The Dissertation Committee for Sean Matthew Carroll Certifies that this is the approved version of the following dissertation:

Strategies for Generating Therapeutic Antibodies

Committee:

George Georgiou, Supervisor

Brent Iverson, Co-Supervisor

Phil Tucker

Jennifer Maynard

Hal Alper

Strategies for Generating Therapeutic Antibodies

by

Sean Matthew Carroll, B.S.

Dissertation

Presented to the Faculty of the Graduate School of

The University of Texas at Austin

in Partial Fulfillment

of the Requirements

for the Degree of

Doctor of Philosophy

The University of Texas at Austin

August 2012

Dedication

To my mother,

for her enduring inspiration

Acknowledgements

I would like to thank my advisor Dr. George Georgiou for his constant support and encouragement throughout my graduate career. Additionally, I would like to thank my co-supervisor Brent Iverson for his help and guidance.

I would also like to thank Dr. Sai Reddy, Dr. Jason Lavinder, Dr. Greg Ippolito, for their many helpful conversations and advice. I would also like to thank Kam Hon Hoi and Christien Kluwe for working with me on projects throughout my time in the BIGG lab.

It has been an extraordinary pleasure to work with the members of the BIGG group.

Strategies for Generating Therapeutic Antibodies

Sean Matthew Carroll, Ph.D.

The University of Texas at Austin, 2012

Supervisors: George Georgiou and Brent Iverson

Monoclonal antibodies have become essential therapeutic tools and currently dominate the therapeutic protein market. Consequently, there is continued demand for new therapeutic antibodies and their discovery techniques.

In one part of this work, we report the discovery of a new therapeutic antibody candidate with a novel mechanism for inhibition of a therapeutically relevant biochemical pathway: the classical complement pathway. In order to inhibit classical complement, an antibody was developed that modulates the signaling subcomponent of the pathway initiating C1 complex, C1s. This work includes novel protocols and strategies used for discovery and characterization of antibody D, which binds and inhibits C1s protease activity. By regulating C1s activity, antibody D is shown to regulate classical complement. It is further shown that affinity maturation of antibody D results in higher levels of complement inhibition at various antibody concentrations. This work marks the first example of an antibody that specifically regulates the classical complement pathway by targeting the C1s protease on the pathway initiating C1-complex.

Next, we characterize the human immune cells produced by humanized NSG mice, most notably the B and T lymphocytes, engraftment with human $CD34^+$ HSC cells. We detected development of naïve human B and T cells and their various subtypes, as

well as other human immune cells from engrafted mice. However, attempts to generate a robust antibody response to antigens were unsuccessful. Therefore, we conclude that NSG humanized mice developed in this study are suitable for studying the antibody repertoire of naïve B cells, however they are not suitable for the analysis of activated B-cells.

Last, we introduce a novel strategy for the generation of polarized antibody repertoires for use in therapeutic monoclonal antibody discovery. This technique combines targeted antigen delivery to a specific lymph node and a frequency based antibody selection approach in order to directly select antigen specific antibodies *in silico*. By directly selecting antigen-specific antibodies, this approach circumvents laborious and time consuming screening techniques. We expect that this work will be the foundation of an overall improved protocol for monoclonal antibody discovery that accelerates the speed and enhances the simplicity of discovery techniques.

Table of Contents

List of Tables

List of Figures

Chapter 1.

Engineering Antibodies

INTRODUCTION

Humans are under constant threat from a vast array of infectious agents. The skin and mucosal membrane act together as the primary barrier to keeping pathogens at bay; their function is to serve as a physical barrier keeping pathogens from gaining entry into the body. However, these barriers are occasionally breached by disease -causing pathogens leading to an infection and activation of the immune system. The immune system is composed of serum proteins, cells, tissues and organs that act in concert to detect, neutralize and dispose of invading pathogens. Pathogens, in turn, are quick to evolve to avoid detection and escape the immune system. In order to combat the vast array of ever evolving pathogens attempting to gain a foothold in the body, the immune system employs two general strategies to recognize pathogens and mark them for destruction: (1) recognize common features of invading organisms and (2) develop new receptors that recognize the unique features of a specific invading organism. The components that comprise the former non-specific strategy collectively form what is called the innate immune response and the components of the latter highly specific strategy form the adaptive immune response (1).

The innate immune response is initiated when common features of invading pathogens are recognized by pattern recognition receptors (PRRs) on secreted serum proteins or the surface of cells such as phagocytes and granulocytes (2, 3). PRRs on the phagocytes (primarily macrophages and neutrophils) are often the first to recognize an invading microorganism. Once recognition of the microorganism has occurred, the phagocytes quickly internalize and destroy the invaders. Occasionally a microorganism is

able to overcome innate immune defenses and avoid destruction by the phagocytes. The ability to escape the initial innate immune response distinguishes pathogenic from non-pathogenic microorganisms. Once a pathogenic microorganism gains a foothold in the body, macrophages and other cells of the innate immune system secrete chemokines and cytokines to stimulate both inflammation and antigen presentation by the phagocytes, thus initiating the adaptive immune response (4).

The innate immune system is limited because it can only control pathogens that express a limited set of molecules with defined molecular patterns that are distinct from those of the macromolecules expressed by the host. In order to control a much wider range of pathogens, the adaptive immune system has evolved to recognize a far greater breadth of molecules (antigens) expressed by invading pathogens. Importantly adaptive immunity displays memory in that re-exposure to antigen decades later elicits a strong humoral immune response very quickly involving host molecules that are largely derived from those induced by the first exposure (5).

The adaptive immune response is further divided into two components: humoral immunity and cell-mediated immunity. The cell-mediated aspect of the adaptive immune response involves T-lymphocytes that are able to either induce apoptosis in host cells displaying epitopes of foreign antigen on their surface (cytotoxic T cells) or assist other immunological processes, including the maturation of B cells into memory B cells and plasma cells and activating cytotoxic T cells and macrophages (6). Secreted immunoglobulins, known as antibodies, comprise the humoral aspect of the adaptive immune response.

Antigens are recognized with low affinity by immunoglobulins expressed on the surface of naïve (non-antigen stimulated) B cells. B-cells displaying antigen-recognizing immunoglobulins undergo expansion and differentiation, eventually resulting in antibodies

with very high affinity and selectivity that are secreted by terminally differentiated form of B cells, called plasma cells (7). Antibodies differ from the innate immune PRRs in that each antibody has been selected to target a specific antigen with high specificity in order to help control the pathogen that expresses that particular antigen. Antibodies are very stable proteins and have a long half-life with some isotypes capable of remaining in circulation for up to three weeks (8). By comparison, proteins other than antibodies having the same molecular weight and charge are removed from circulation within 1-3 days. Once bound to an antigen, antibodies confer protection through three pathways: neutralization of the pathogen which is prevented from infecting the host, activation of complement (complement dependent cytotoxicity, CDC), and recruitment of phagocytes for opsonization (antibody dependent cell cytotoxicity, ADCC) (9). Antibodies can recognize a wide variety of antigens including proteins, small molecules, lipids, carbohydrates and nucleic acids.

Antibodies have become widely utilized as therapeutics and thus antibody discovery and engineering have evolved into a multi-billion dollar industry. The first FDA approved clinical use of an antibody in humans occurred in 1982 (muromonab, a mouse IgG used as an immunosuppressant; it destroys human T cells by binding surface antigen CD3), and in 1997 the first anticancer antibody received approval (rituximab, a chimeric antibody that binds to the B cell surface marker CD20; it is used to treat diseases characterized by excessive B cells such as lymphomas) (10). As of May 2012, there were 39 monoclonal antibodies approved by the FDA (fda.gov, list below). The impact of antibody therapeutics is specifically demonstrated by the fact that they have generated ~$18.5 billion in sales for 2010, the highest of all biological drugs (11). Their importance in diagnostics and therapy cannot be understated.

#	Trade Name	mAb	#	Trade Name	mAb
1	Orthoclone OKT3	Muromonab-CD3	21	PROSTASCIN T	CAPROMAB PENDETIDE
2	ACTEMRA	TOCILIZUMAB	22	RAPTIVA	EFALIZUMAB
3	ADCETRIS	BRENTUXIMAB VEDOTIN	23	REMICADE	INFLIXIMAB
4	ARZERRA	OFATUMUMAB	24	REOPRO	ABCIXIMAB
5	AVASTIN	BEVACIZUMAB	25	RITUXAN	RITUXIMAB
6	BENLYSTA	BELIMUMAB	26	SIMPONI	GOLIMUMAB
7	BEXXAR	TOSITUMOMAB; IODINE I 131 TOSITUMOMAB	27	SIMULECT	BASILIXIMAB
8	CAMPATH	ALEMTUZUMAB	28	SOLIRIS	ECULIZUMAB
9	CEA-SCAN	ARCITUMOMAB	29	STELARA	USTEKINUMAB
10	CIMZIA	CERTOLIZUMAB PEGOL	30	SYNAGIS	PALIVIZUMAB
11	DERMABET	BETAMETHASONE VALERATE	31	TECHNETIU M	TECHNETIUM (99m Tc) FANOLESOMAB; NEUTROSPEC
12	ERBITUX	CETUXIMAB	32	TYSABRI	NATALIZUMAB
13	HEMABATE	CARBOPROST TROMETHAMINE	33	VECTIBIX	PANITUMUMAB
14	HERCEPTIN	TRASTUZUMAB	34	VERLUMA	NOFETUMOMAB
15	HUMIRA	ADALIMUMAB	35	XGEVA	DENOSUMAB
16	ILARIS	CANAKINUMAB	36	XOLAIR	OMALIZUMAB
17	LUCENTIS	RANIBIZUMAB	37	YERVOY	IPILIMUMAB
18	MYLOTARG	GEMTUZUMAB OZOGAMICIN	38	ZENAPAX	DACLIZUMAB
19	MYOSCINT	IMCIROMAB PENTETATE	39	ZEVALIN	IBRITUMOMAB TIUXETAN
20	PROLIA	DENOSUMAB			

Table 1.1: Current List of FDA Approved Monoclonal Antibodies (http://www.fda.gov/ May 2012)

ANTIBODY STRUCTURE

Antibodies are composed of two identical heavy and light chains that come together to form the "Y" shape molecule shown in the figure below. The heavy chain and light chains are organized into multiple immunoglobulin domains that are held together into their large complex by disulfide bonds.

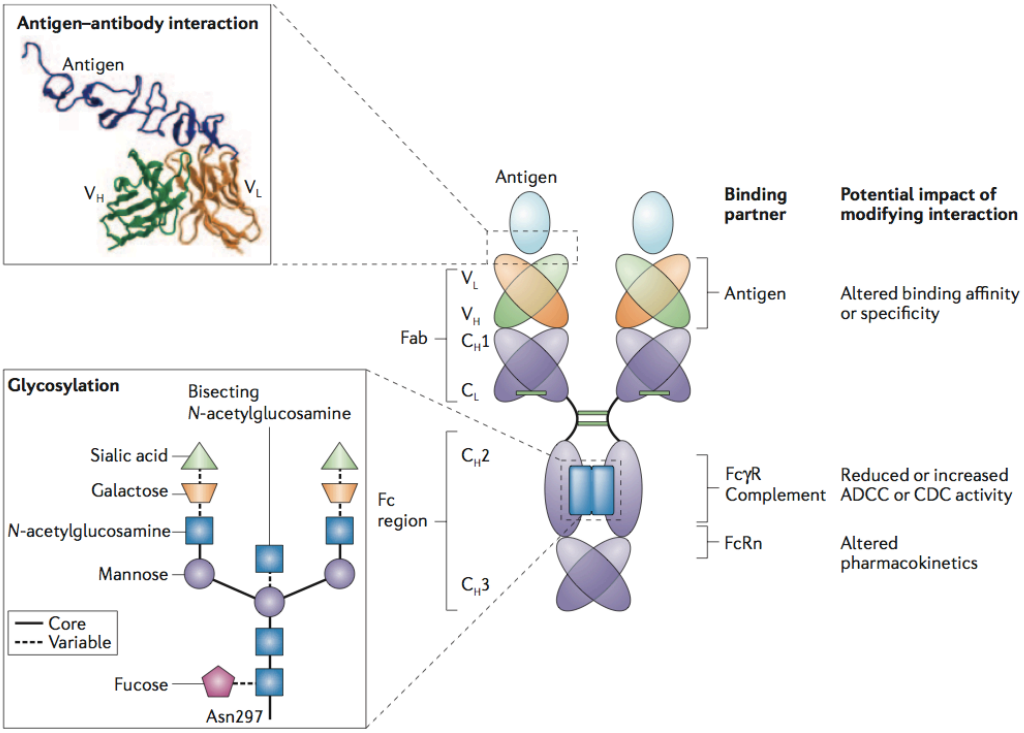

Figure 1.1: Antibody domain structure (IgG) and antigen binding sites (12).

An antibody monomer is comprised of two identical antigen-binding fragments (FAB); the antigen binding domains are linked together by the constant domain (F_c) that recruits immune cells to dispose of the bound antigen. In the human immune system, there are different constant domains and they define the respective isotypes: IgA, IgD, IgG, IgE, IgM. Each isotype has a different F_c domain structure that controls the types of effector cells that can be recruited by the antibody, whether the antibody can activate the complement pathway and avidity. The most common isotype in serum and the only one used therapeutically so far is IgG (13). IgA and IgG isotypes are further divided into subclasses (IgG1, IgG2, IgG3, IgG4 and IgA1 and IgA2). The subclasses are >95% homologous but differ in their ability to activate effector responses.

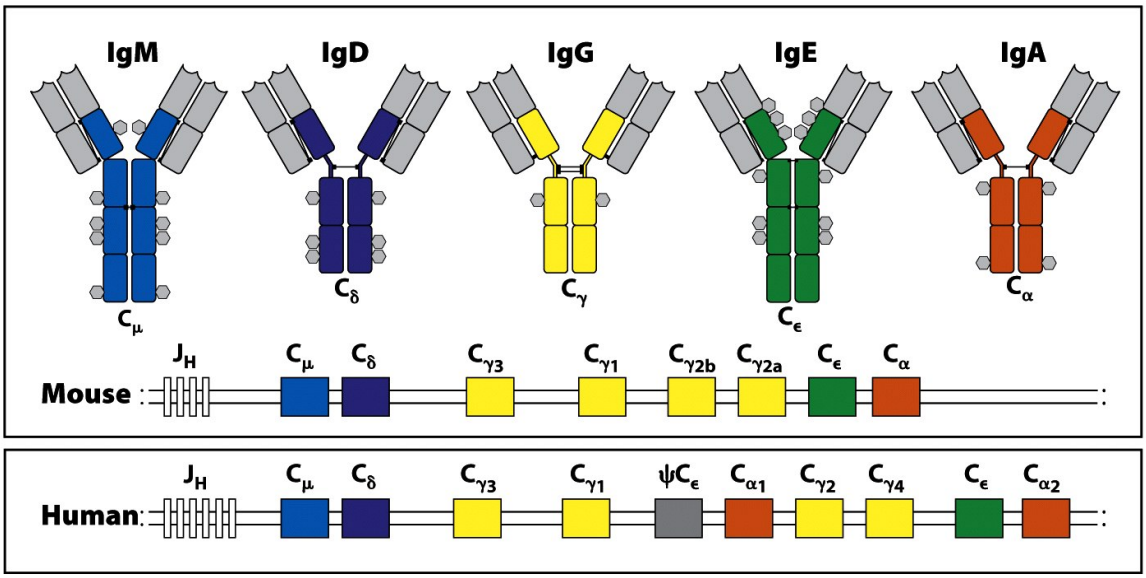

Figure 4-17 Immunobiology, 7ed. (© Garland Science 2008)

Figure 1.2: Structural comparisons of antibody isotype and subclass and their relative chromosome location (1)

Each antibody has two identical fAb fragments composed of two light chain and heavy chain immunoglobulin domains. The antigen-binding site is located within the variable domain at the N terminus of each chain; each variable domain contains three complementary determining regions (CDRs) that establish antigen binding. The heavy and light variable regions of the antibody come together to create the complete antigen-binding site.

Antigen Recognition and the Variable Domains

The antibody antigen binding sites are found within the first globular protein domain on the N terminus of the heavy and light chains. These antigen recognition domains are called variable domains because of the vast diversity of peptide sequences found within these domains. The majority of the diversity in each variable domain occurs

at the antigen binding loops are called the complementary determining regions (CDRs) or hyper variable regions.

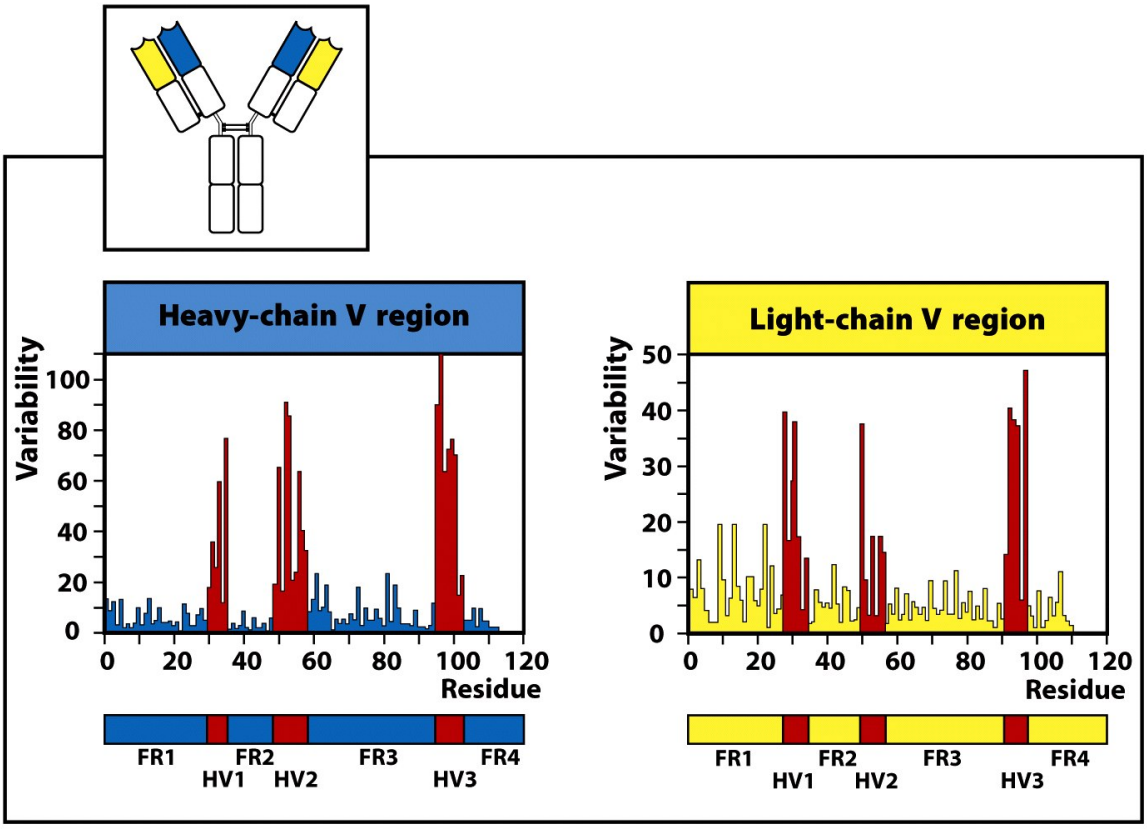

Figure 3-6 Immunobiology, 7ed. (© Garland Science 2008)

Figure 1.3: A variability plot derived from the amino acid sequences of several dozen heavy and light chain V domains is shown. The red areas of higher variability are the CDRs (1)

Both the heavy and light chain have three CDR loops giving each fAb arm six CDRs with which to bind one antigen epitope. The third CDR of the heavy chain, termed the CDRH3, is the most variable CDR loop and the most significant loop in determining binding specificity. The CDRH3 is so diverse because it is formed at the junction of the genetic recombination of the three different fragments, named the heavy chain V, D and J regions (14). The human genome has many V, D and J regions that can recombine during

B cell development in order to produce many different functional heavy chains (14). Besides combining three different immunoglobulin gene segments, the mechanism of genetic recombination also stochastically introduces additional diversity by adding or deleting nucleotides. This recombination event can produce a near CDH3 infinite diversity at the site.

The two other CDR loops found on the heavy chain are not the product of a recombination event; therefore the number of germline V gene fragments determines the initial diversity of these loops. However, through a mechanism called somatic hypermutation, these loops are often mutated in order to increase the affinity of the antibody. The light chain forms in a similar manner except that it is the product of a recombination event that has only two genetic fragments, termed light chain V and J fragments. Because the light chain CDRL3 is the product of only two genetic fragments coming together, there is significantly less diversity.

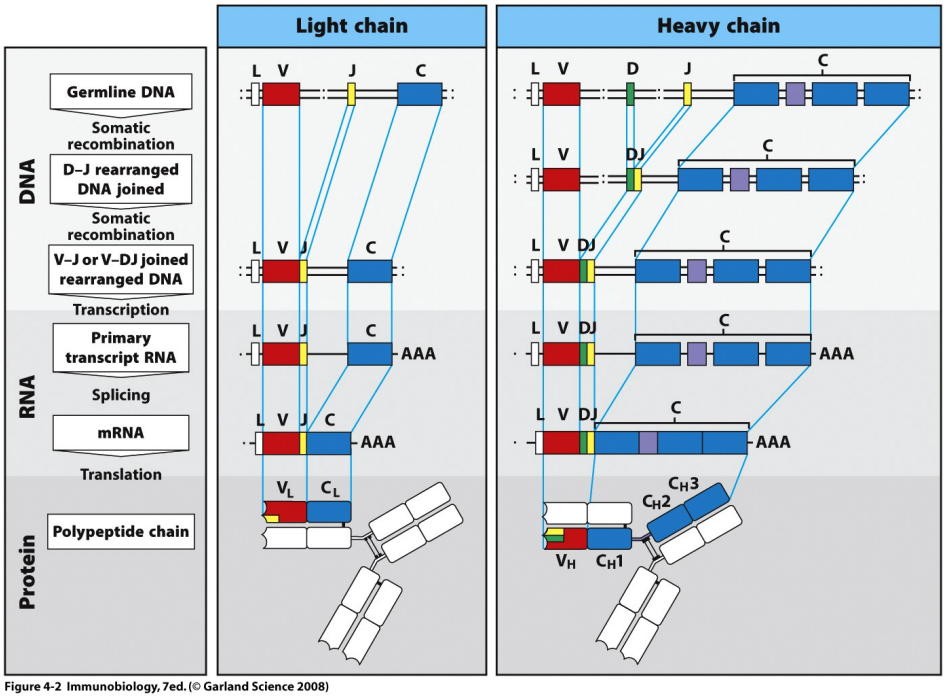

Figure 1.4: V gene construction from V-region gene segments (1).

Antibody Effector Function

Antibodies interact with the innate immune system through the Fc (constant region) portion of the antibody. The F_C interacts with the host environment and the innate immune system in three main ways: (1) By binding cell surface receptors on innate immune cells to induce reactions critical for pathogen clearance. (2) By initiating the cytolytic cascade of serum protein activation collectively known as the classical complement pathway. This interaction beings when the F_C interacts with the pathway initiating C1 complex binding; antibody activation of this process is referred to as CDC, complement dependent

cytotoxicity. (3) Mediating the presentation of antigens to dendritic cells and other innate immune cells that in turn trigger adaptive immune responses to the pathogen.

The various antibody isotypes and subclasses have different affinities for Fc receptors and C1 complex. The avidity and interaction between the Fc and cell surface receptors or serum proteins determines the nature of the response elicited by the complement pathway or by effector cells. For example, human IgG4 cannot bind C1 complex while the other three IgG subclasses can.

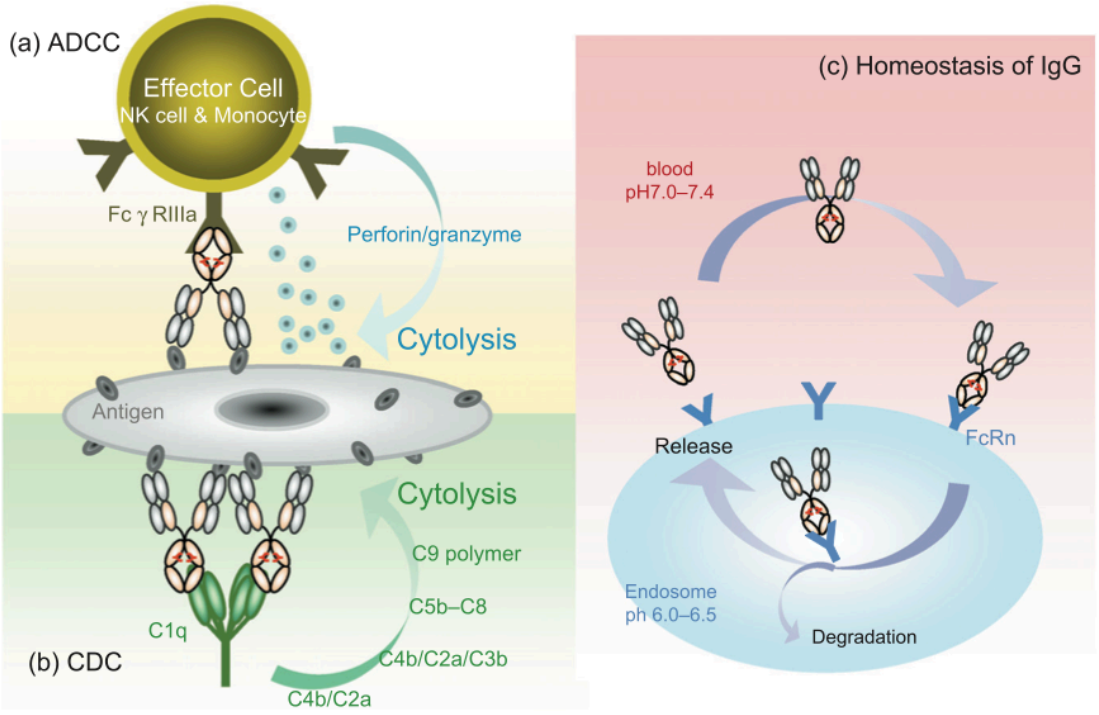

Figure 1.5: Outline of effector functions dependent on antibody Fc. ADCC(a), CDC (b) and FcRn binding are shown. Phagocytosis is not shown (9)

Present on most cells of the immune system are Fc receptors (FcRs) that bind the constant region (Fc) of specific immunoglobulin (Ig) isotypes and isotype subclasses.

Different cells express different FcRs depending on the function of the cells and the Igs to which they respond. Cellular internal signaling cascades initiated by immune complexes that bind the FcRs are commonly activating signals that result in phagocytosis of the immune complex that initiated the signal. In other cases, activation of mast cells can lead to an allergic reaction when IgE binds its receptor, while activation on NK cells by IgG leads to release of its granules. One IgG molecule is insufficient to activate FcγRs (IgG binding FcRs). Instead, the key to signal transduction is the cross-linking of receptors by immune complex. After the pathogen is bound by the Fc receptors of the phagocyte, the pathogen is ingested and destroyed by the in a process called phagocytosis.

FcRs on non-phagocytes can actively destroy target pathogens through a different mechanism know as antibody dependent cell cytotoxicity (ADCC). ADCC is a process in which effector cells lyse a target cell coated in antibody without engulfing or ingesting, a process primarily carried out by natural killer cells (NK), ADCC occurs when the FcR expressed on NK cells (called FcγRIII) binds to immune complexes formed by pathogen and antibodies bound to it (15). Upon activation by immune complexes, NK cells secrete cytokines and cytotoxic granules that enter the pathogen and promote cell death and apoptosis.

Another very important function of the Fc region is to increase the serum half-life and aid in the transport of antibodies across cellular barriers by interacting with the neonatal Fc receptor (FcRn) (16, 17). FcRn is presented on a many different cell types, including the endothelial cells that form the interior surface of the blood and lymphatic vessels. The FcRn prolongs *in vivo* half-life by binding IgG that has been ingested into an acidified endosome via non-specific vesicle mediated uptake of fluid by the cell. Once bound, IgG is recycled back to the cell surface where it is released in the mildly basic pH of blood, thereby preventing it from undergoing degradation in the endosome. Without

FcRn binding ability, the half-life of antibodies is reduced dramatically from 21 days to 7 (18, 19).

Classical Complement Pathway

Antibodies also engage the complement system in order to eliminate pathogens and toxins. The complement pathway system is a complex and powerful component of the immune system that is essential for proper clearance of immune complexes and apoptotic or damaged cells. The complement system is made up of a large number of plasma proteins that cooperate via a biochemical cascade to destroy a pathogen and induce an inflammatory response that helps fight infection. Complement is organized into three semi-independent pathways (classical, alternative and lectin), each of which is activated by different physiological conditions. Any one or more of the three pathways shown in the figure 1.16 can activate the complement cascade. Once a pathway is activated, a biochemical cascade is initiated by the activation of a zymogen protease (inactive) that cleaves and activates the next zymogen substrate in order to propagate and continue the cascade. Complement is an autocatalytic process, therefore activation of a pathway leads to the pathogen surface being coated with complement defense proteins that mark it for destruction and provide a signal for removal by immune cells.

One route that activates this process, called the classical complement pathway, occurs when complement proteins recognize a pathogen coated with antibodies. The classical complement protein complex C1 binds the either the C-reactive protein (CRP) or the Fc region of IgM or IgG1-3 initiates an attack on the pathogen. This pathway ultimately results in the formation of membrane attack complexes (MACs) that disrupt the phospholipid bilayer on a target cell, resulting in cell lysis and death. In addition to

MACs, the complement pathway also deposits a protein called C3b on the surfaces of target cells, which promotes their destruction by phagocytosis. Complement activation also results in the release of cytokine-like molecules C5a and C3a, which results in chemotaxis and activation of leukocytes.

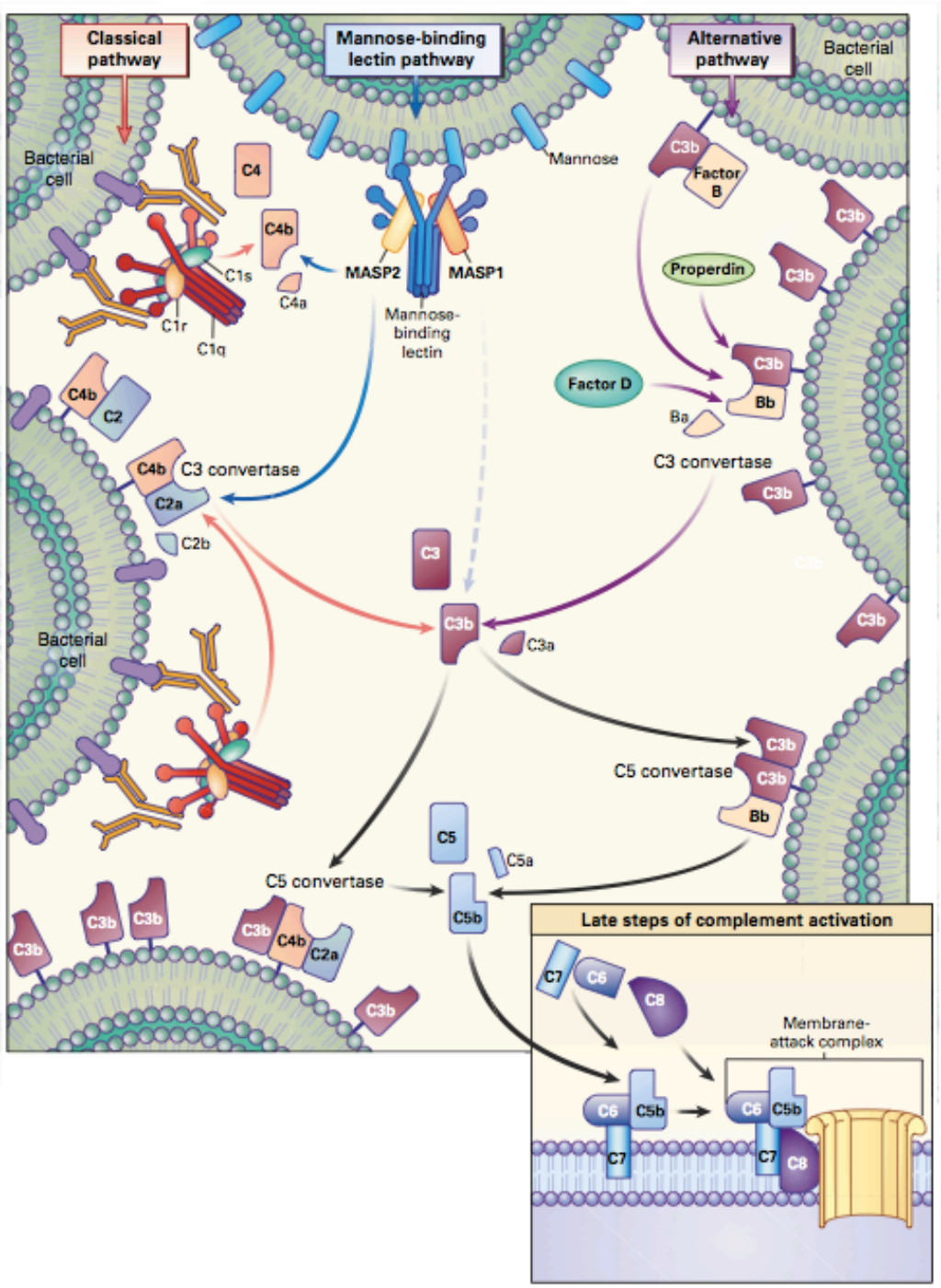

Figure 1.6: Complement overview: the classical (red), lectin (blue) and alternative (purple) pathways are initiated by different protein complexes that recognize different conditions, but the pathways ultimately use the same downstream proteins (20)

The classical complement pathway is comprised of nine protein complexes, yet only the pathway-initiating C1 complex is an exclusive member of the pathway. Whereas the other complement pathways – lectin and alternative - share the other constitutive proteins found in the classical pathway. Thus, targeting the initiation complex (C1) for intervention and inhibition of classical complement is the logical option to control this pathway without adverse consequences to the other essential pathways.

The function of C1 complex is to first recognize physiological conditions for activation of complement and then begin the classical complement cascade. It is composed of one C1q molecule with six terminal C1q globular heads, which recognize initiation conditions, two C1r proteases that activate C1s upon initiation, and two C1s proteases that transmit the activation signal by cleaving serum complement components C2 and C4 (21). Classical complement pathway begins when C1q globular heads recognize surface bound IgG, IgM or C-reactive protein (CRP) then undergo a conformational change. These conformational changes induce C1r to self-activate, which in turn activates C1s, the protease that propagates the activation signal to other serum proteins.

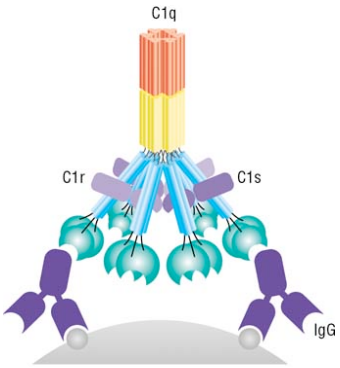

Figure 1.7: C1s in complex with C1q and C1r while recognizing IgG (22)

C1s is a 75kDa serine protease with an identical domain organization to C1r and MASP-1, MASP -2, and MASP -3 of the complement lectin pathway of complement activation(23). Each member of this family is composed of five non-catalytic domains followed by a C terminal chymotryipsin-like serine protease domain.

Development of B cells

Immature B cells are produced in the bone marrow, where V(D)J recombination occurs and self-reactive B cells are apoptosed (here called clonal deletion). Immature IgM^{+}/IgD- B cells travel from the bone marrow and travel through the blood to the spleen; once in the spleen, they are subjected to further rounds of clonal deletion before becoming fully mature (24). In the presence of a supporting microenvironment, immature B cells become mature long-lived naïve B cells (follicular B cells) and recirculate through secondary lymphoid organs in search of signs of infection (25). A small number developing B cells become immobile marginal zone (MZ) B cells instead of follicular B cells; the decision to become a MZ B cell is though thought to be in part related to the strength of B cell receptor signaling (26). MZ B cells home to the spleen and can be activated in a T-cell independent manner. Follicular B cells are the most common naïve B cell and they home primarily to B cell follicles in the secondary lymphoid organs. B cell follicles are always located in secondary lymphoid organs near T cell zones, an arrangement that allows for activated T helper cells to quickly activate follicular B cells that have bound antigen.

Once follicular B cells are activated by T helper cells and antigen recognition, they can proliferate and differentiate to form either plasma cells capable of antibody secretion or memory cells that provide long lived memory against subsequent infections (27). Most

plasma cells generated upon activation of naïve B cells are short lived plasma cells that primarily remain in the extramedullary region on the secondary lymphoid organ (28); a small fraction become long lived plasma cells primarily home to the bone marrow where they can persist for many years. Activated B cells can also travel to the germinal centers (GC) where GC reactions provide a cellular milieu for the mutation and affinity maturation of the B cells (25).

Recombinant Antibody Fragments

Advances in molecular cloning techniques have enabled the production of antibody variable domains without the constant region domains. Antibody variable domains are the only domains required for antigen binding.

The most common host for heterologous expression of antibody genes is *E. coli*. Expression of full-length antibodies is relatively more difficult and can result in the production of an appreciable amount of misfolded protein. Therefore for bacterial expression antibody fragments, namely fAb, scFv or scAb formats (see figure below) are much more widely employed. Antibodies in scFv format comprise only the variable heavy and light domains linked by a short peptide sequence. Fab antibodies consist of the entire VL chain and the variable heavy as well as the first constant region of the VH. A disulfide bond in the constant regions is responsible for linking FAB heavy and light chains. Additional formats are shown in the figure blow. Multivalent antibody fragments are occasionally desirable because they provide an increase in functional affinity (avidity) or can be engineered to have multiple specificities(29, 30).

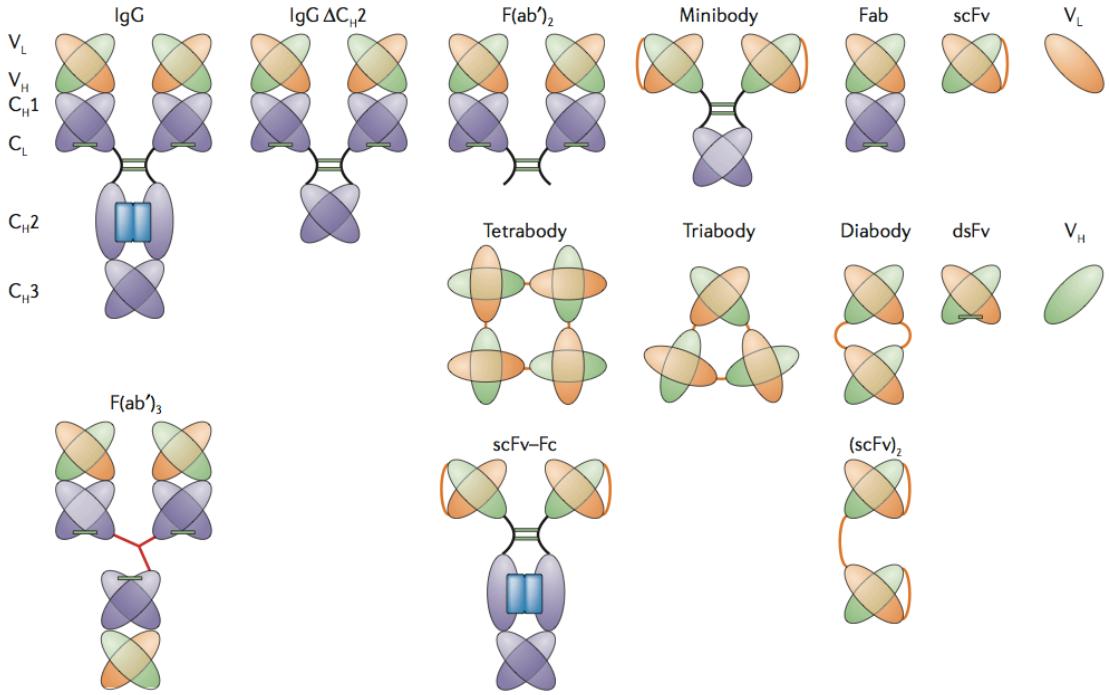

Figure 1.8: Representative antibody formats created through genetic manipulation and protein expression (12). Constant regions are purple, heavy chains are green, light chains are orange, and sugars are blue. scAbs are important in this study, they are scFvs with the light chain constant domain C-kappa attached at the C-terminus of the peptide.

ANTIBODY SPECIFICITY AND AFFINITY

As discussed above, the antigen-binding site of antibodies lies within the variable region. The specific residues on an antigen that interact with amino acids in the antigen-binding site of the antibody constitute the binding epitope. The two most important characteristics of an antibody Fab region are its specificity and affinity for the epitope it binds. Specificity is the ability of the Fab region to recognize and bind one antigen over another. An antibody that binds and forms an immune complex with many similar epitopes is said to have "poor specificity". Conversely, an antibody that binds one antigen epitope but will not bind another highly similar epitope is said to have "high specificity".

Antigen affinity is often used as the standard quantitative measure of the quality of an antibody. The affinity of the Fab region for an antigen can be generally thought of as the "tightness" of the interaction. In order to numerically define affinity, first it is necessary to desirable the interaction in a quantitative way. The formation of immune complexes is a reversible process, therefore the formation of immune complex can be written as the following:

$$[Antibody] + [Antigen] \leftrightarrow [Antibody{:}\,Antigen]$$

The association rate (forward reaction) is governed by the rate constant k_{on} ($M^{-1}s^{-1}$) and the dissociate rate (reverse reaction) is governed by the off rate constant k_{off} (s^{-1}). These rates are dependent on the concentration of the antibody and antigen, but reach the same values at equilibrium; at that point the concentrations of the complex, antibody and antigen are constant. Once the reaction reaches equilibrium, the ratio between immune complex and the separated component parts is constant and can be written in the following manner:

$$K_D = \frac{[Antibody][Antigen]}{[Antibody{:}\,Antigen]} = \frac{k_{\text{on}}}{k_{\text{off}}}$$

The constant K_D, called the dissociation constant, is the most common measure of antibody affinity. The smaller the dissociation constant, the greater the propensity for the antibody to be in complex with antigen; thus smaller dissociation constants are indicative of tighter bonds between antigen and antibody. There are various methods for determining the dissociation constant and the individual rate constants. Two important technologies for determining the dissociation constant considered here are surface plasmon resonance and kinetic exclusion assay.

Surface Plasmon Resonance (BIACore)

SPR is the most popular way to measure the equilibrium dissociation constant and kinetic parameters for two interacting molecules. The most attractive feature of this technology is that does not require a secondary probe or fluorophore conjugate in order to detect an interaction; therefore SPR is free from the compilations that can arise from the labeling of molecules. The most popular instrument used for SPR is BIACore. BIACore and other similar SPR instruments are microfluidic devices that immobilize one of the binding partners on the surface of a sensor chip then flow the other binding partner over the surface. When an interaction occurs between the fluid phase and immobilized binding partners, there is a slight change in mass on the surface of the chip. This minuscule change in mass is monitored by a change in the reflected light directed at the other side of the chip. The greater the change in mass, the higher the deflection of the reflected light. The measure of the change in mass near the surface is used to create a real-time interaction profile called the sensorgram. One such example of a sensorgram is shown in the figure below. In an experiment, many of these sensorgrams are generated using different concentrations of unbound material followed by interpretation of results via mathematical software order to calculate the equilibrium dissociation constant K_D, and the association and dissociation rates (k_{on} and k_{off})

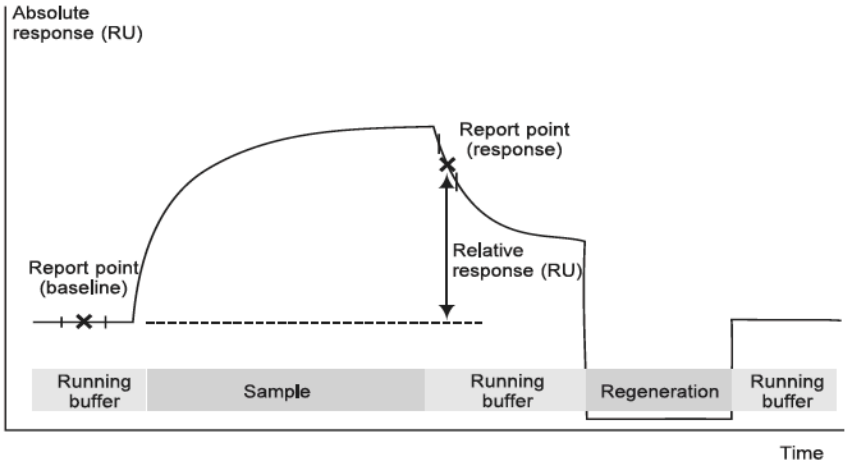

Figure 1.9: Schematic illustration of a sensorgram with bars below indicating the solution passing over the sensor surface. The x-axis is time and the y-axis is an aribtraty unit (RU) which correlates with the mass on the surface of the sensor. Extracted from BIACore handbook.

Kinetic Exclusion Assay (KinExA)

The kinetic exclusion assay experiment measures the equilibrium dissociation constant K_D and association rate k_{on} directly; multiplying the two experimental values together calculates the off rate. The advantage of this method is that equilibrium is measured with both components in the solution phase. Other technologies, such a SPR, require one of the components to be immobilized to a surface, which can distort and destabilize the delicate proteins.

The most popular machine for running this sort of assay is called a KinExA. In order to determine the K_D of an antibody, first one of the binding partners (usually the antigen) is immobilized to a solid bead support (usually through adsorption to polystyrene beads). Immobilized antigen is then used as a probe to capture the free component of the other partner (antibody) once equilibrium is reached between solution phase antibody and

antigen. This exposure time is quick enough that any antibody in a preformed complex with antigen in solution will not have the time needed for dissociation. A secondary antibody conjugated to a fluorophore is then used to detect antibody captured by the immobilized antigen for each solution of antibody and antigen.

For each experiment, a series of solutions containing different concentrations of antigen and a constant concentration of antibody are equilibrated before being exposed to the solid phase antigen in order to capture free antibody. It is important to note that even though immobilized antigen is used as a capture agent, equilibrium is still being measured from liquid phase interactions.

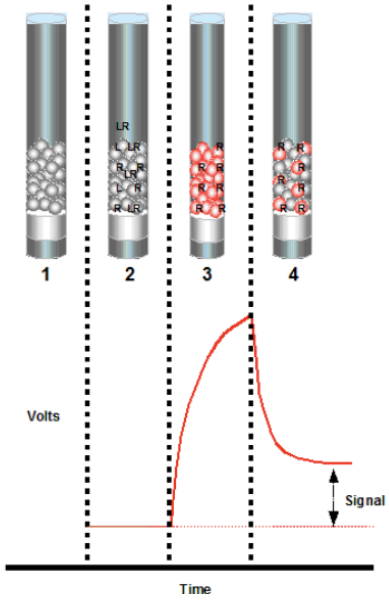

Figure 1.10: Steps involved in kinetic exclusion assay and representative signal output. R= receptor (antibody), L= ligand (antigen), LR=ligand-receptor complex. 1. Immobolized antigen (L) is loaded into the detection well. 2. Antigen antibody mixture at equilibrium is flown over the beads. The beads capture antibody not in complex with antigen, but antibody in complex is not. 3. Secondary fluorescent probe is flown over beads 4. Buffer is run over beads, leaving only bound secondary probe. Extracted from the KinExA guidebook.

In each experiment, output signals are measured from a series of solutions with different antigen concentrations and a constant antibody concentration. After a series is measured in duplicate, mathematical software calculated the dissociation constant K_D. Binding kinetics can be determined by further experiments in which the measurements are collected "pre-equilibrium".

THERAPEUTIC ANTIBODIES AND THEIR DISCOVERY

Antibody therapy in humans began in the 1890s when Emil von Behring and colleagues discovered that transferring serum from animals immunized with diphtheria could protect humans from the same disease (31). At the time they did not know the protection was a result of the antibody transfer, so they named this processes "serum therapy". Serum therapy brought with it significant complications because antibodies could not be separated from the serum, resulting in intense immune reactions to the foreign serum proteins. Over time, purification of the antibody fraction became possible; however this fraction was still very impure by modern standards because it contained both unintended antibodies and other with impurities that could not be removed. During the early 1900s, advances in vaccination and antibiotics would largely overshadow this technology (32). It was not until the mid 1970s that antibody technology would see its next major advance: a breakthrough technology that enabled the mass production of a single antibody clone.

Hybridoma Technology

In the mid-1970s an important breakthrough occurred, which would be known as the beginning of modern antibody engineering: hybridoma technology (33). Before the advent of the hybridoma method, investigators could only produce polyclonal serum antibodies; this required large numbers of immunized animals and did not immortalize the antibody-producing cells. Therefore production was a cumbersome process requiring many animals in order to produce more antibodies and each preparation was different that the one before. To overcome this problem, a technology was needed that could produce an infinite number of the same antibody. The easiest solution was to extract one of the antibody-secreting lymphocytes from immunized animal and grow it indefinitely in culture, however antibody-secreting cells have a finite lifespan and will not continue living or dividing in culture for very long. In order to overcome this limitation, Köhler and Millstein developed a method to create an antibody producing cell line capable of dividing and living indefinitely outside of an animal; these cultures produced a near infinite amount of the same monoclonal antibody clone (mAbs) (33). The two scientists achieved this feat by fusing antibody-secreting lymphocytes with myeloma cells; the resulting cell was a sort of cancer cell that would grow indefinitely in culture while producing only one type of antibody (34). These fusion cells are called hybridomas.

Hybridomas can now be created in most any biological lab today. Production of a monoclonal hybridoma cell line requires a multistep protocol that can take months in order to create cell line producing an antibody specific to an antigen. The first step necessary is to immunize mice with antigen followed by B-cell isolation from the spleen or other lymphocyte-containing anatomical locations. B cells are then pooled with mouse myeloma cells that do not secrete antibody before being incubated in media that promotes cellular fusion. The fusion process is stochastic and results in B-cell / B-cell, B-cell / myeloma

(hybridoma), and myeloma / myeloma products. The B-cell / B-cell product and single B cells do not survive long, and due to a key genetic mutation, the myeloma cells that have not fused with a B-cell will eventually die in the presence of aminopterin. Therefore after culturing in aminopterin, the only surviving cells have are a fusion of at least one B-cell and myeloma cell. The surviving hybridomas are then diluted into single cell compartments where they grow indefinitely and produce antibodies. The antibody-containing supernatant is assayed for specificity to the antigen desired, and wells containing antigen-specific antibodies have successful hybridomas that are expanded, cultured and further characterized.

The hybridoma technique remained the dominant method for discovering and expressing monoclonal antibodies for a long time and is still commonly used to in industry today. However, this technology is not without drawbacks; the process in very long. It can take month to immunize mice, wait for an appropriate immune response, then create and expand the hybridomas. Competing technologies such as phage display with a synthetic library (discussed in subsequent sections) offer antibody isolation in weeks. Furthermore, hybridoma produced antibodies commonly have sub-optimal dissociation constants, because the murine antibodies isolated from hybridoma technology often have roughly nano-molar range dissociation constants while many therapeutic antibodies today have pico-molar constants (12, 35, 36). Affinity maturation is often required in order to have a therapeutically relevant antibody. Another complicating factor associated with antibodies produced from hybridomas is that murine Fc regions are not readily recognized by human FcRs. As a result, mouse antibodies are not very effective at soliciting a response from human effector cells. The most significant drawback of therapeutic antibodies produced from hybridomas is their immunogenicity (37). Antibodies produced from mice are often recognized by the human immune system as foreign. Therefore after repeated treatments,

the immune system mounts an immune response that fights against the foreign antibodies, a process known as human anti-mouse antibody (HAMA) response.

Humanized Antibodies

In order to circumvent complications associated with injecting murine antibodies into humans, antibodies with a human framework were necessary. Only very recently have reports of human hybridomas become a seemingly viable technology; however there are still many technical and ethical issues limiting their widespread adoption (38, 39). Instead the first and still most common solution was to produce human-like antibodies from mice. This was first accomplished by linking the variable domains found using hybridoma technology to the constant domains of human antibodies. These murine-human antibody chimeras remove much of the murine sequence, resulting in less immunogenicity and engagement of the human FcRs. The FDA has approved several chimeric antibodies, however the remaining murine sequences still result in HAMA response (40).

The immunogenicity of chimeric antibodies has been further reduced by continued humanization. The next iteration of antibody humanization is to further reduce the amount of murine antibody sequence by CDR grafting. In this process the murine CDR loops that bind the antigen are grafted onto human variable frameworks (41). This produces an antibody with even less murine sequences, resulting in less frequent and less severe immunogenicity. CDR grafting also has drawbacks: the human variable frameworks supporting the CDR loops are not identical to the supporting mouse framework; therefore when CDR loops are grafted onto different frameworks, they are not necessarily displayed in the same way. The consequence of the different frameworks is that CDR grafted antibodies often have a significantly reduced affinity for the antigen. Additionally these

loops are oftentimes slightly immunogenic, however, much less so than chimeric antibodies. Despite these problems, CDR grafted humanized antibodies are the most common type of FDA approved antibody.

Human Antibodies from Mice

Creating fully human antibodies is one of the most important goals in the field of antibody engineering for therapeutic purposes, but the obvious ethical and practical considerations of using humans for production prevent any direct methods for being employed. There have been advances in creating human hybridomas, however the use of this technology is still limited in application(38, 39, 42). Instead, a few very cleaver indirect methods have been devised to create fully human antibodies in mice.

Transgenic Mice

The most commonly explored method for attaining human antibodies from mice is through proprietary transgenic mouse models (or transchromosomic), meaning mouse immunoglobulin genes have been inactivated and replaced by human immunoglobulin variable and constant regions. This technology has proven extremely effective at producing human antibodies, as evidenced by all four of the clinically approved antibodies in 2009 came from such transgenic mice(43). Examples of this technology include:

Medarex - UltiMab platform

Abgenix - Xenomouse technology. (acquired in April 2006 by Amgen)

Regeneron - VelocImmune technology

Kirin Brewery Co - Kirin TC Mouse

Humanized Mice

The other technology that produces human antibodies from mice involves the engraftment of human hematopoietic cells or tissues in immuno-deficient mice. The advantage of this model is that it provides an opportunity to study human cells and biological processes *in vivo* (44). This is the model is significantly more difficult to use because engraftment requires expert training and engraftment levels are quite variable. Despite the inherent difficulties, this model pursued in studies today because it offers the rare opportunity to study fully human cells *in vivo*; therefore studies involving humanized mice have relevance to human immunology in addition to the therapeutic value of the antibodies produced from them.

Since the creation of the first humanized mice, increases in human lymphocyte populations and activity has been enabled by the systemic reduction of immune cells produced by the host mouse (45). Reduction in background immune cell production in the host is important to prevent competition with or rejection of human $CD34^{+}$ cells once engrafted. One of the most popular mouse strains developed to date, and the one used in this research, is termed NSG (NOD.Cg-Prkdc^{scid} Il2rg$^{tm1Wjl/SzJ}$ mice). The genetic modifications introduced to this strain in order to reduce host immune function are the following:

1. Non-obese-diabetic (NOD) – The genetic background derived from the NOD mouse line contributes reducing in innate immunity such as macrophage dysfunction, absent complement hemolytic activity, and reduced NK activity (46).

2. DNA-dependent protein kinase (Prkdc) – Commonly known as the severe combined immunodeficiency (SCID) mutation, this mutation results in inactive T cells and B cells (47). The *PRKDC* gene encodes a protein that resolves DNA strand breaks that occur during V(D)J recombination, resulting in significantly reduced numbers of T and B cells.
3. IL-2 receptor γ chain – Disruption of the IL-2R common γ chain (γc) results in a loss of NK, B and T cells and dendritic cell dysfunction since γc is required for multiple cytokine signals that are indispensible to immune cell development (IL-2, IL-4, IL-7, IL-15, etc) (45)

Additionally, exposing pups to 100cGy of gamma radiation 24-48 hours after birth ablates additional background immune cells and allows for optimal human HSC engraftment (48). Within 12 weeks of engraftment, the human $CD34^+$ stem cells development a fully populated human immune system within the mouse (49-51). The development and effectiveness of the immune cell repertoire is sufficient and have to elicit a T and B cell response (50).

The limitation of current humanized mice technologies such as the one described previously is that the B cell environment does not provide the appropriate cytokine signals in order to create numerous amounts of fully developed naïve B cells(52). This results in an immune repertoire that resembles a developing infant(53). In addition to further depleting the ability of the host to reject human cells, future progress in this field will focus on improving the cellular milieu of the mouse strains engrafted with human progenitors such that development, differentiation, and sustenance human lymphocyte population is better supported.

In vitro Discovery Technologies

Since its inception, hybridoma technology has been an essential method for discovering and expressing monoclonal antibodies and is still commonly used to in industry today. However, the process is very low throughput; it is not possible to screen large collections of antibody producing cells. In order to find the rare binding antibody from a pool of millions, major innovations were necessary. The collection of a large pool of antibody genes is called a library. Before the innovations enabling screening of large libraries could be established, essential molecular biology techniques would be required in order to create and express the libraries to be screened. Once the requisite tools were developed, they were used in many creative ways to build large antibody libraries and the systems used to discover the rare desirable clones.

The many technologies invented for screening and sorting large antibody libraries are the topic of the following subsections. The first technology, called phage display, was invented first and is the most popular method. After phage display technology, other screening platforms were developed that offered alternatives to the limitations of phage display screening. The common element each of screening platform possesses is the connection between genotype and phenotype(54). The type of link varies and each type link has unique advantages and disadvantages over the original phage technology. Each technology shares a common general methodology: enrichment of the library by applying selective pressure, amplification of the enriched population, and subjecting the enriched population to further rounds of selective pressure until the library is sufficiently enriched. The subsequent sections will focus on the many distinctive and creative ways to link genotype and phenotype and the screens or selections developed to discover antibodies from large libraries using the common strategy of applying iterative rounds of selective pressure.

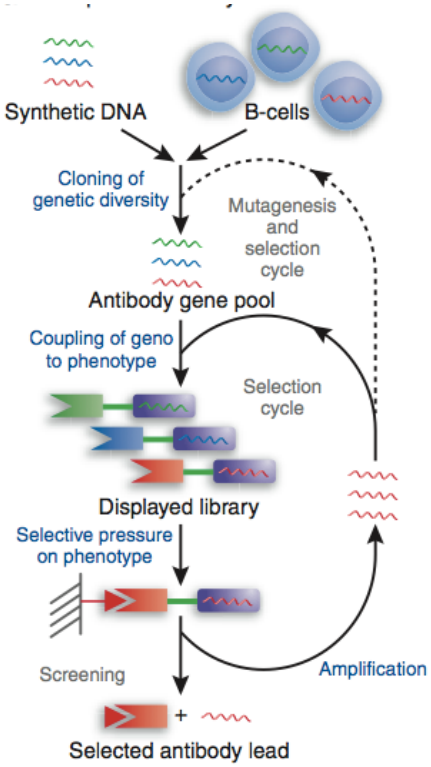

Figure 1.11: Outline of the common process of discovering antibodies from large libraries of antibody genes for immune or synthetic sources (54).

The processes and enabling technologies used to discover antibodies from large libraries can be broadly categorized as either screens or selections. Screens are processes that look at every individual within a library and keep only the desirable clones. Screens can be quite tedious and therefore very high throughput machines are employed to look at millions of clones quickly. Fluorescent Activated Cell Sorting (FACS) of cellular displayed antibodies is an example of a technique that utilizes a screening machine. Selections are methods that result in only desirable clones present when the selection is over, washing away unbound clones or selecting for a trait necessary for survival removes

the undesirable clones. An example of a selection the will be discussed in subsequent sections is phage panning.

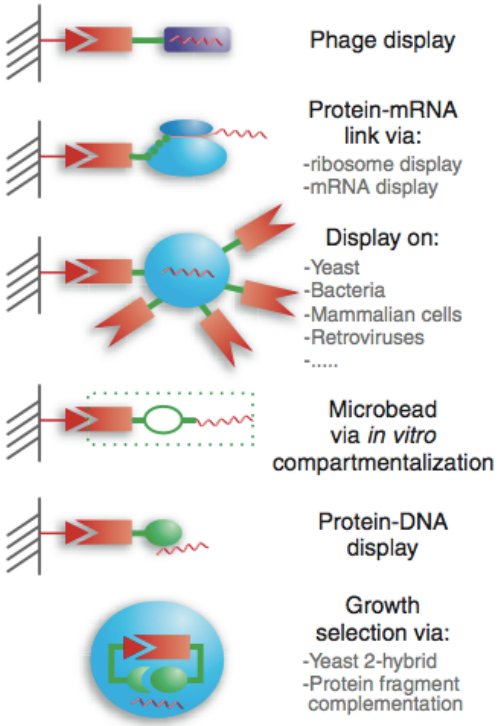

Figure 1.12: A condensed diagram depicting some of the many technologies linking genotype to phenotype (54).

Phage Display Technology

Once the requisite molecular cloning technologies became available, the first and most popular technique for discovering antibodies was established: phage display. In this screening technique antibody fragments are expressed on the surface of filamentous phage, a virus that infects only bacteria (55). This technology quickly became a routine method to isolate relevant antibodies from highly diverse libraries originating from a vast array of source genes (human, murine, naïve, immunized, or synthetic) (56-58).

Phage displaying antibodies on their surface are created in *E. Coli*. The most commonly used bacteriophage for phage panning are M13, fd and f1; the following explanation described M13 bacteriophage but other bacteriophages are highly similar (59). Each phage is made of two components: the genetic material and the protein coat. M13 carries a genome that encodes 11 genes; five of these genes encode coat proteins displayed in the figure below, while the rest of the genes encode proteins necessary for viral assembly and replication.

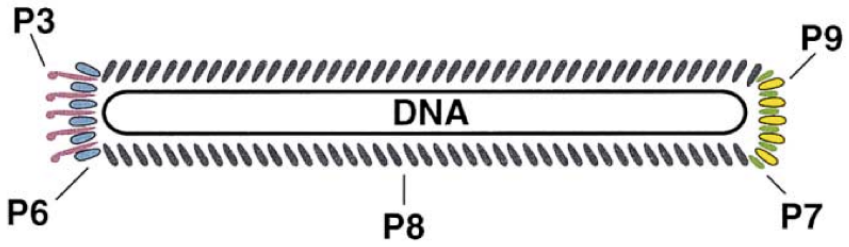

Figure 1.13: A representation of the proteins of a bacteriophage. Roman numerals and Arabic numerals are used interchangeably (60)

The bacteriophage lifecycle begins when P3 binds the F pilus on the surface of the bacterial cell (61). Upon binding, the single stranded DNA (ssDNA) inside the bacteriophage is translocated into the bacterial cytoplasm. Once inside the cytoplasm, invading phage ssDNA is replicated, double stranded, and used as a template to create many phage particles. Before the assembly of a new phage particle, the coat proteins are embedded into the surface of the *E. Coli* inner membrane. P9 and P7 are the first of the coat proteins to be assembled into a new budding viral particle, followed by many thousands of P8 proteins. P8 proteins are continuously incorporated into an elongating phage until the bacteriophage genome is fully packaged into the budding particle, thus a bigger genome would result in a longer bacteriophage. P3 and P6 proteins are the last two proteins to be incorporated into the growing phage particle; once completed the assembled

phage particle is released into the extracellular environment. The budding of M13 phage is not a lytic process, therefore the infected bacteria will continue to grow and produce.

Phage display technology manipulates the bacteriophage lifecycle in order to create hybrid phage particles that display antibodies on their surface and incorporate the antibody gene into the plasmid packaged within the particles. A plasmid that contains the necessary sequences for incorporation into a phage particle is called a phagemid. Hybrid phage can be produced a number of ways, the most common method fuses the antibody gene to an additional copy of the P3 phage protein. The antibody-P3 fusion is encoded by a phagemid that does not encode any of the other phage proteins but preferentially packages into new budding bacteriophage. In order to produce the other proteins required to create a new phage particle, an additional infection step is required with M13 helper phage. Helper phages have all the genetic information necessary to create a complete phage particle, however a mutation in the helper phage genome results in preferential packaging of the antibody containing phagemid instead of the helper phagemid into budding phage particles. Helper phage infection of an *E. coli* cell with an antibody-containing phagemid results in the production of hybrid phage with both an antibody displayed on the surface of the particle and the antibody gene incorporated within it; thus a link between antibody genotype-phenotype is established.

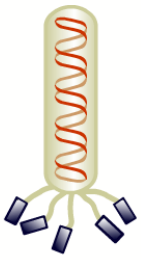

Figure 1.14: A phage with antibody gene inside the coat and antibody fragments fused to the surface coat proteins (blue). Adapted from http://www.dyax.com/

The ability to isolate the rare antibodies that bind an antigen of interest from a large library is accomplished by successive rounds of antibody selection, whereby the antibody population is repeatedly enriched for those that bind to an antigen of interest. For each round of selection, the phage-displayed-antibody library is incubated with an antigen immobilized to a surface (i.e. polystyrene or magnetic beads); unbound phage are washed away and bound phage are recovered for another round of screening, often this process is repeated for 3-8 rounds (62). Once successfully enriched, the library contains a large fraction of antibodies that bind the target antigen and relatively few clones (<100) need to be analyzed in order to isolate a binding antibody.

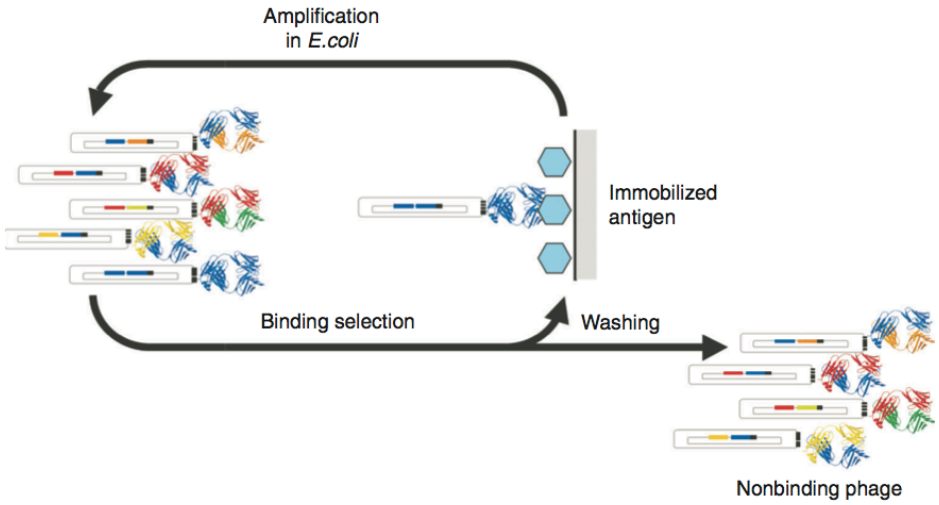

Figure 1.15: An outline of phage display with antibody fAbs are displayed on the surface of phage (63). Multiple rounds of this process enrich phage displaying an antibody that binds the immobilized antigen.

FACS and Surface Display Techniques

Surface display is a technique used to select for proteins within large libraries with a desired characteristic. The technique requires the protein to be anchored to the surface of a cell in order to provide a link between genotype and phenotype (64, 65). A fluorescent

probe is then incubated with the cells and a florescent activated cell sorter (FACS) measures the florescence of each cell and separates a populations based on user defined criteria. This technique can be applied to the surfaces of mammalian, yeast, and bacterial cells (66). After cells displaying protein that meets the user-defined criteria are selected, they are amplified and this process is repeated until the library is sufficiently enriched. This process is outlined in the figure below.

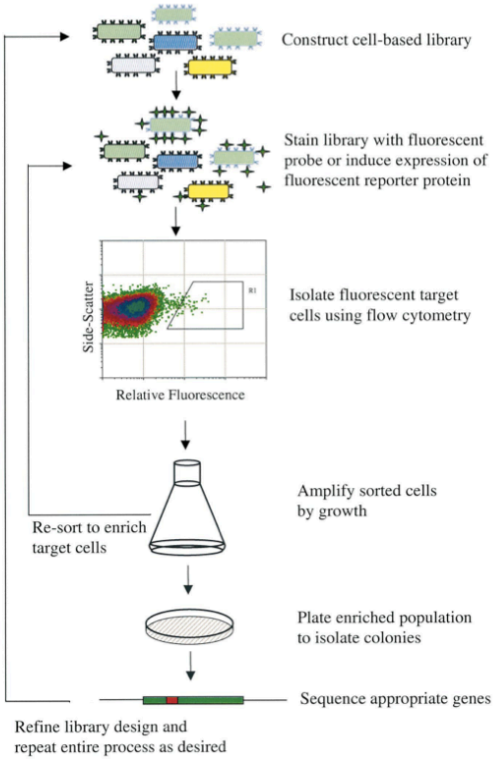

Figure 1.16: The FACS sorting process outline for surface display (64)

The advantage of this technology is that cells are much larger than phage and can be subjected to screening by fluorescence associated cell sorting (FACS). FACS combines high-throughput cell sorting with real-time quantitative analysis, allowing for library enrichment based on more than one criterion, such as antibody expression and affinity

(67). However, this technology is limited by the transformation efficiency of *E. coli* (thus limiting library size) and the sorting rate, both of which affect the ability for antibody screening.

The surface display and selection process outlined in the figure above can be applied to select for different characteristics of many different protein types (68). One interesting example involves using FACS selection and surface display in order to engineer a protease with novel proteolytic activity for a peptide conjugated to a fluorescent probe (69, 70). In this example, the native peptide carried many charged amino acids but no net charge, while the cleaved peptide was highly positively charged and thus adhered to the negatively charged *E. Coli* membrane. Cells displaying highly proteases cleave more fluorescent peptide and thus these cells become brighter than cells with less active proteases. Rounds of FACS sorting that select for the most fluorescent cells enriched for protease variants with the desired specificity.

When surface display is utilized for large antibody libraries, the antibody is anchored to the cell surface and the fluorescent probe is the antigen conjugated to a fluorescent molecule. Cells displaying antibodies that bind the antigen become fluorescent when they capture antigens conjugated to a florescent fluorophore; cells presenting antibodies with a stronger affinity for the fluorescent antigen capture more fluorescent molecules and thus become brighter than cells with weaker affinity. The FACS machine diverts the brighter cells in a separate collection tube order to create a population enriched for antigen binding activity.

FACS Technology

Flow cytometry is a high throughput technique that analyzes the size and fluorescence of individual particles at a very high rate (>10^9 events/hr for the fastest machines) (71). Heterogeneous mixtures of cells in suspension are passed single file across multiple laser points. The light signals from the particles are registered and correlated to qualities such a cell morphology, protein expression, gene expression, and cellular physiology. The user can select cells with desired qualities and the machine will deflect these cells into a separate container. This separation happens exceptionally fast, is highly accurate, and is not destructive to the cell. The applications to biotechnology are vast and essential for many modern practices (71, 72).

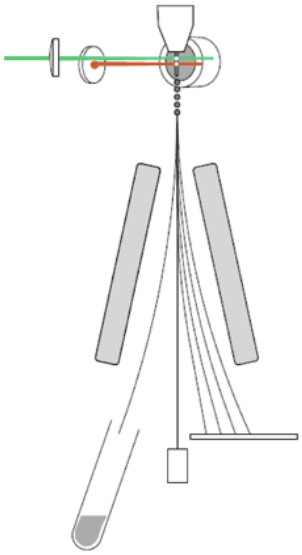

Figure 1.17: The essential process of the FACS machine (65). Cells in individual droplets are flown past multiple lasers (green and red) and their fluorescence is measured. Individual cells with a user-defined fluorescence are directed into a separate collection tube by the magnetic blocks (grey).

Bacterial Cell Antibody Surface Display

The first *E. coli* based surface display methods were developed in the late 1980s; these early techniques fused foreign epitopes to the endogenous outer membrane proteins (73). In the early technologies, antibodies displayed on the surface are anchored to the endogenous outer membrane protein A (OmpA). Using this technology, successful enrichment of a library for a specific antibody was demonstrated using outer membrane protein expression (74). This system displays antibodies on the surface of the cell by fusing an antibody scFv to a hybrid of endogenous *E. coli* outer membrane proteins Lpp and OmpA.

The utility of antibody surface display via the Lpp-OmpA system is limited to scFv format antibodies binding small molecule antigens. Successful studies demonstrating antibody binding to larger more complicated antigens have not been reported using this system in *E. Coli*; such complications are likely because the outer membrane of bacteria is full of LPS which carry a high negative charge that could restrict access for large globular protein antigens. Recently, other bacterial strains have been found to accommodate large protein-antibody interactions, but by the time these discoveries were published, the field had already evolved towards other solutions for bacterial surface display of antibodies (75).

The first evolution of bacteria display technology away from the outer membrane problems associated with the Lpp-OmpA system was to move antibody production from the outer surface to the bacterial periplasm. The periplasm is the space between the inner and outer membranes. Periplasmic Expression with Cell Sorting (PECS) is an "anchor-less" technology for discovering ligand-binding proteins where proteins are expressed in the periplasmic space then incubated the cells with fluorescently labeled ligand (76). Because the ligand-binding proteins are too large to diffuse through the outer membrane,

the cell acts as the link between genotype and phenotype. Usually only molecules smaller than 650Da can diffuse through the outer membrane of *E. coli*, however, this technology uses conditions such that up to 10kDa proteins can diffuse through the membrane. Cells expressing ligand-binding proteins in their periplasmic space bind and retain fluorescent ligand; the tighter the binding interaction the more ligand is retained in the periplasmic space and thus those cells become more fluorescent. Successive rounds of cell sorting for the brightest bacteria have been shown to enrich for ligand binding proteins. PECS has been employed to select for antibody scFvs that bind the small molecule digoxigenin conjugated to a 10kDa fluorophore (76).

PECS does not allow for selection of large protein-protein interactions because the technology relies on the diffusion of one ligand through the outer membrane of the bacterium. This problem was solved by anchored periplasmic expression (APEx): an *E. coli* based display technology that links the ligand-binding protein to the periplasmic face of the inner membrane of the cell. APEx is a particularly important advance because it allows for selection of scFv antibodies that bind large proteins. Periplasmic anchoring allows for outer membrane permeablization without the scFv antibody diffusing away and thus terminating the link between genotype and phenotype (77). Once the outer membrane has been permebleized, large proteins (up to 240kDa) can diffuse into the periplasmic space where they can be retained by scFv antibodies. Cell sorting can then be used once again to sort a library of scFvs for antigen binding.

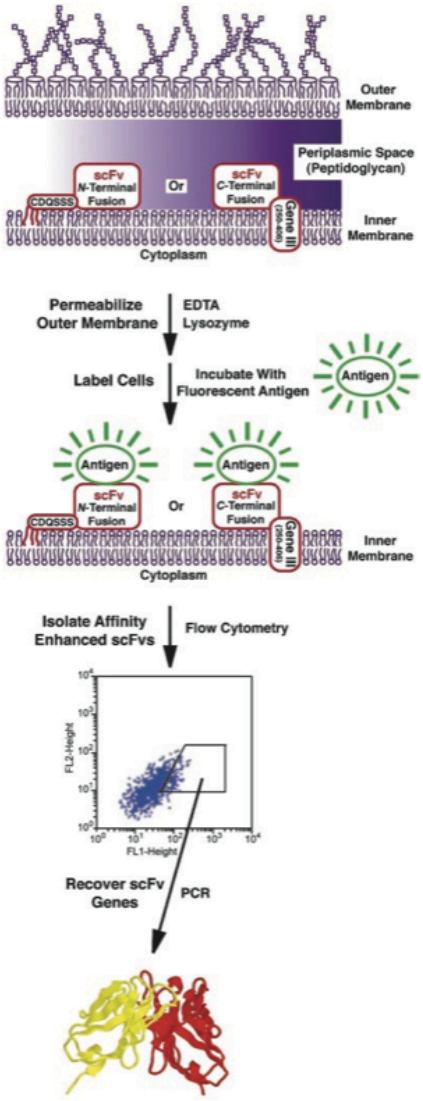

Figure 1.18: Method outline for the APEx system (77). After removal of the outer membrane and cell wall, cells are labeled with fluorescent antigen and sorted with a FACS machine in order to enrich for antigen binding cells.

Permeablization of the outer membrane is also called spheroplasting. Under typical spheroplasting conditions, a cell is treated the following way:

1. Cell pellets are resuspended in a hypertonic tris-sucrose solution
2. Outer membrane is solubilized by EDTA, which chelates the magnesium ions stabilizing the cellular outer membrane

3. Lysozyme is added to break the cell wall down
4. $MgCl_2$ is added to quench the EDTA and stabilize the outer membrane

The spheoplasting procedure kills the cells (lysozyme is commonly known as the antibacterial enzyme from hen egg white). Since the cells are not able to grow upon sorting, their genes are instead recovered by PCR, which generally increases the time between cell sorting cycles by at least one day.

All of the bacterial cell surface display technologies discussed thus far use scFv antibody fragments instead of full length IgGs. Monovalent scFv and Fab fragments are commonly used because they're relatively simple to express in *E. coli*, however they are not always ideal therapeutic formats because of their short serum half-life and low thermostability(78). Therefore, antibody scFvs isolated using phage display, surface display or other techniques are converted into the full-length IgG format for therapeutic efficacy testing. However, scFvs converted into full-length IgG format often show reduced or completely lost antigen-binding ability. Additionally, scFvs discovered using anchored display technologies, such as phage panning and APEx, are occasionally dependent on anchoring in order to fold correctly and bind antigen. *E*-clonal technology addresses these problems by producing full length IgG in the periplasmic space and "capturing" the full length IgGs via anchored ZZ protein, a protein A derivative that binds the Fc of IgG (67, 79). Capture instead of anchoring is an valuable improvement because the ZZ protein will only recognize correctly assembled Fc fragments, ensuring selection of properly folded IgG. Selection of full length antibody IgGs removes the necessity for format conversion in order to pursue studies that further characterize the effectiveness of the antibody(80). The scheme has been successfully used to discover antibodies that bind the protective antigen of the pathogen *Bacillus anthracis*. The format for the *E*-clonal system outlined in the figure below.

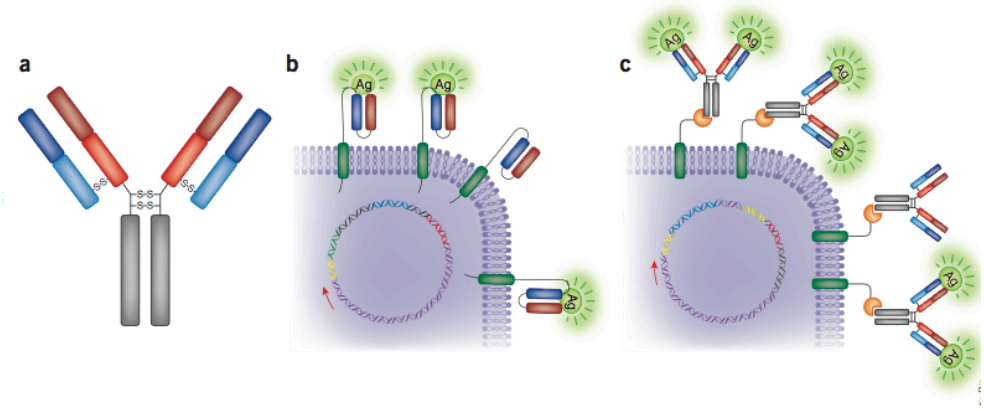

Figure 1.19: a comparison of APEx technology (b) and *E*-Clonal technology (c) with reference full-length antibody (a). APEx technology displays scFv antibody fragments anchored to the inner membrane of bacteria while *E*-Clonal technology attaches full length antibodies to the inner membrane that are captured by an anchored protein A domain. (80)

Yeast Display

Yeast display was first described in 1997 as an alternative screening technology to bacterial display(81). This technology display a library of antibody scFvs fused to the C-terminus of the yeast a-agglutinin on the surface of *Saccharomyces cerevisae*. An important feature of this technology is that it circumvents the unpredictable expression biases that occur when eukaryotic proteins are expressed in *E. coli*. Bacteria possess a limited ability to solubly express many disulfide bonded mammalian proteins, such as antibodies, because they lack the eukaryotic proteins that help chaperone and fold a protein. *S. cerevisae* have a surprisingly homologous folding and secretory machinery when compared to mammalian cells, therefore expressing mammalian cell proteins such as antibodies in *S. cerevisae* is an important improvement over bacterial expression. The ideal scenario for surface expression that would exclude any machinery biases and provide mammalian glycosylation profiles would be mammalian cell surface expression. These technologies have been developed, but slow culture times and inefficient cloning

techniques required to regulate expression levels and library size make these technologies limited in application (82, 83).

Display on the surface of *S. cerevisae* is accomplished by fusing the scFv to the two-subunit protein a-agglutinin. The Aga1p subunit anchors the protein fusion to the cell wall by β-glucan linkage; the subunit Aga2p is anchored to the Aga1p subunit through two disulfide bonds.

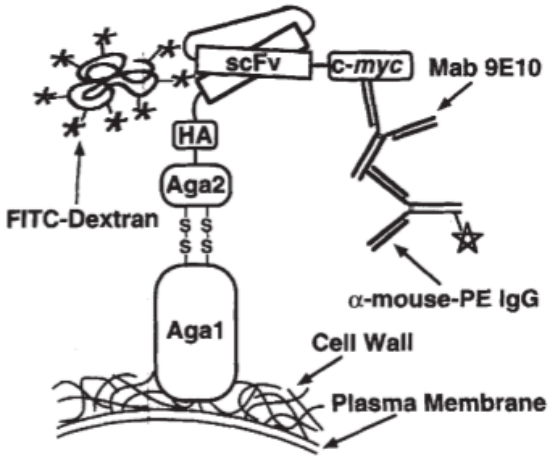

Figure 1.20: Yeast display antibody selection platform as depicted in the original 1997 paper from Dane Wittrup (81)

This usefulness of this technology was originally demonstrated to by affinity maturation of an scFv. Studies have further validated the usefulness of this technology by discovering ligand binding by non-immunoglobulin proteins, discovering an antibody with 48fM dissociation constant, and creating a non-immune human antibody library of over 10^9 variants (84-87).

Cell Free Technologies: Ribosome display

Ribosome display is an interesting and useful technology because it can select binders from a large library without using cells at any step(88). This is particularly important because the library size of cell based techniques is limited by the transformation efficiency of the cell (10^7-10^8 cells/ug DNA for yeast and 10^9-10^{10} cells/ug DNA for *E. coli*), while *in vitro* display technologies such as ribosome display can handle libraries with up to 10^{14} members(89). Another advantage of an entirely *in vitro* approach is that random mutations can be introduced after each round, as no library diversification step is required.

Ribosome display creates a link between genotype and phenotype during an *in vitro* translation by stabilizing a complex comprising the ribosome, mRNA, and the folded antibody(90). In order to create this link, the library of antibodies is genetically fused to a spacer sequence without a stop codon. When the space sequence is translated it is still attached to the tRNA and occupies the ribosome, thus allowing for an attachment of the antibody to its mRNA. Selections are performed on the complex in a similar way to phage panning. The recovered fraction is then subjected to reverse transcription and PCR in order to amplify the DNA of the recovered fraction for another round of screening. This process is outlined in the figure below.

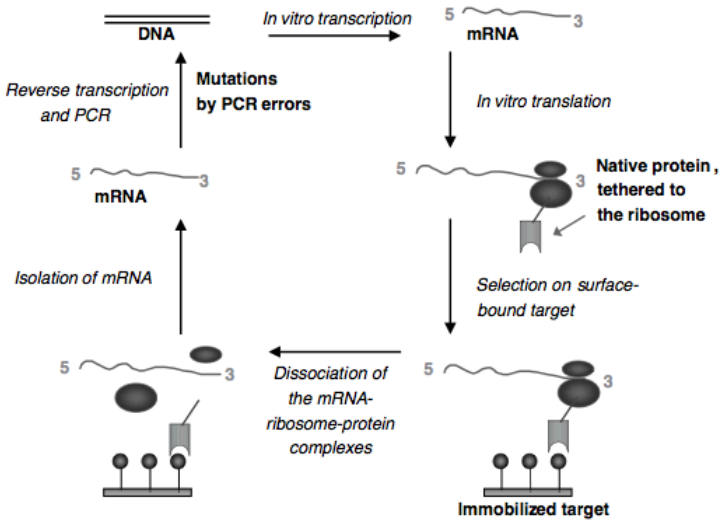

Figure 1.21: The principal of ribosome display (91).

Ribosome display has proven a useful addition to the repertoire of technologies and techniques available for antibody discovery. This technology has been used to discover picomolar affinity antibody from a fully synthetic native library (91).

Similar cell free display technologies have been utilized with similar results. For example, mRNA display technology achieves the covalent link between protein and mRNA through a puromycin adaptor (92).

Chapter 2

Antibody-Mediates Inhibition of Human C1S and the Classical Complement Pathway

Regulating the complement system with antibodies has recently become a high profile drug discovery strategy following the FDA approval of the first complement specific drug, eculizumab, and its further investigation in 39 clinical trials registered with the US National Institute of Health (93). This work expands on the strategy of systemic regulation of complement (as is the case with eclulizumab) by instead inhibiting a specific arm of complement, the classical complement pathway. In order to inhibit that the classical complement pathway, an antibody was developed that modulates the signaling subcomponent of the pathway initiating C1 complex, C1s. This work includes novel protocols and strategies used for discovery and characterization of antibody D, which binds and inhibits C1s protease activity. Through numerous cell and plate based assays, antibody D is shown to regulate classical complement when the pathway is selectively activated by surface bound immunoglobulin. It is further shown that affinity maturation of antibody D results in higher levels of complement inhibition at various antibody concentrations. In summary, this work marks the first example of an antibody that specifically regulates the classical complement pathway by targeting the C1s protease on the pathway initiating C1-complex.

INTRODUCTION

The complement pathway is critical for the proper clearance of pathogens and apoptotic or damaged cells. The complement system comprises three semi-independent pathways: classical, alternative and lectin-mediated (20). The classical complement reaction cascade is initiated when the C1-complex, the only dedicated component of this pathway, binds to immune complexes or to C-reactive protein (CRP) deposited on apoptotic or damaged cells. The C1 complex is composed of one C1q molecule containing six terminal C1q globular heads, two C1r protease molecules and two C1s molecules. Binding of C1q to immune complexes formed by IgM or by certain IgG subclasses (IgG1, IgG2, IgG3) results in the activation of C1r which in turn cleaves and activates C1s. Subsequently, the active form of C1s specifically cleaves the serum complement proteins C2 and C4 (21) forming, respectively, C2b and C4b which associate into the C2bC4b complex that constitutes the C3 pro-convertase. The subsequent steps in the reaction pathway ultimately result in opsonization, release of anaphylaxins (C3a, C5a) and in the deposition of the membrane attack complex that forms holes on the membrane of the target cell thus mediating cell killing.

Disregulation of classical complement activation is associated with numerous human diseases including rheumatoid arthritis, transplant rejection, ischemic reperfusion injury (94, 95) and neurological disorders (96). Therefore, pharmacological inhibition of complement is highly desirable and the subject of intensive research (97, 98). Eculizumab (trade name Soliris), which inhibits the processing of C5 and formation of the anaphylatoxin C5a, interferes with a reaction that is common to all three complement reaction cascades and has been approved for the treatment of the orphan disease, paroxysmal nocturnal hemoglobinuria (93). So far only one upstream inhibitor of the classical pathway, human plasma-derived C1 inhibitor (C1-inh, trade names CINRYZE

and Berinert for the blood isolated protein and Rhucin for the recombinant C1-inh) has been approved for treatment of hereditary angioedema (99) a disease caused by a genetic defect in endogenous C1 inh. C1-inh is a serpin with broad substrate specificity that irreversibly inactivates several serum proteases including C1r, C1s, MASP-1, MASP-2, thrombin and other enzymes of the fibrinolytic, clotting and kinin pathways (100).However, high doses of C1-inh are associated with increased incidence of thrombotic events (http://www.fda.gov). Further, supra-physiological levels of C1-inh downregulate all pathways of complement activation (101) and therefore they can negatively impact the beneficial effects of complement in pathogen and malignant cell elimination. It is of note that at over $300,000 per year per patient, both Eculizumab and CINRYZE are the two highest priced approved drugs (102).

Inhibitors of the classical pathway displaying improved selectivity relative to CINRYZE are highly desirable. Such high selectivity can be achieved using antibodies. In earlier studies, antibody fragments that block the globular heads of C1q and thus prevented the binding of immunoglobulins or CRP were reported (103, 104). However, when C1q-specific antibody fragments are present in an IgG, which is therapeutically more relevant because of its much longer serum persistence, the bivalency of the molecule results in complement activation instead of inhibition.

In this work we describe the engineering of human antibodies that inhibit the catalytic activity of C1s. Phage display of a very large synthetic library resulted in the isolation of an F_{AB}, (clone D), that bound to C1s with nanomolar affinity and an even higher apparent affinity when formatted as an IgG molecule, due to avidity effects. Further, affinity maturation of the scfv D resulted in a variant, D.35 with sub-nanomolar monovalent affinity. Importantly, D and D.35 were shown to inhibit C2 and C4 processing in serum and complement deposition and lysis of antibody-sensitized cells. However,

unlike C1-inh, they did not bind to other serum proteases. These findings suggest that C1s inhibitory antibodies may be of interest for the inhibition of the classical complement pathway in disease settings.

RESULTS

Antibody Isolation and Affinity Maturation

Our initial efforts to generate inhibitory antibodies to human C1s, either from animal immunization and V gene repertoire analysis (105) or by panning of scFv libraries from immunized animals led to the isolation of several clones which bound with high affinity (e.g. Reddy et al. 2010) but failed to inhibit the formation of C2b by activated C1s. Similarly, phage panning of a very large human synthetic $(F_{AB})_2$ library constructed by Sidhu and coworkers (106) resulted in the isolation of two antibodies (clones A and B) which displayed subnanomolar apparent affinity according to ELISAs (Table 2.2) however also failed to inhibit the cleavage of C2 *in vitro* (data not shown). C1s comprises, starting from the N-terminus, a CUB module (107), an epidermal growth factor (EGF)-like module, a second CUB domain, two complement control protein domains (CCP) and a C-terminal chymotrypsin-like serine protease (SP) domain (23). We reasoned that only antibodies to SP are likely to be inhibitory and that the use of intact C1s as the immunogen may be resulting in the generation of antibodies to one or more of the N-terminal, non-catalytic domains. To test this hypothesis, a truncated form of C1s lacking the two CUB domains as well as the EGF-like domain and comprising only of the two complement control domains and the protease active site (CCP_2-SP) was expressed in insect cells and purified to near homogeneity (Figure 2.14). We found that, as had been expected, antibodies A and B failed to bind to CCP_2-SP and therefore must recognize the N-terminus

of C1s. To isolate antibodies with inhibitory function, the synthetic library was subjected to two rounds of panning against activated CCP_2-SP followed by additional panning with full length protein in order to ensure that clones specific to the catalytic domain can also bind to it in the context of the intact protein (Figure 2.1). After a total of 5 rounds of panning, five distinct clones (Tables 2.1, Sequences C-G) were isolated of which 4 were specific for CCP_2-SP (Figure 2.2).

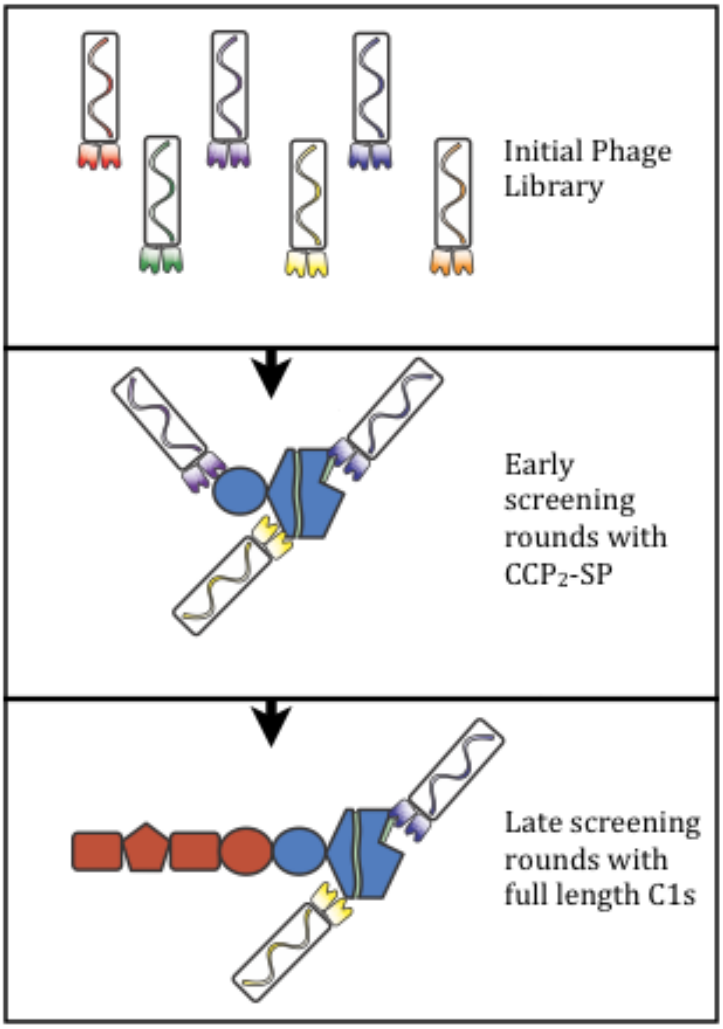

Figure 2.1: Phage panning overview used for discovery of antibodies reactive against the complement C1s serine protease. A human synthetic antibody phage library was enriched for binding to the C1s active domain (second CCP domain and serine protease domain: CCP_2-SP) by three rounds of panning against the CCP_2-SP antigen. A further three rounds of panning was performed against the entire C1s protease. Library is further described in Materials and Methods.

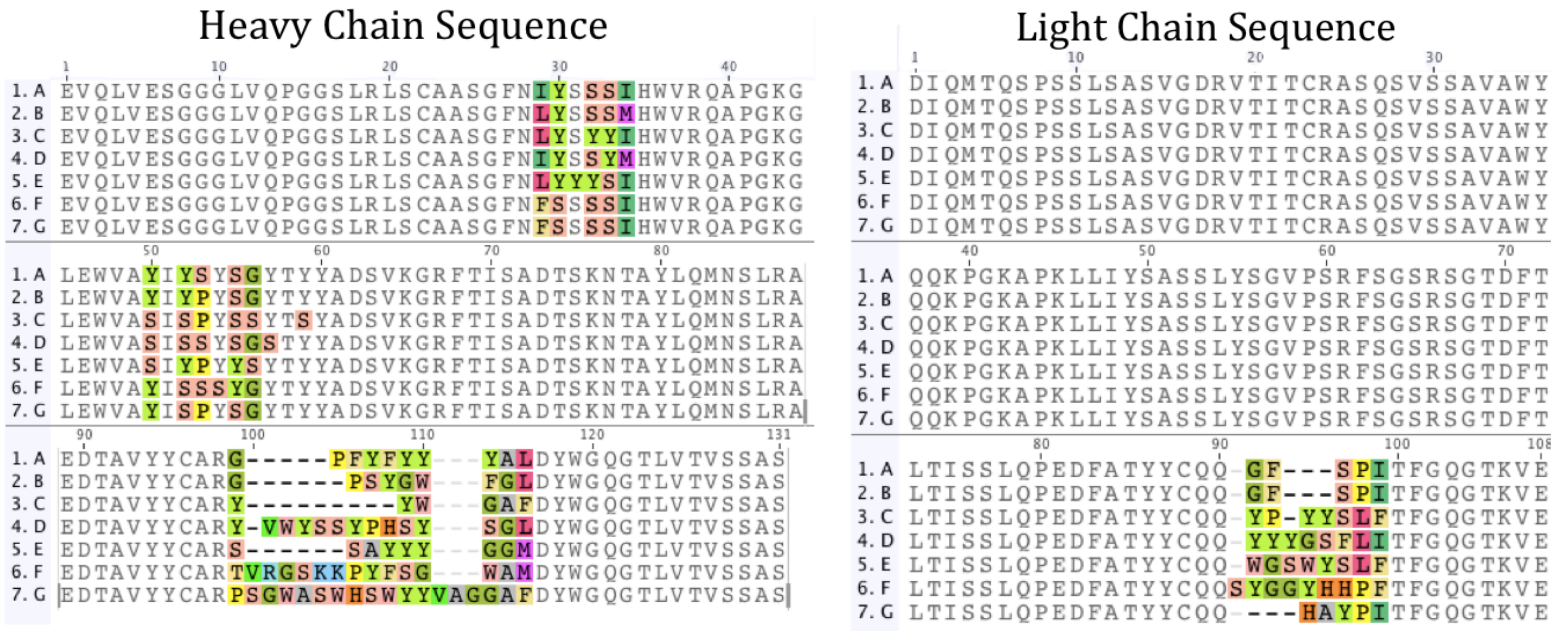

Table 2.1: Antibody Heavy and Light Chain Sequences. This table reports the heavy chain sequences of the variable region of each of the reported antibodies with color used to highlight differences.

Antibody	Kd	CDRH3 length
A	20pM	14
B	20pM	13
C	130pM	10
D	2nM	18
E	4nM	13
F	90nM	19
G	35nM	22

Table 2.2 Antibody Properties. Affinity and CDR-H3 length as determined by ELISA and IMGT/V-QUEST respectively

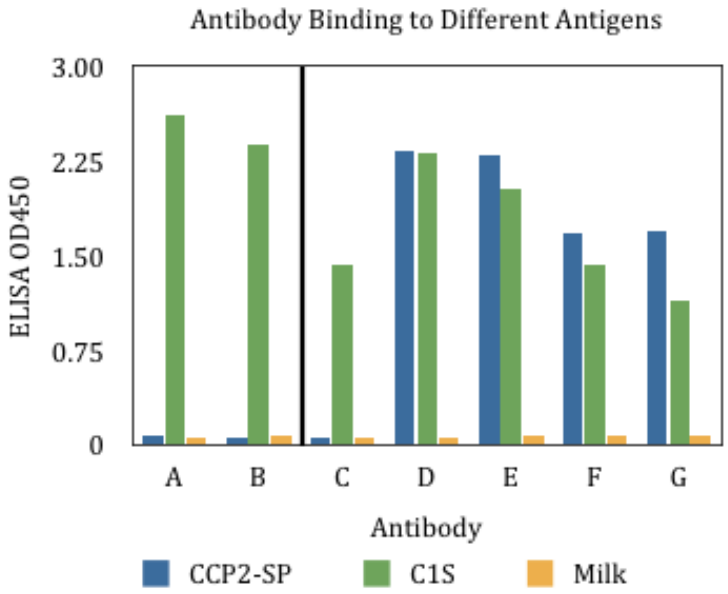

Figure 2.2: Evaluation of phage binding to C1s. CCP_2-SP, C1s, or milk were coated as capture antigens (400 nM) for ELISA testing of phage binding specificity described in Materials and Methods. Antibodies A-B (left of bar) were isolated from panning against C1s antigen only, whereas C-G were isolate with the scheme depicted in Figure 2.1. Nearly all antibodies isolated usin this scheme were reactive with both the CCP_2-SP truncated antigen and the full length C1s protein.

Antibody fragments were expressed as monomeric F_{AB}s and were tested for inhibition of the proteolytic activity of activated C1s was determined using a FRET peptide substrate (108). One $F_{AB,}$ (antibody D) exhibited significant inhibition in this assay and was characterized further (Figure 2.3).

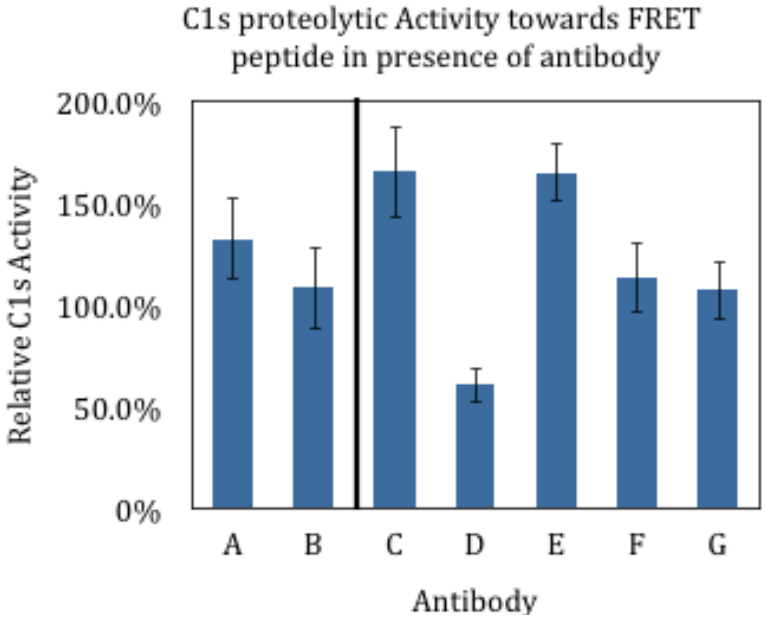

Figure 2.3: Fluorescence resonance energy transfer (FRET) peptide proteolysis assay. Relative activity of C1s in the presence of an excess of antibody. Activity was measured by comparing signal from cleaved FRET substrate in the presence of excess antibody compared to no antibody control. Among the several isolates (antibodies C-G), Antibody D displayed the greatest inhibition of C1s protease activity. Measurements were made in triplicate. Error bars depict standard deviation.

Antibody D contained an 18 aa long V_H CDR3 significantly longer than the mean CDR3 length for mice or humans (12 aa Human, 9 aa mouse (109)). The equilibrium dissociation constant to C1s was determined by kinetic equilibrium exclusion analysis using a KinExa instrument and was found to be 1.7 nM (95% confidence 1.1-2.2nM) in close agreement with the value determined by competition ELISA. Expression of this

antibody as a full length human IgG in HEK293T cells resulted in more potent inhibition of C2 by SDS-PAGE as expected from the higher avidity of the bivalent antibody format (Figure 2.4)

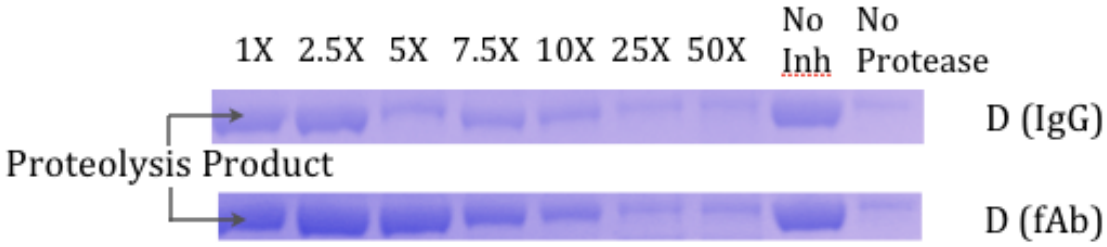

Figure 2.4: C2 inhibition assay with IgG and fAb format antibody D. Ratios of inhibitor antibody to C1s are shown above bands. Accumulation of proteolysis products from the C1s substrates C2 were detected by SDS-PAGE and indicated by the arrows drawn. Reactions were run in the presence of different molar ratios of Fab or IgG antibody to C1s (indicated above each column).

To improve the equilibrium binding affinity of antibody D for C1s, first it was expressed as scAb (a scFv fused to a human Ck which improves expression in *E.coli*). Purified D scAb was shown to display a binding affinity identical to that of the F_{AB} ELISA (Figure 2.5).

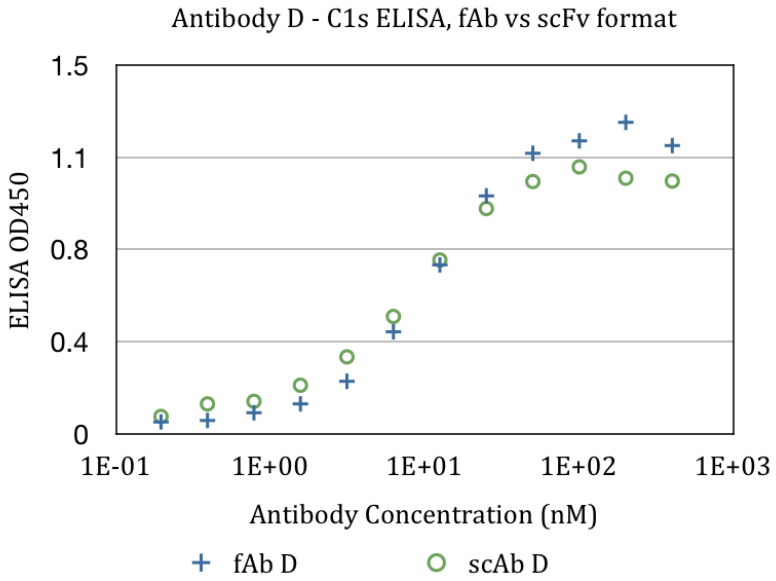

Figure 2.5: Affinity of D in various formats. Serial ELISA dilutions were performed using antibody D in scAb and fAb format. Dissociation constants were estimated by ELISA to be identical.

Then the corresponding scFv domain was subcloned into plasmid pAPEx1 for anchoring on the inner membrane of *E.coli* to enable flow cytometric screening by the anchored periplasmic display (APEx methodology, Figure 2.6). Following random mutagenesis by error prone PCR, a library of $>10^7$ transformants was subjected to 3 rounds of screening fluorescently labeled C1s at 20nM. Three rounds of screening resulted in a 3.5-fold increase in the mean cell fluorescence. 10 clones from the third round were grown individually and the scFv from one clone, D.35 displaying the highest fluorescence was expressed in soluble form (Figure 2.7). KinExa analysis indicated that the D.35 scFv displays a K_D= 0.95nM (95% confidence interval (1.1-0.76nM Table 2.3) a 2-fold improvement relative to the parental scFv (Table 2.3).

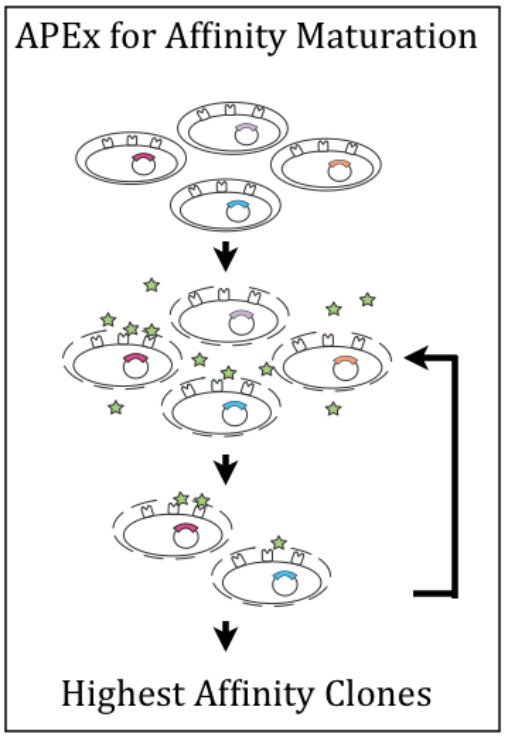

Figure 2.6: Anchored periplasmic expression (APEx) schematic for affinity maturation of anti-C1s antibodies. Mutagenic libraries of the parental anti-C1s antibody (hereafter referred to as Antibody D) were expressed as anchored scFvs on the inner membrane of *E. coli*. Bacteria were spheroplasted and incubated with fluorescent antigen before being subjected to FACS sorting. After multiple rounds of screening the highest affinity clones were selected for further analysis.

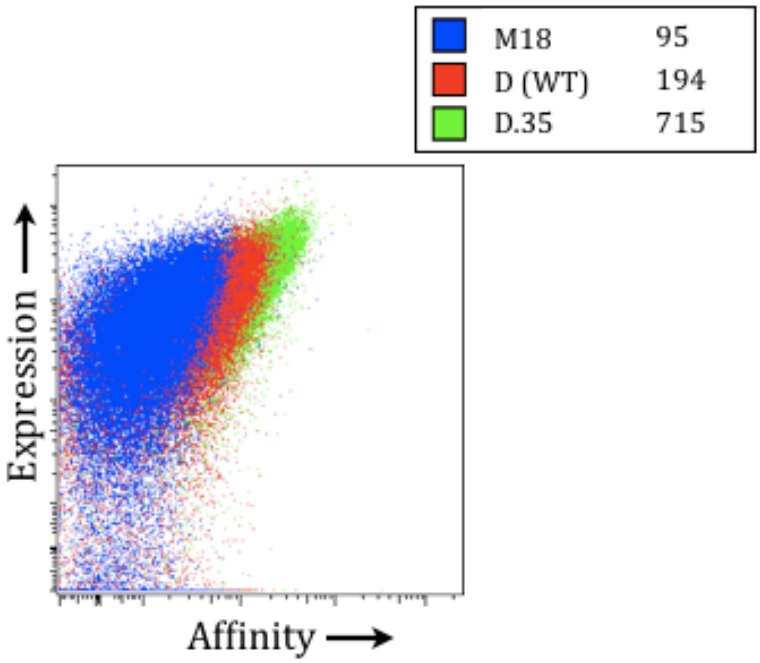

Figure 2.7: Fluorescence activated cell sorting (FACS) to select high-affinity variants of the D anti-C1s antibody. FACS signals of individual clones were compared by mean fluorescence intensity (MFI): FACS signals of negative control antibody M18 (blue), wild-type antibody D (red) and affinity matured antibody D.35 (green).

	K_D	95% High	95% low
D	1.7	2.2	1.3
D.35	0.95	1.1	0.76

Table 2.3: KinExa Analysis of Antibodies. Affinity of D and D.35 as determined by KinExA. 95% confidence intervals are also reported.

The light chain mutation S56P is the D.35 mutation (Table 2.1). Further attempts at affinity maturation though random mutagenesis failed to give any further K_D improvement in contrast to other studies that generated 35-270-fold improvements using similar techniques (77, 110, 111). Attempts at affinity maturation through phage panning

a library with diversified light chain CDRs constructed as described by Ge *et al*. were also unsuccessful (112). The inability to further affinity mature antibody D may be a consequence of the antibody-antigen interface created exclusively by the long (18 aa) CDRH3 loop. If this is indeed the case, future mutagenesis should focus on exclusively on CDRH3.

The affinity-enhanced antibody (D.35) was then investigated for increased C1s inhibition by direct detection of C1s mediated proteolysis substrates C2 and C4. C1s, antibody, and substrate were incubated for 50 minutes at different antibody/C1s ratios and immediately ran on an SDS-PAGE gel. D.35 was determined to better inhibit C1s activity by inspection of the intensity of the commassie bands from the proteolysis products (Figure 2.8).

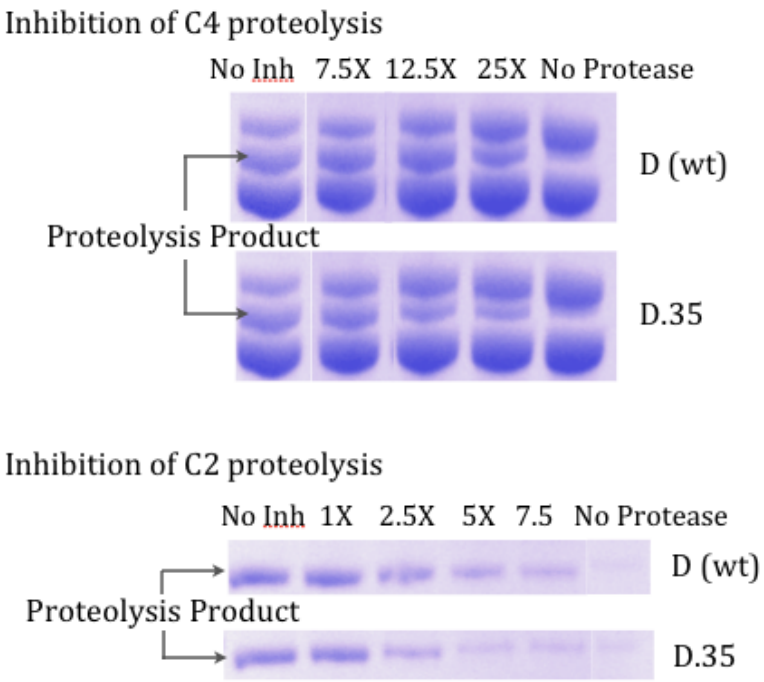

Figure 2.8: Antibody-mediated inhibition of C1s proteolytic activity. Accumulation of proteolysis products from the C1s substrates C2 and C4 were detected by SDS-PAGE and indicated by the arrows drawn. Reactions were run in the presence of different molar ratios of F_{AB} antibody to C1s (indicated above each column).

Inhibition of the classical complement activation pathway

Ramos is an EBV-negative, lymphoblastoid cell line derived from a B cell lymphoma that expresses high levels of the B cell surface marker CD20 (113). The anti-CD20 therapeutic antibody rituximab mediates the ablation of CD20 expressing cells to a large part via the activation of complement on target cells (114) and is used for the treatment of lymphomas and in autoimmunity. The ability of the D and D.35 F_{AB}s to

inhibit the activation of the classical complement pathway was evaluated by monitoring the deposition of the C3b convertase on the surface of antibody-sensitized target cells. Activation of C2 and C4 by C1s results in the formation of the C2bC4b complex, or C3 convertase, which promotes cleavage of the very abundant protein C3 into C3a and C3b. The latter is deposited on the cell surface where, together with C2bC4b forms the C5 convertase. The deposition of C3b on the surface of rituximab-sensitized cells in the presence or absence of inhibitors was determined by flow cytometry using a fluorescently labeled anti-C3b antibody in the presence of 40% of fresh human serum. The presence of 9uM C1 inh reduced C3b deposition detected by FACS signal approximately 25 %. The same level of inhibition of complement activation was observed with F_{AB} D while the affinity matured variant D.35 conferred approximately 2-fold greater inhibition resulting in approximately 46% reduction in C3b deposition relative to control cells incubated without inhibitor.

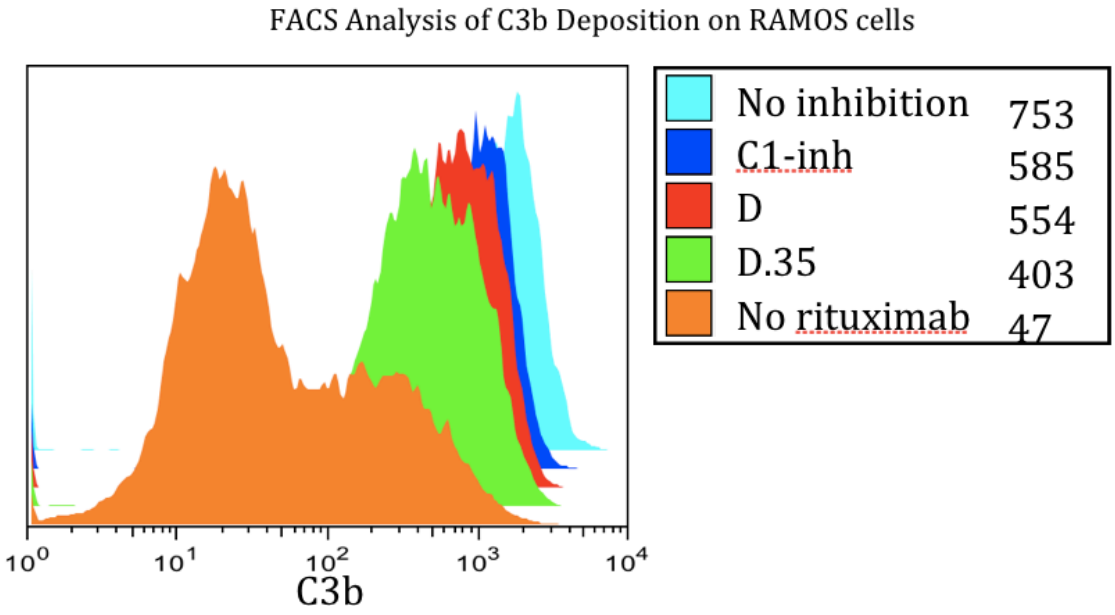

Figure 2.9: FACS detection of surface bound complement component C3b on rituximab sensitized Ramos cells in the presence of selected inhibitors. C3b is a complement protein near the middle of the complement cascade that binds surfaces undergoing complement attack. C3b levels were detected with fluorescent antibody after cells Ramos were incubated with 25uM inhibitor and 33% Normal Human Serum (NHS).

IgM is a potent activator of the classical complement pathway, and activation of the classical complement biochemical cascade occurs when C1 complex binds a single surface bound IgM molecule. The deposition of late complement component C5-9b was detected on IgM coated ELISA plates in the presence of 35% serum. Several dilutions of each inhibitor from 9.2uM to 1.8uM were incubated in 35% serum for 50 minutes. At 9.2uM, the maximum concentration of each inhibitor, D.35 and D exhibited 43% ± 6% and 56% ± 6% of the C5-9b signal from uninhibited serum deposition while 81% ± 1% C5-9b signal was detected on cell in the presence of exogenous C1-inh (figure 2.10).

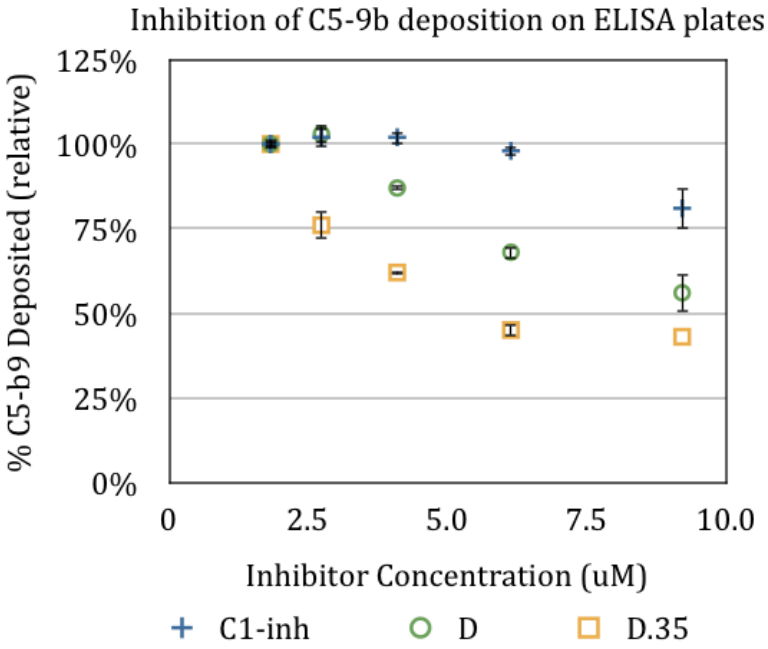

Figure 2.10: Inhibition of complement protein C5-9b deposition onto IgM coated ELISA plates. C5-b9 is a late complement protein deposited onto surfaces undergoing attack by complement. C5-b9 was detected with a C5-9b specific antibody conjugate after complement was activated in the presence of various concentrations of inhibitors between 9.2-1.8uM. OD_{405} values for wells were divided by uninhibited activated complement to give relative levels.

Finally, to monitor the inhibition of complement mediated lysis of Ramos cells sensitized with rituximab, we monitored the release of calcein. Cells were incubated with calcein-AM which readily diffuses into cells where active cellular esterases cleave the acetomethoxy group to generate highly florescent calcein that can no longer diffuse through cellular membranes. Thus the fluorescence in the culture supernatant is indicative of the extent of cell lysis. Cells were sensitized with 0.1ug/ml rituximab in 40% fresh human serum with several dilutions of each inhibitor from 9.2uM to 1.8uM for 25 minutes at which point the supernatant was collected and the fluorescence was

monitored. At the maximum concentration of each inhibitor, D.35 and D exhibited -3% ± 21% and 15% ± 9% of the calcein released from uninhibited serum deposition while 62% ± 5% calcein release was detected on cell in the presence of exogenous C1-inh (figure 2.11).

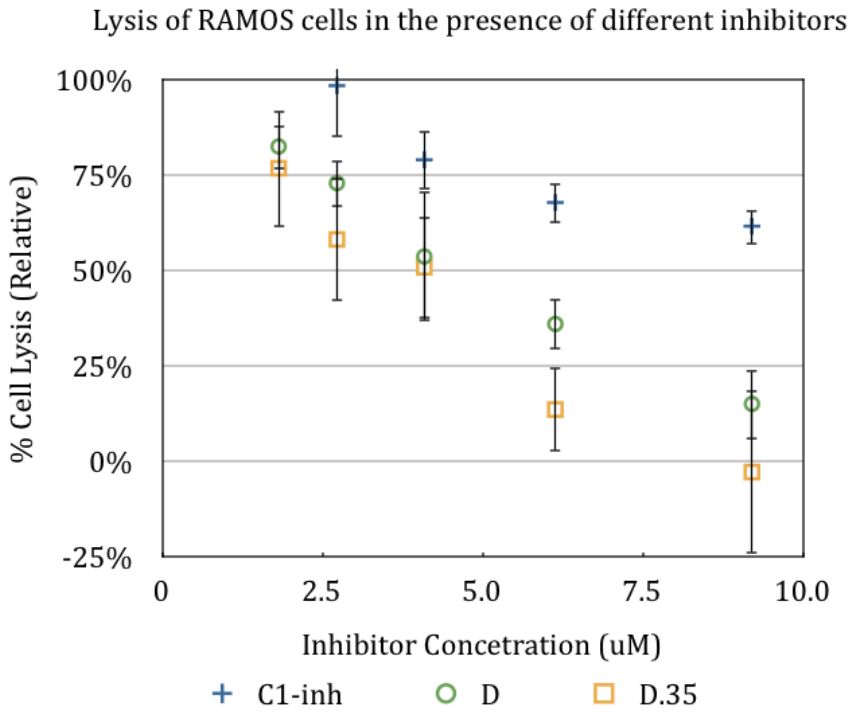

Figure 2.11: Lysis of Ramos cells in the presence of rituximab and selected inhibitors. Cell lysis by complement occurs when pores are formed on the cell surface by terminal membrane attack complexes. Cell lysis was measured by the complement-mediated release of fluorescent calcein in the presence of inhibitor concentrations between 9.2 and 1.8uM. Relative values were calculated by dividing the specific release of wells with inhibitor by the specific release from uninhibited wells.

Together these three assays demonstrate that an antibody that binds and inhibits the C1s protease on the C1 complex can regulate classical complement activity.

Furthermore, affinity maturation of Antibody D to D.35 improved classical complement regulation compared to the wild type Antibody D.

The Specificity of Antibody D

Specificity is an important aspect of any antibody. Many monoclonal antibodies fail to be therapeutically useful because they bind both the intended protein and an unintended homologous protein, resulting in unintended consequences. Because C1s is homologous to many proteins, including the other constitutive protease of the C1 complex, C1r, it is important to determine the specificity of D for its intended target C1s.

A capture ELISA was run in which C1s, C1r, or unactivated proenzyme C1s (pC1s) was adsorbed to the plates. Serial dilutions of antibody F_{AB} D were incubated with the adsorbed antigen followed by detection with anti-Flag-HRP. The results indicate that F_{AB} D is highly specific to C1s, the was no observed binding to homologous protein C1r and the affinity for pC1s was observed to be ten-fold less than the C1s signal.

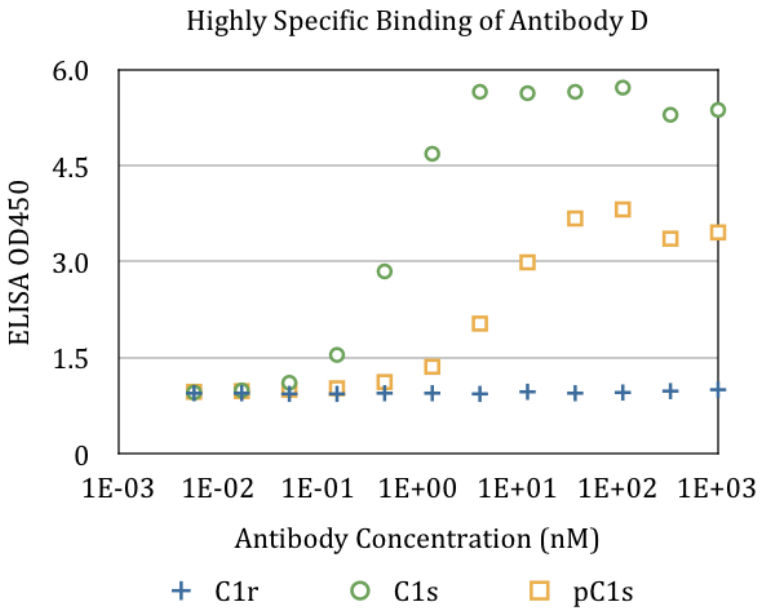

Figure 2.12: Antigen specificity of D. Serial ELISA dilutions were performed by incubating antibody D against different immobilized antigens. The specificity of D to the active form of C1s is indicated by the higher ELISA signal and lower antibody concentrations. Antibody D has no detectable binding to C1r. EC_{50} of F_{AB} D is estimated to be ~1nM for C1s and ~20nM for proenzyme C1s.

Discussion

Abnormal classical complement activation contributes to the pathogenesis of many diseases such as rheumatoid arthritis, transplant rejection, and even neurological disorders such as Alzheimer's disease (94-96); therefore therapeutic regulation of classical complement is a highly desirable goal. In this work, we developed an antibody that inhibits the signaling protease of the pathway-initiating C1 complex, C1s. Specificity is an extremely important quality of a potential therapeutic inhibitor, and poor specificity is often the reason many protease inhibitors are not very effective (115). In earlier

studies, C1s was targeted by a small peptidomimetic molecule and was shown to be effective in reducing classical complement activation in rabbits (116). However the short half life and low specificity of this molecule have prevented its further development as a drug candidate (97). In contrast human antibodies are ideal therapeutic molecules because of their high specificity, long half-live in circulation and low immunogenicity (117). In this work, phage display using a large diversity library was used to isolate antibody D, which binds activated C1s with nanomolar affinity and inhibits its proteolytic activity.

Antibody D preferentially binds the active C1s molecule compared to the inactivate form and exhibits 20 fold lower EC_{50} for active C1s than the proenzyme form (Supplemental figure 3a). It contains an unusually long CDR3 (18 aa) which may be important for binding to the active site cleft of C1s. Long CDR3s have been observed in several antibodies selected for their ability to inhibit hydrolytic enzymes (115, 118).

A variety of approaches were employed in an effort to isolate affinity improved variants of the D antibody fragment from libraries generated by either random mutagenesis or by DNA shuffling (112, 119) and screened by phage display in solution or alternatively by APEx. A variant displaying a modest 2-fold higher affinity could only be isolated by using three rounds of APEx; further mutagenesis and screening failed to yield any clones displaying further improvement in the equilibrium dissociation constant to C1s. This is in contrast to other studies from our lab and others where affinity improvements from the nM range to 10s of pM could be obtained by surface display for a variety of antibodies (77, 110, 111). The difficult in achieving a significant enhancement in the affinity of antibody D may be due to its unusually long CDR3. In this case, further affinity improvements may need introducing mutations within the CDRH3 loop in order further optimize the contact interface.

The F_{AB} D and its affinity improved variants D.35 F_{AB} were shown to inhibit the deposition of C3b on CD20 expressing cells sensitized with the anti-CD20 antibody rituximab and also the formation or the C5-9b complex at 9.2uM in 35% serum. Importantly, the D.35 F_{AB} was shown to protect CD20 expressing cells from complement-mediated lysis more effectively than the clinically used complement inhibitor C1-inh in the presence of 40% serum.

The C1 complex is a very attractive target for selective inhibition of the classical complement pathway because it is the only member of the classical pathway that does not participate in the other complement pathways. There are two possible strategies for blocking the activation of the C1 complex: (1) preventing the C1q heads from recognizing substrate and (2) blocking signaling upon complex activation by targeting the C1s protease. Inhibition of C1s rather than C1q offers several advantages: (1) there are three times fewer C1s molecules relative to C1q globular heads. (2) Because the inactive C1s zymogen is structurally different than the active C1s, it is possible to generate inhibitors that block only activated C1 complex (3) Inhibition of C1q by full length antibodies is undesirable because the avidity effect of bivalent IgG can actually induce C1q activation (103) . Full length IgG molecules are much more desirable as therapeutics because of their higher apparent affinity relative to monovalent antibody fragments (nearly 10-fold) (120) and their significantly increased serum half-life due to the interaction of the Fc region of the antibody with the neonatal Fc receptor (17).

Complement regulation is made difficult by high serum concentration of its constitutive proteins, requiring high concentrations of inhibitors to counteract them. C1 complex is normally found at 240nM in serum, therefore C1s and C1q are found at nearly 480nM and 1.440uM respectively (121). In this study, complement mediated lysis of RAMOS cells was greatly reduced when 9.2uM of antibody D.35 was used in 40%

serum, which implies that 23uM of antibody would be required for similar effectiveness in potential patients (100% serum). Therefore, further improvement of the antibody D.35 is required to in order to achieve effectiveness at therapeutically relevant concentrations (<1uM). Potential methods for improvement could come from continued affinity maturation or through bivalency, which generally results in a 10-fold apparent affinity improvement (120).

In order to address the exceedingly high concentration of F_{AB} D.35 inhibitor required for complement inhibition, a combination of antibody inhibitors might be a desirable approach to limit complement activation at lower antibody concentrations. It is therefore particularly relevant that we have shown novel methodologies for discovering and affinity maturing such antibodies that can be easily tailored to different classical complement proteins or an entirely different pathway. Alternative antibody-based classical complement inhibition strategies that prevent C1 complex signaling could be developed by slightly modifying our discovery scheme for development of antibodies that bind the proenzyme form of C1s or C1r.

MATERIALS AND METHODS

Insect Cell Expression and Activation of C1s active domain

The active domain of C1s (second CCP domain and the serine protease domain, CCP_2-SP, aa 358-688) was expressed with an N terminal 6X-His tag in Sf9 insect cells grown in Insect-XPRESS media (Lonza, 12-132A) with 5% FBS and 1x Penicillin-Streptomycin (Invitrogen, 15070-063) essentially as described earlier (122). After 6 days

of cell culture 500mL of supernatant was aspirated and dialyzed using SnakeSkin dialysis tubing (10kDa MWCO Thermo, product #68100) 2X for 12hrs in 4L PBS, pH 7.5.

Inactive CCP_2-SP was purified from dialyzed supernatant by Ni-NTA chromatography. Briefly, 25mM imidazole was added to 500mL of dialyzed supernatant then passed three times over 1ml of Ni-NTA slurry (Qiagen, 30250) in a polypropylene column (Thermo, 29922). The column was washed by passing 10ml of PBS, pH 7.5, 25mM imidazole before eluting twice with 0.5ml of PBS, pH 7.5, 250mM imidazole. 1ml of eluent was collected and dialyzed into 500 ml PBS, pH 7.5 with a Slide-A-Lyzer dialysis kit (Thermo, #66003). Purified inactive CCP_2-SP was quantified by measuring absorption at A_{280} in a NanoDrop instrument and adjusted to 6uM in PBS, pH 7.5 (ext coefficient 66975 $M^{-1}cm^{-1}$ (calculated via http://web.expasy.org/protparam/) protein M.W. 39kDa).

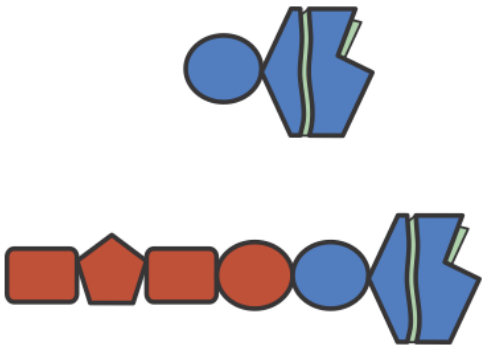

Figure 2.13: Visual comparison of the domain structure of CCP_2-SP vs C1s. Domain structure of CCP_2 from left (N terminal) to right: CCP_2, SP. Domain structure of C1s from left (N terminal) to right: CUB1, EGF, CUB2, CCP_1, CCP_2, SP. Glycosylation sites are found on the EGF domain and the CCP_2 domain.

Activated CCP_2-SP was generated by incubating 6 uM CCP_2-SP with 0.2uM C1r (Complement Tech, #A102) in PBS, pH 7.5 at 37°C for 2 hours. Activated CCP_2-SP was

then adjusted to 20% glycerol and stored at -80°C until needed. Activation of CCP_2-SP was confirmed by monitoring C2 proteolysis as follows: 1ul of 6uM activated CCP_2-SP was incubated with 3 ug of C2 (ComplementTech, A112) in 10ul PBS, pH 7.5 at 37°C for 30 min. The activated CCP_2-SP and C2 solution was then boiled in 1X non-reducing SDS-PAGE buffer (Invitrogen, LC2677) and analyzed by SDS-PAGE (NuSep, NG21-420) (Figure 2.14).

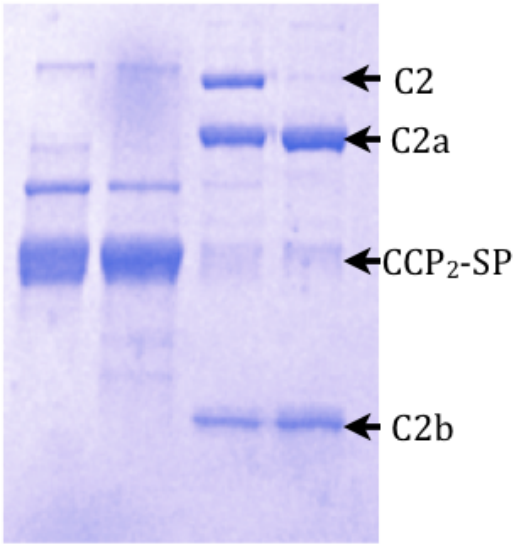

Figure 2.14: Insect cell expression of C1s active domain (CCP_2-SP)**.** Lanes 1-4 : (1) Inactive CCP_2-SP, (2) activated CCP_2-SP, (3) C2 incubated with unactivated CCP_2-SP, (4) C2 incubated with activated CCP_2-SP.

Phage Panning

The human synthetic $(F_{AB})_2$ phage library F constructed on the phagemid F_{AB}-C (106) was generously supplied by Sachdev Sidhu (59).

CDRH1		**29**	**30**	**31**	**32**	**33**	**34**															
	Template sequence	F	S	S	S	S	I															
	Allowed diversity	IL	YS	YS	YS	YS	IM															
CDRH2		**50**	**51**	**52**	**52a**	**53**	**54**	**55**	**56**	**57**	**58**											
	Template sequence	S	I	S	S	S	Y	G	Y	T	Y											
	Allowed diversity	YS	I	YS	PS	YS	YS	GS	YS	T	YS											
CDRH3		**94**	**95**	**96**	**97**	**98**	**99**	**100**	**100a**											**100x**	**100y**	101
	Template sequence	R	T	V	R	G	S	K	K	P	Y	F	S	G	W					A	M	D
	Allowed diversity	R	X	X	X	X	X	X	X	X	X	X	X	X	X	X	X	X	X	AG	FILM	D
				X = Y/S/G/A/F/W/H/P/V (1-17 aa)																		

		90	**91**	**92**	**93**	**94**				**95**	96
CDRL3	Template sequence	Q	S	S	Y	S				L	I
	Allowed diversity	Q	X	X	X	X	X	X	X	PL	FI
				X = Y/S/G/A/F/W/H/P/V (3-7 aa)							

Table 2.4: The sequence diversity allowed for LibF

Before panning, 3 ml activated CCP_2-SP or full length active C1s (ComplementTech, A103) at 4 ug/ml in PBS, pH 7.5 was adsorbed onto immunotubes (Nunc #444202) overnight by rotating at 4°C. Coated tubes were then blocked with PBS, pH 7.5 containing 2% milk for 2 hours at room temperature. Coated and blocked tubes were then incubated with 3 ml of PBS, pH 7.5, 2% milk with 10^{13} freshly purified phage at 25°C for 2 hours. Following incubation with phage, the immunotubes were washed 20X with PBS, pH 7.5, 00.05% Tween-20. Phage bound to the immunotubes after washing were eluted by incubation with 1mL of 100mM triethylamine (TEA) for 8 minutes followed by neutralization with 1ml of 1M Tris-base, pH 8.0. Recovered phages in elution-neutralization buffer were then used to infect 10mL of *E. coli* XL1-Blue cells at OD_{600} 0.3 for 1 hour in 2XYT media at 37°C. Infected cells were recovered by plating on 2XYT +200 ug/ml carbenicillin plates and the plates were incubated overnight at 37°C. Colonies recovered from plates were scraped and to prepare phage for the next round of panning according the standard protocol outlined by Fellouse and Sidhu (59). The first three rounds of panning were performed using immunotubes with activated

CCP_2-SP adsorbed to the surface followed by three rounds panning using immunotubes with full length C1s adsorbed to the surface.

After six rounds of panning, individual clones were evaluated by monoclonal phage ELISA. Colonies recovered from the final round of panning were grown in 150 ul 2XYT media with 200 ug/ml carbenicillin in 96-well culture plates (Cellstar 650 180) by shaking overnight at 37°C. 2 ul of overnight cultures were subcultured into 170 ul media and grown for another 90 minutes in the same media at 37°C. Cultures were then infected with M13K07 helper phage (NEB, #N0315S) by adding 10 ul of $5x10^{11}$ phage-per-ml and incubating without shaking at 37°C for 1.5 hours. 2 ul of 5 mg/ml kanamycin was added to infected cultures followed by overnight shaking at 37°C. Overnight infected cultures were centrifuged at 3500 x *g* for 10 min then the supernatant was collected by pipette. 100ul of supernatant was mixed with 100ul of PBS, pH7.5, 2% milk then 50ul of the solution was added to high binding ELISA plates (Costar 3590). ELISA plates were previously incubated with either 4ug/ml C1s or BSA control antigen and blocked with PBS, pH7.5, 2% milk. After incubation with supernatant-PBS milk mixture for 1 hour at 25°C, ELISA plates were washed 3X with PBS, pH 7.5, 0.2% Tween-20. Following washing, wells with bound phage were incubated with 50 ul of 1:5,000 anti-M13-HRP (GE 27-9421-01) in PBS, pH7.5, 2% milk for 30 minutes at 25°C. Plates were washed three more times, then bound phage was detected by adding 50ul Ultra TMB (Thermo, 34028) to the plates and incubating for 15 minutes. Following incubation with TMB, plates were quenched with 50ul of 1M H_2SO_4. Absorbance at 450nm was measured using a 96-well plate reader and positive clones were determined by 5-fold higher 450nM signal on antigen-coated plates compared to BSA-coated plates.

In order to enable soluble expression of F_{AB} antibodies, phagemids from positive clones were modified with mutagenic primers such that a 10X poly-His tag followed by

two stop codons was inserted between the CH1 heavy chain constant domain and the gene3 fusion. Soluble F_{AB} antibodies were generated from the mutated phagemid by overnight culture in 500 mL 2XYT at 37°C with 200uhg/ml carbenicillin followed by osmotic shock and Ni-NTA purification essentially as described (123).

Antibody ELISAs

ELISAs were performed in order to detect binding and estimate the EC_{50} values of F_{AB} or scFv antibody fragments binding to antigen. 50 ul of 4ug/ml antigen in PBS, pH 7.5 were adsorbed to 96 well high binding ELISA plates (Costar #3590) by incubating at 4°C overnight. Plates were blocked by incubating with 250 ul PBS, pH 7.5, 2% milk at 25°C for 2 hours. Serial dilutions of antibodies in PBS, pH 7.5, 2% milk were added to the plates in duplicate in order to cover a wide range of antibody concentrations then incubated on the plate for 1 hour at 25°C with mild shaking. After washing 3X with PBS, pH 7.5 0.2% Tween-20, plates were incubated with 1:5,000 anti-EC5 HRP (Bethyl Labs, #A190-102P) for 30 min at 25°C with mild shaking. Plates were washed three additional times then bound antibody fragments were detected by adding 50 ul Ultra TMB (Thermo, 34028) to the plates and incubation for 15 minutes. The TMB solution was quenched with 50ul of 1M H_2SO_4 and absorbance was measured at 450nm using a 96-well plate reader. EC_{50} values were estimated to be the 450 nm reading corresponding to half the maximum 450nm absorbance detected at saturating concentration of antibody fragment.

Affinity Maturation of antibody D

The variable heavy and light chains of antibody D were subcloned into the scFv format with the light chain at the N terminus followed by a $(Gly_4Ser)_4$ linker and the heavy chain. Soluble expression of antibody fragments and ELISA assays to measure EC_{50}s towardsC1s were performed essentially as described above. The dissociation constant of scFv format antibody D was estimated to be the same as the F_{AB} format antibody. The scFv gene of antibody D was then subjected to random mutagenesis by error prone PCR (119). Following ligation into pAPEx1 (77) and transformation into *E.coli* Jude-1 cells (67), $>10^7$ transformants were obtained on selective plates. Sequencing of 10 randomly selected clones revealed a mutation rate of ~2.5 nucleotide substitutions per gene (0.3% bp nucleotide error rate). Overnight cultures of transformants were induced by 1/100 subculture into terrific broth (TB) (BD, #243810) with 2% glucose and 1mM IPTG (EMD Millipore, #420322) for 4 hours and 37°C. Induced cultures were spheroplasted and incubated with 1/2000 anti-flag PE (Prozyme PJ315) and 20nM of C1s conjugated to Alexa Fluor647 (Invitrogen #A-20173) then subjected to three rounds of APEx sorting using a BD FACS Aria as previously described (111).

Individual clones encoding scFv genes isolated from the third round of sorting were grown as above; the cells were, spheroplasted, and analyzed for expression and antigen binding via FACS. Clones exhibiting a higher Alexa Flour647 signal (indicative of improved binding to C1s conjugated Alexa Fluor 647) were selected for further analysis via ELISA and KinExA.

Determination of Dissociation Constant via KinExA

Kinetic exclusion assays were performed with a KinExA 3200 instrument. C1s was adsorbed onto Poly(methyl methacrylate) (PMMA) particles (Sapidyne #440176) by mixing 1 vial of particles with 10ug of C1s in 1ml of PBS, pH 7.5 and rotating for 2 hr at room temperature. Beads were then blocked by incubation with 10mg/ml BSA and rotated for another 2 hours at room temperature. A range of C1s concentrations from 500 nM to 0.03 nM were incubated in PBS, pH 7.5, 1mg/ml BSA, 0.02% sodium azide with F_{AB} antibody at either 1 nM or 0.1 nM for 24 hours at room temperature. The solution was then applied to the beads using the KinExA 3200 autosampler followed by detection of free antibody was detected using 0.5ug/ml anti-human IgG Dylite 649 (Jackson Immuno #109-495-088). Data were collected in duplicate and equilibrium dissociation constants were determined using the KinExA n-Curve analysis software.

C1s activity inhibition assays

Purified soluble F_{AB} proteins expressed from pFAB-S (pMAZ360-IgG vector with 10XHis-2Xstop introduced between CH1 and CH2) were incubated in triplicate at 500nM with 35nM C1s and 1uM synthetic C1s FRET peptide substrate (Anaspec 61318) at 37°C with shaking in flat bottom optical 96 well plates (Thermo Fisher 265301). After 10 minutes, the fluorescence intensity was determined using an excitation wavelength of 320 nm and an emission wavelength of 420 nm. Relative C1s activity was calculated by dividing the emission value from test wells by the emission value from wells without antibody (only C1s and substrate). Antibodies exhibiting inhibition of C1s generated relative C1s values less than 1.

The inhibition of C2 or C4 (ComplementTech A112, A105c) processing by activated C1s was determined by SDS-PAGE as follows: 10nM active C1s

(ComplementTech, A103) was preincubated with various stoichiometric ratios of F_{AB} in PBS, pH 7.5 at 25°C for 5 minutes. Subsequently, either 2.5ug of purified C2 or 8ug of C4 were added then incubated for an additional 2 hours at 37°C. Following incubation, samples were boiled for 5 minutes in 3x-SDS-PAGE buffer; proteins were resolved on a 4-20% acrylamide gel (NuSep, #NG21-420) following the manufacturer's instructions. Gels were then stained with gel-code blue (Thermo Scientific #24592).

Treatment of Human Serum

Blood (~15ml) was collected from human volunteers under IRB protocol #IRB000007066 approved by the Scott & White Hospital and by the University of Texas at Austin IRB committees. The blood was allowed to clot for 30 minutes at room temperature, the centrifuged for 10 min at 1000 x *g*, and the supernatant (serum) was collected into fresh vials. Sera were combined from 5 volunteers at a time and stored until use at 4 °C but for no more than one week.

Complement Deposition and C5-b9 detection on IgM coated plates

To monitor C5b-9 deposition, high binding ELISA plates (Corning, 3590) were prepared by adsorbing 50ul of 10ug/ml purified human IgM (Jackson ImmunoResearch, 009-000-012) in PBS, pH7.5 at 4°C overnight then blocking with 250ul PBS, pH 7.5, .05% gelatin for 2 hours at room temperature. Samples were prepared by diluting 200ul of fresh human serum with 80ul of F_{AB}, C1-inh (ComplementTech, A140) or PBS control in Dulbecco's PBS (dPBS), pH 7.5 (Thermo, SH30028.02) and 280ul gelatin veronal buffer (GVB++, Complement Tech, B102). 50ul of each sample was added in triplicate to plates then incubated for 50 min at 37°C with mild shaking. Plates were washed 3X

with wash solution included in the COMPL CP 310 kit (Euro-Diagnostica) followed by incubation with 50ul of alkaline phosphatase labeled antibody (also included in COMPL CP 310 kit). An additional 3X washes were performed with included wash buffer, then C5-b9 was detected according to manufacturers instructions (Euro-Diagnostica, COMPL CP 310).

Relative percent of classical complement mediated C5-b9 deposition was determined by dividing the absorbance at 405nm from test wells by the absorbance from wells with serum without inhibitor.

Complement deposition and lysis of Rituximab sensitized cells.

C3b deposition on Ramos cells, a Burkit cell lymphoma line, sensitized with the anti-CD20 antibody Rituximab was evaluated by flow cytometry as follows: cells were grown according to the ATCC protocol, centrifuged at 500 x *g* for 10 minutes at room temperature, then resuspended to approximately $5x10^5$ cells per 100 ul in Dulbecco's PBS, pH 7.5 (dPBS, Thermo, SH30028.02) with .1% BSA (dPBSB). Cells were then incubated with 10 ug of Rituximab (generously provided by Dean Lee, MD Anderson Cancer Center) per 10^6 cells for 1 hr at 4°C while rotating. Antibody sensitized cells were centrifuged at 500 x *g* for 10 minutes at room temperature, washed by resuspending with dPBSB and then in dPBS 2X. Following washing and centrifugation, aliquots of 10^5 cells were resuspended in a mixture of 40 ul of NHS, 55 ul of gelatin veronal buffer, and 15 ul F_{AB} antibody or C1-inh in dPBS resulting in a final concentration of 25 uM, and then incubated for 45min at 37°C while rotating. After incubation, cells were washed by centrifugation at 500 x *g* for 10 minutes and resuspended in dPBS and then in dPBSB 2X. The deposition of C3c on the surface of the cells was determined with 100ul of 1/20

FITC labeled C3c antibody (Abcam, ab4212) in dPBSB for 30min at 4°C. Cells were washed again with dPBSB and FITC signal was analyzed using BD FACS-Aria flow cytometer.

Complement mediated lysis of Ramos cells in the presence of either F_{AB} or C1-inh was determined by calcein release upon lysis. Cells were loaded with Calcein by incubating $5x10^5$ Ramos cells in 1 ml PBS, pH 7.5 with 4uM calcein-AM (Sigma, C1359) at 37°C for 45 minutes. The cells were then washed 2X with PBS, pH 7.5 by centrifugation at 500 x *g* for 10 min followed by resuspension in 1 ml PBS, pH 7.5. Aliquots of 10^5 cells were resuspended in a mixture of 120 ul NHS, 120 ul gelatin veronal buffer, and 60 ul of a solution of F_{AB} antibody or C1-inh in PBS, pH 7.5 resulting in final concentrations between 9.2 and 1.8 uM. 100 ul aliquots of cell suspension were transferred to 96 well round bottom plates (Costar, 3799), supplemented with 5 ul of 2 mg/ml Rituximab in PBS, pH 7.5 and incubated for 25 minutes at 37°C with mild shaking. Following incubation, cells were pelleted at 1000 x *g* for 5 minutes then 50 ul of supernatant was transferred to flat bottom optical plates (Thermo Fisher #265301) containing 50ul of PBS, pH 7.5. Calcein release was measured by reading the fluorescence of supernatant using a microplate reader with 485nm excitation and 535nm emission.

The percent of specific calcein release was determined by the following equation:

$$\%\ Specific\ Release = \frac{(Test\ release) - (Spontaneous\ Release)}{(Maximum\ Release) - (Spontaneous\ Release)}$$

Incubating cells in serum/inhibitor solution without rituximab determined spontaneous release. Maximum release was estimated by incubating cells in 2% Triton

X-100 (Sigma T8787). Relative cell lysis was determined by dividing the specific percent release from test wells by the percent specific release from wells with Rituximab antibody and no inhibitor.

Chapter 3

Characterizing Humanized Mice

INTRODUCTION

Humanized mice are generated through the engraftment of human $CD34^+$ hematopoietic stem cells into immune-deficient mice. Once engrafted, the human stem cells home in to the bone marrow where they divide and differentiate into human cells of the myeloid and lymphoid lineages (45). Humanized mice are rather difficult to use because engraftment requires expert training and the level of lymphoid and myeloid cells formed post engraftment is quite variable. Nevertheless, they are highly utilized in biomedical research because these mice provide an unparalleled opportunity to study human cells and biological processes *in vivo* (124). In particular, humanized mice provide an important preclinical model that enables the investigation of human-specific infectious diseases in order to better understand the mechanism of disease pathogenesis and evaluate therapeutics (44). One of the predominant applications of humanized mice has been the study of diseases such as HIV, Dengue virus and Epstein-Barr virus (EBV) infections (125-127). Detailed understanding of the B cell repertoire produced in these mice has significant relevance to human immunology and the study of human-specific diseases in addition to being a potential source of fully human antibodies.

Since initial development of humanized mice, continued improvements in the mouse strains used for engraftment have resulted in the systematic reduction of mouse immune cells thereby allowing improved development of human lymphocyte populations in the animal (45). Reduction in background immune cell production in the host is

important to prevent competition with, or rejection, of engrafted human $CD34^+$ cells. One of the most popular mouse strains developed to date, and the one used in this research, is termed NSG (NOD.Cg-Prkdc^{scid} Il2rg$^{tm1Wjl/SzJ}$ mice). The *PRKDC* gene encodes a protein that resolves DNA strand breaks that occur during V(D)J recombination, resulting in significantly reduced numbers of T and B cells (47). Disruption of the IL-2R common γ chain (γc) results in a loss of NK, B and T cells and dendritic cell dysfunction since γc is required for multiple cytokine signals that are indispensible to immune cell development (IL-2, IL-4, IL-7, IL-15, etc) (45) .12 weeks after engraftment of human $CD34^+$ stem cells into NSG mice, the lymphocyte progenitors develop into the full population of human immune cells (49-51). However, immune cell development from mouse to mouse is heterogeneous and dependent on the quality of $CD34^+$ stem cells and the skill in which they are engrafted. Therefore, we seek to characterize the human immune cells that develop in NSG mice and the immune response they generate following immunization.

We analyzed the B and T lymphocyte subpopulations that develop either 6 or 12 weeks post engraftment in NSG mice engrafted with human $CD34^+$ HSC cells. Repeated immunizations with a highly immunogenic antigen failed to yield significant antigen-specific IgM or IgG antibodies in these mice. Mice were characterized with florescent antibodies that bind cell surface markers that indicate cell type (see Figure 3.4 and Table 3.1). Important cell types determined in this study were $CD3^+$ T cells including the $CD4^+$ helper and $CD8^+$ cytotoxic T cell subtypes, as well as $CD20^+$ B cells including the $CD27^+$ memory B cell and $CD138^+$ plasma cell subtypes. Based on these results, we conclude that NSG humanized mice are suitable for studying naïve mature B cells and T cells, however they are not suitable for the analysis of activated B-cell subsets in response to immunization.

RESULTS

FACS Scans for Characterization of Humanized Mice Lymphocytes

10 Non-obese diabetic-*scid-IL2Rγ*^{null} (NOD-*scid- IL2Rγ*^{null}) mice were engrafted with umbilical cord blood (UCB) CD34^{+} hematopoietic progenitors and analyzed at either 6 weeks or 12 weeks post engraftment. Spleen, bone marrow and thymus (when present) were collected, labeled with flourochrome conjugated antibodies as discussed later, and analyzed using flow cytometry (FACS Aria). Peripheral blood (PB) and lymph nodes (LN) lymphocytes were too few to analyze via flow cytometry.

Human lymphocytes express the surface protein CD45^{+} cells. Cells labeled with an anti-CD45 antibody, and therefore correspond to total human lymphocytes in the mouse, were quantified via FACS from the spleen for both the 6 and 12-week-old mice populations. The frequency of CD45^{+} cells varied among the 6 and 12-week post engraftment mice. CD45^{+} human lymphocyte frequencies from the total spleen population were 10% ± 7% in six-week-old mice and 34% ± 37% (between 1-90%) in the same population in twelve-week-old mice. From each spleen, CD3^{+} T lymphocytes comprised <2% of CD45^{+} cells in the spleens of mice analyzed six-weeks-post engraftment mice and 32% ± 22% in mice analyzed twelve-weeks post engraftment, suggesting maturation of T-cells largely occurs after 6-weeks following engraftment. In contrast, the fraction of CD20^{+} B cells within each spleen was surprisingly consistent: CD20^{+} B cells comprised approximately 50% ± 10% of CD45^{+} human lymphocytes in the spleen from both 6 and 12-week-old mice.

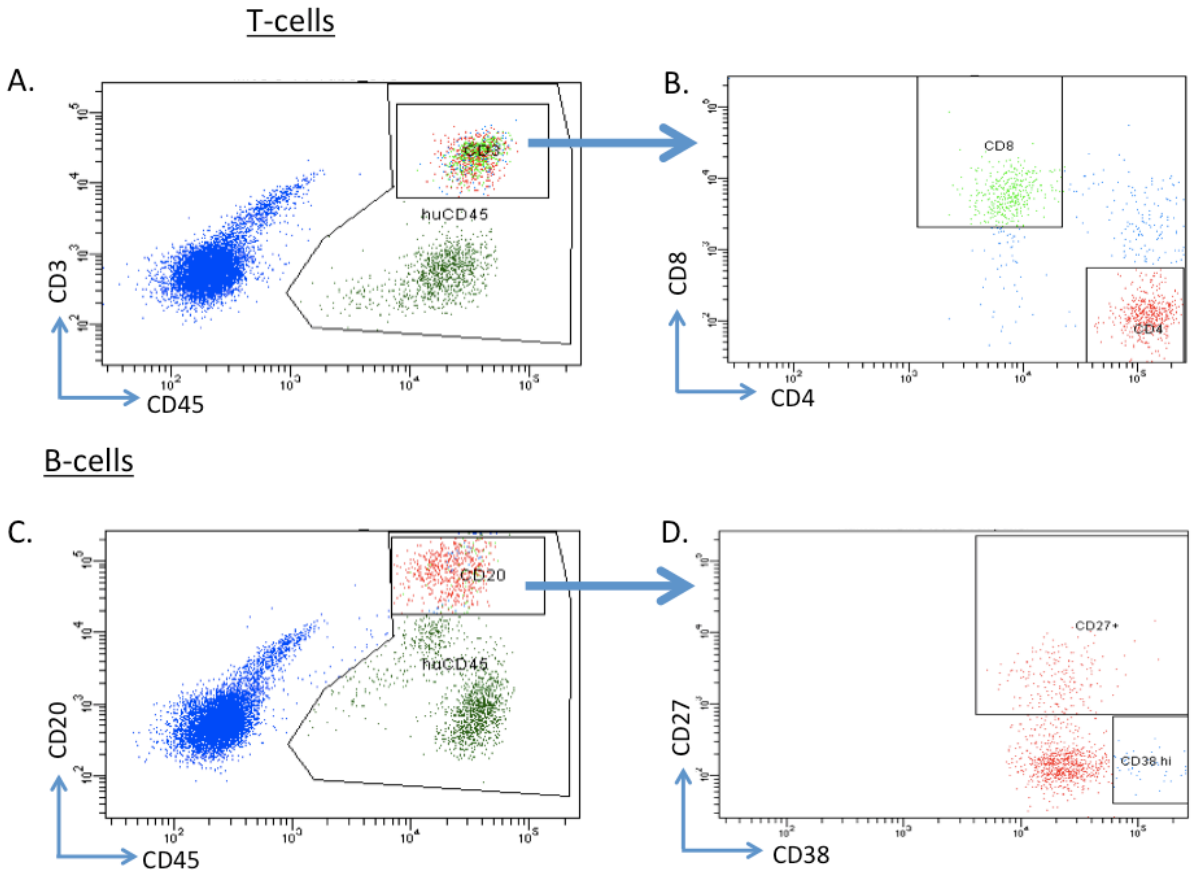

Figure 3.1: FACS scans of the spleen of a representative a 12-week-old humanized mouse. Results representative of N=4 12 week old humanized mice. $CD45^+$ / $CD3^+$ T cells from panel (A) were further analyzed in panel (B) for $CD4^+$ T helper cells and $CD8^+$ cytotoxic T cells. $CD45^+$ / $CD20^+$ B cells from panel (C) were further analyzed in panel (D)

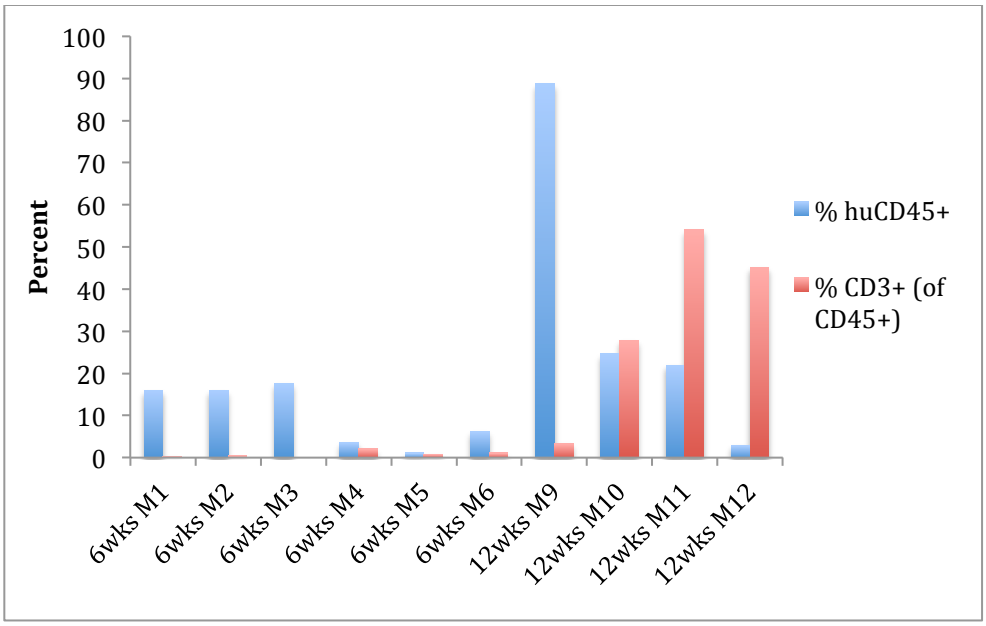

Figure 3.2: Engraftment levels and T cell populations from the spleen of humanized mice at different ages.

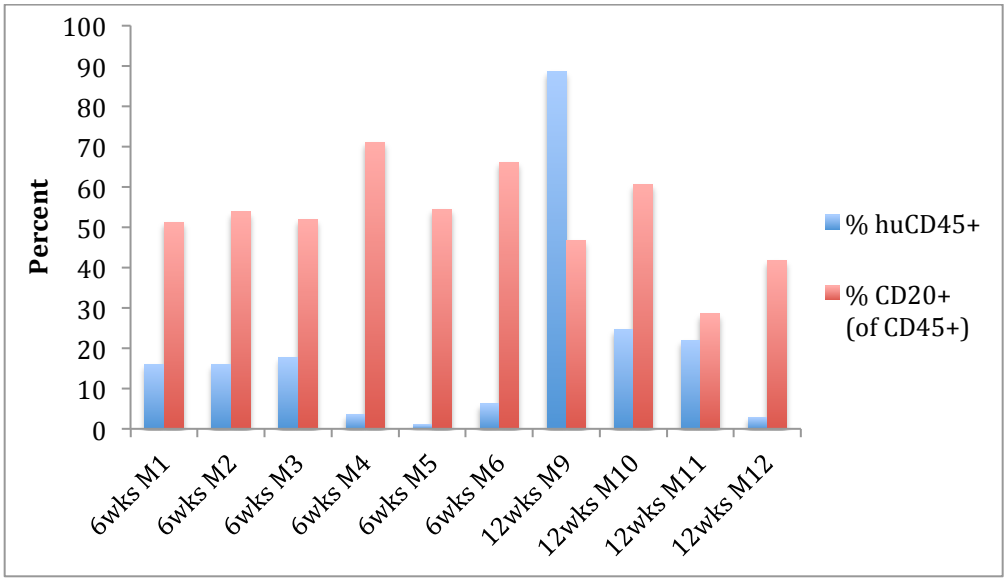

Figure 3.3: Engraftment levels and B cell populations from the spleen of humanized mice at different ages

The spleen, thymus (when present) and bone marrow from twelve-week old mice were further analyzed via antibody staining and FACS for the presence of specific B-cell and T-cell subtypes and other $CD45^+$ lymphocytes. Of $CD20^+$ B cells, approximately 5.7% ± 1.8% of the spleen B cells and 1.3% ± 1.0% of the bone marrow B cells were $CD27^+$ B memory cells; 13.3% ± 5.7% of the spleen and 15.7% ± 3.5% bone marrow $CD20^+$ B cells were $CD38^+$ plasma cells. Of the $CD3^+$ T lymphocytes analyzed, the thymus contained predominately $CD4^+/CD8^+$ developing T lymphocytes, while T cells that had migrated to the spleen had largely differentiated into $CD4^+$ helper T cells or $CD8^+$ cytotoxic T cells.

Non-B and T-cell leukocytes were also analyzed. $CD11c^+$ dendritic cells, which mainly function as antigen presenting cells, were present at 2.3% ± 1.3% and 2.35% ± 1.2% in the spleen and bone marrow respectively. $CD33^+$ monocytes, mast cells and myeloid progenitors, which are non-lymphoid white blood cells that play other roles in immunity, are present at 4.2% ± 1.9% and 12.1% ± 6.3% in the spleen and bone marrow respectively. These leukocyte development levels are nearly identical to those published by Ishiwaka et al (50).

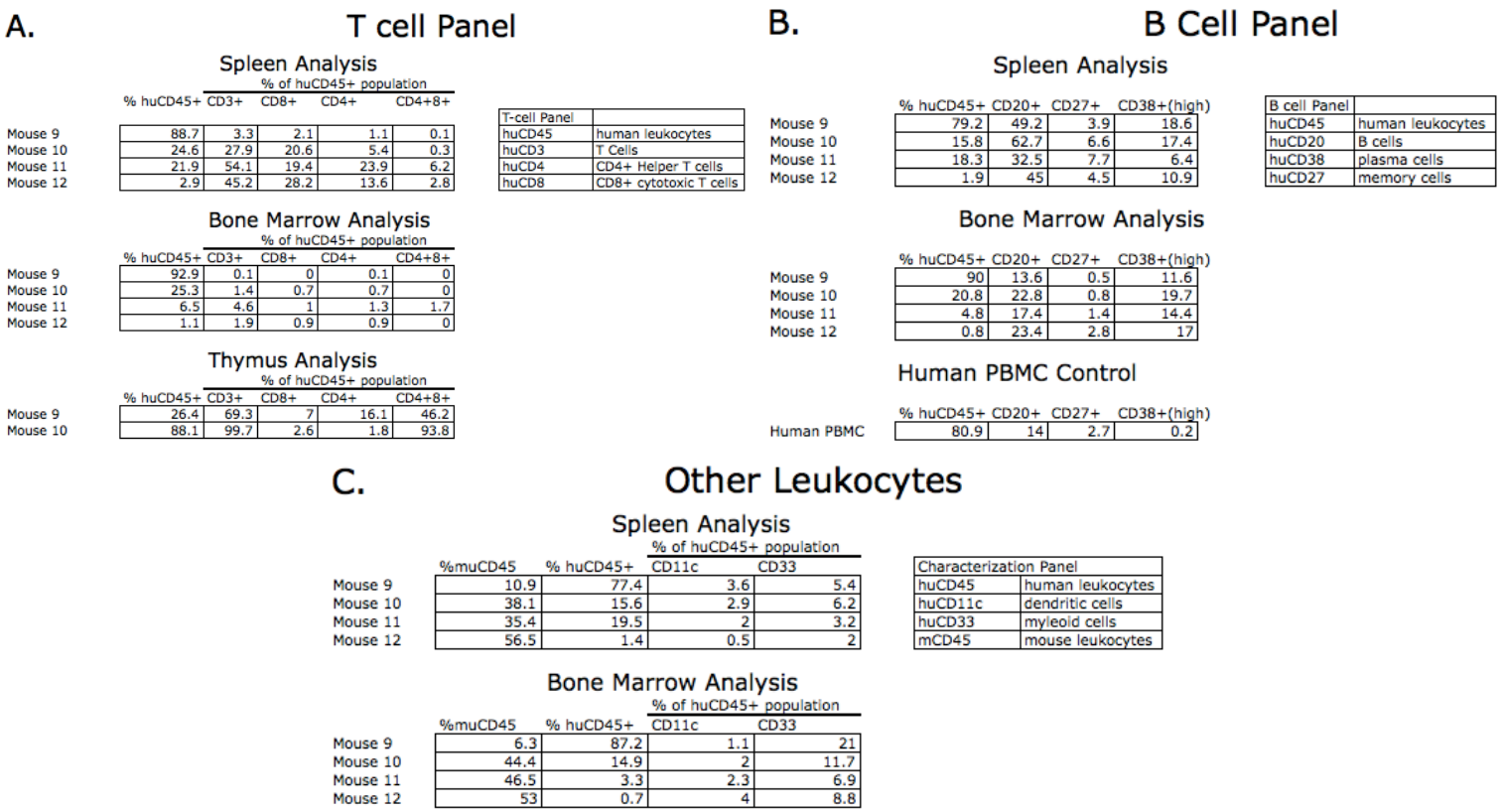

Figure: 3.4: Engraftment Levels of Leukocytes in 12-week-old humanized mice determined by FACS. (A) T-cell engraftment levels and subsets. $CD8^+$ and $CD4^+$ cells are reported as a percent of $CD3^+$ population. (B) B cell engraftment levels and subsets. $CD20^+$ engraftment levels are reported as a % of the total $CD45^+$ population; $CD27^+$ and $CD38^+$ subsets of B cells are reported as a percent of $CD20^+$ B cell population. (C) Other leukocyte subsets. Engraftment levels of human subsets are reported and a percent of the $CD45^+$ population.

Immunizations of Humanized Mice

The 10 Non-obese diabetic-*scid-IL2Rγ*^{null} (NOD-*scid- IL2Rγ*^{null}) mice were engrafted with umbilical cord blood (UCB) CD34^{+} hematopoietic progenitors. 12 weeks post- engraftment, mice were immunized into the peritoneum with an emulsion of 50ug of the highly immunogenic protein *Concholepas concholepas* hemocyanin (CCH) and complete Freund's adjuvant (CFA). Each mouse received a subcutaneous booster injection 3 weeks later composed of an emulsion of 50ug of CCH and incomplete Freund's adjuvant (IFA). Two weeks after boost immunization, blood was drawn from the mice via tail vein snip and an ELISA was performed to measure IgG and IgM antibody titers against CCH.

IgM and IgG antibody titers were determined as 3-fold above background OD450 reading for each of the 10 mice. Each mouse produced antigen specific antibodies at lower than 1/1,000 dilution, indicating a significantly reduced ability to produce human antigen-specific antibodies. Standard laboratory BALB/c mice immunized in this fashion produce antibody titers between 1/50,000 and 1/500,000.

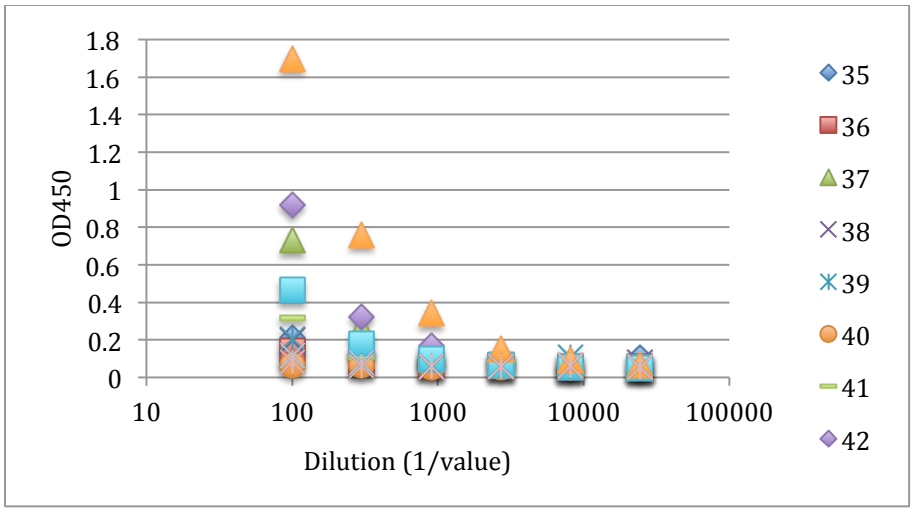

Figure 3.5: CCH-specific antibody titers for mice at following two immunizations. The numbers in the legend represent the identity of the humanized mouse. IgM and IgG (cross reactive detection antibody was used) antibody titers are determined as the point where signal is 3-fold above background OD450 signal. Therefore, none of these mice have antibody titers higher than 1000.

DISCUSSION

Here we analyzed the lymphocytes and immune responses in humanized NSG ((NOD.Cg-Prkdc^{scid} Il2rg$^{tm1Wjl/SzJ}$) 6- and 12-weeks post-engraftment. For the 12-week old mice studied in this work, numbers for dendritic cells, B cells and T cells appropriately reflect engraftment levels observed previously 12-weeks post engraftment by Ishikawa et al. (50). Their results did show slightly more B cells, (ex. 47% ± 12% in the spleen in our studies vs 60% ± 14% in their work), however they used a different B cell marker (theirs CD19 vs CD20 ours) that may explain the different levels recorded. At 6-weeks, CD3$^+$ T cells were nearly non-existent but CD20$^+$ B cells were found in

significant numbers; by 12-weeks post engraftment both cell types were present at levels in agreement with previously published data.

The numbers of mouse $CD45^+$ cells were inversely correlated with human $CD45^+$ cells in the animals. We suspect that the presence of murine $CD45^+$ cells is a result of insufficient ablation of host $CD45^+$ cells during γ irradiation of pups. It is poorly understood how murine $CD45^+$ cells develop (the IL2-Rγ mutation should prevent them from developing), these cells have been recorded before in previous studies characterizing NSG mice (50). Therefore, this result underscores the importance of expertise required in order to achieve high engraftment levels and the necessity to characterize each mouse within the study.

The lymphocytes cells produced in NSG mice are sufficient to elicit a T and B cell response following antigen stimulation (50). However, previous studies have found that despite the presence of a total $>10^6$ $CD20^+$ B cells and $CD3^+$ T cells in the spleen, antigen specific IgG titers are nearly undetectable following immunization in this animal model (50, 128). One reason thought to be partially responsible for the weak antibody response is that human T cell selection occurs against murine MHC I / II thereby altering human T cell help to mature B lymphocytes (129). Additionally, previous accounts describing the mature naïve B cell subsets generated in NSG humanized mice have not thoroughly characterized the B cell antibody repertoires in depth.

Follow up work on these mice using identical procedures and flourochrome labeled antibodies that detect B-cell development stage (CD19, IgM, IgD), revealed that ~90% of the B cells were IgM/IgD^+, indicating the B cells were naïve (53). Similar results, indicating normal naïve adaptive immune cells but little production of antigen specific antibodies, have been found in similar mouse strains (50, 130, 131). Results from Watanabe et al. using the similar mouse strain NOD/shi-scid/γc^{null} (NOG) further

investigate the B-cell development (131). We therefore concluded that naïve mature B cells developed in these mice were suitable for antibody repertoire study. Follow up work confirms that the B cell repertoire is indeed very similar to the native human repertoire (53).

Following repeated immunization of these mice, we saw nearly negligible antigen specific IgG and IgM antibody titers. Subsequent published studies confirm the lack of antigen specific antibodies produced using humanized mice (50, 128). We therefore concluded that insufficient IgM/IgG development in response to immunization excluded the mature repertoire from further study. Improvement of the milieu provided by the host mouse strain is necessary in order to achieve a functional human adaptive immunity in mice. One such innovation is the transgenic mouse strain NGS-HLA-A2/HHD, which has backcrossed the human HLA class I transgene onto the NHS background (129). This improvement is significant because these mice have a humanized immune microenvironment expressing HLA class I, allowing for the mouse facilitate proper intrathymic selection of human T cells in a HLA-restricted manner and thereby resulting in active cytotoxic T lymphocytes and $CD4^+$ T helper cell subsets. Another promising improvement to B cell survival is the introduction of the human B lymphocyte survival factor, BLyS, which is shown to increase serum Ig levels 40-fold in response to thymus-independent antigens (132). Therefore, we suspect that in the near future, humanized mouse strains improvements or supply of exogenous survival factors will support a more complete human adaptive immune response in mice, capable of producing significant quantities of antigen specific IgG.

MATERIALS AND METHODS

Ethics Statement

The animals used in this study were housed in under pathogen-free barrier conditions at the Animal Resource Center at the University of Texas at Austin. The experiments were conducted following the Institutional Animal Care and Use Committee guidelines (approved protocol number AUP-2009-00035).

Engraftment of Humanized Mice

NOD-*scid- IL2Rγ*^{null} mice were irradiated at 1-2 days old with 100cGy of gamma irradiation laregly following the protocol of Pearson et al. (48). Intracardiac injection of $3x10^4$ Umbilical Cord Blood $CD34^+$ hematapoetic progenitors (Lonza, 2C-101A) in 50ul of PBS, pH 7.5 was performed once mice were irradiated.

FACS Scans

At 6-12 weeks post engraftment, spleen, bone marrow from the tibia and fibia, and thymus were collected into ice cold buffer 1 (PBS, pH 7.5, 0.1% BSA, 2mM EDTA). A single cell suspension was made from isolated organs by passing cells through a 70uM strainer into a 50mL conical tube (large gauge needles and the rubber stopper of a 3mL syringe are extremely helpful to break up the organ and allow single cells to pass). An additional 5ml of buffer 1 was used to rinse strainer. Cells were then centrifuged at 500 x *g* for 10 min in a swinging bucket rotor and resuspended in 1ml of buffer 1.

Washed cells in 1ml of buffer 1 were incubated on ice for 5 minutes with 2ul of FC Block. Following block, 100ul aliquots of cells were incubated with flourochrome-labeled antibody panels according to the table below then incubated for 20 minutes at

4°C, centrifuged at 500 x *g* for 10 min, resuspended in 100ul of buffer 1, and analyzed via FACSAria flow cytometer. Analysis was performed using FACS Diva software.

	T-cell Panel		Vendor	Prod #	vol (ul)/aq
V450	huCD45	human leukocytes	BD-pharma	560367	5
FITC	huCD3	T Cells	BD-pharma	555332	20
PE	huCD4	$CD4^+$ T cells	BD-pharma	555347	20
APC	huCD8	$CD8^+$ T cells	BD-pharma	555369	20

	B cell Panel		Vendor	Prod #	vol (ul)/aq
V450	huCD45	human leukocytes	BD-pharma	560367	5
FITC	huCD20	B cells	BD-pharma	555622	20
PE	huCD38	plasma cells	e-bioscience	12-0388-42	5
APC	huCD27	memory cells	BD-pharma	558664	20

	Characterization Panel		Vendor	Prod #	vol (ul)/aq
V450	huCD45	human leukocytes	BD-pharma	560367	5
FITC	huCD11c	dendritic cells	e-bioscience	11-0116-73	20
PE	huCD33	myleoid cells	BD-pharma	555450	20
APC	mCD45	mouse leukocytes	BD-pharma	559864	2

None	Fc Block	Block Mouse FcR	BD-pharma	553142	2

Table 3.1: Panels of Antibodies used for various characterizations.

Immunizations

12 week old humanized mice were immunized with an emulsion of 1/3 adjuvant complete Freund's adjuvant (CFA) with 50ug of antigen Concholepas concholepas hemocyanin (CCH) (Pierce, 77130) in dPBS, pH 7.5 (Thermo, SH30028.02) was prepared at RT by mixing with a pipette then brief sonication until a stable emulsion is

achieved (usually 30 seconds). Injection agent was drawn into the 29G syringe (BD, 309306) and mice were immunized subcutaneously into the scruff of the back of the neck. Booster immunizations were performed via intraperitoneal injection three weeks after primary immunizations with Incomplete Freund's adjuvants (IFA) instead of CFA and 50ug of CCH protein in 50ul of PBS, pH 7.5.

Titer Determinations

Mice were bled 2 weeks post boost via tail vein snip, then serum IgG and IgM titers were determined by ELISA serial dilution. Briefly, high binding ELISA plates (Corning Costar 3590) were coated overnight at 4C with 50ul of 4ug/ml antigen in PBS, pH7.5. Plates were aspirated then blocked for 3 hours at 25°C with PBS, pH7.5, 2% milk. Plates were again aspirated then incubated with 50ul of serum diluted 1/200 through 1/437000 in PBS, pH7.5, 2% milk and incubated at 25°C for 2 hours. Plates were washed 3X with PBS, pH 7.5 0.05% tween-20 (PBST) then incubated with 1/5000 anti-Mouse I HRP (Jackson Immuno, 109-035-044) at 25°C for half an hour. Plates were washed again 3X with PBST then incubated with 50ul of TMB substrate for 15 min at 25°C then quenched with 1M sulfuric acid. Plates were read at 450nm and analyzed with GraphPad Prism software. Titers were determined as the point where the non-linear fitted curve determined 3-fold signal above background.

The lack of an antigen-specific antibody response following repeated immunizations with a highly immunogenic adjuvant suggests that only a partial reconstruction of the human adaptive immune system was achieved. Therefore, we conclude that NSG humanized are suited for studies requiring a naïve human adaptive

immune system, but further improvements in the host mice are necessary in order to study the adaptive immune response.

Chapter 4

Generating Highly Polarized Antibody Repertoires in Immunized Mice

INTRODUCTION

Mice have been used as the primary source for generation of monoclonal antibodies since the mid-1970s when hybridoma technology was invented (34). The hybridoma technology involves fusing antibody-producing cells from the spleen of an immunized mouse with myeloma cells in order to produce antibody-secreting cells that can survive indefinitely, thus enabling an unlimited production of a single antibody (33). Limitations of the technology are that it is time consuming and often only 2-3 distinct monoclonal antibodies per animal are isolated. Innovations in the field of therapeutic technology, specifically the development transgenic mice with human antibody variable genes, have made the industry even more dependent on mice for production of therapeutic antibodies, not less (117, 133). The hybridoma technology is still widely used today because it is a straightforward and effective, albeit laborious, process for producing antibodies to a desired antigen. The use of hybridoma technology as they did in the 1970s has significant disadvantages for the production of therapeutic antibodies. Therefore, a technology that circumvents the slow culturing process while maintaining or improving the simplicity and efficacy of antibody discovery from immunized mice is highly desirable.

Reddy *et al*. recently published an antibody discovery technology that avoids the laborious and time consuming screening and culturing procedures of hybridoma technology. Their technology demonstrated that the most highly represented heavy and light V gene sequences from the antibody repertoire isolated from the bone marrow

plasma cells are antigen specific (105). Following repeated immunization of mice and isolation of the bone marrow plasma cell population (BMPC) via FACS sorting, the most frequent antigen specific V genes from the sequenced antibody variable region repertoire were synthesized, expressed either as scFvs or full length IgGs in bacteria or mammalian cells, and specificity was verified via ELISA.

Reddy *et al*. showed that the most abundant antibody V genes (.5-10% frequency) expressed by bone marrow plasma cells (BM-PCs) 7 days post-boost immunization correspond to antigen-specific antibodies. However, not all highly frequency V genes in the BM-PC repertoire are antigen specific necessitating the testing of several combinations of the most frequent VH and VL genes to find antibodies with desired affinity and specificity. Therefore, in order to increase the speed and simplicity of a frequency-based antibody discovery technique, it is desirable to create polarized repertoires composed of a higher frequency of antigen specific antibodies and less irrelevant antibodies. The purpose of this study is to investigate a new method for the generation of even more polarized repertoires composed of antigen specific antibodies for use in the discovery of antigen specific antibodies.

Reddy et al. utilized the well-established fact that plasma cells in the bone marrow produce antigen-specific antibodies that constitute the steady-state serological response to challenge or immunization (28). The cytokines and other signals present in the bone marrow environment allow plasma cells to reside there for more than 60 days in mice (134). Without survival signals, antibody secreting cells such as plasma cells and plasmablasts survive for an average of one week (135). Because the long-lived plasma cells will find residence in the bone marrow irrespective of which secondary lymphoid organ(s) they were selected for expansion and differentiation in, the bone marrow niche is filled with antibody producing cells targeting the large array of antigens to which a

mouse has been exposed, presumably during its entire lifetime up to that point (136, 137). It follows that selection of relevant antigen-specific plasma cells from the bone marrow will be complicated by the many other plasma cells present that do not produce an antibody specific to the antigen of interest, thereby diluting the repertoire with antibodies that bind irrelevant antigens.

The bone marrow is the eventual destination of most long-lived plasma cells, but it is not the anatomical location where plasma cell selection occurs. The origin of these cell types is a germinal center within a lymph node or the spleen. Germinal centers provide a cellular milieu for the expansion, differentiation and affinity maturation (through somatic mutation of the antibody genes) of mature B cells (25). Both the lymph nodes and bone marrow contain plasma cells that produce antibodies specific to the antigen (138). However, only the bone marrow has the signals necessary to sustain long lived plasma cells (135). Among the important signals found within the bone marrow that extend the life of the antibody producing plasma cells include CXCL12, TNF, IL-5, IL-6 and ligands for CD44 (135).

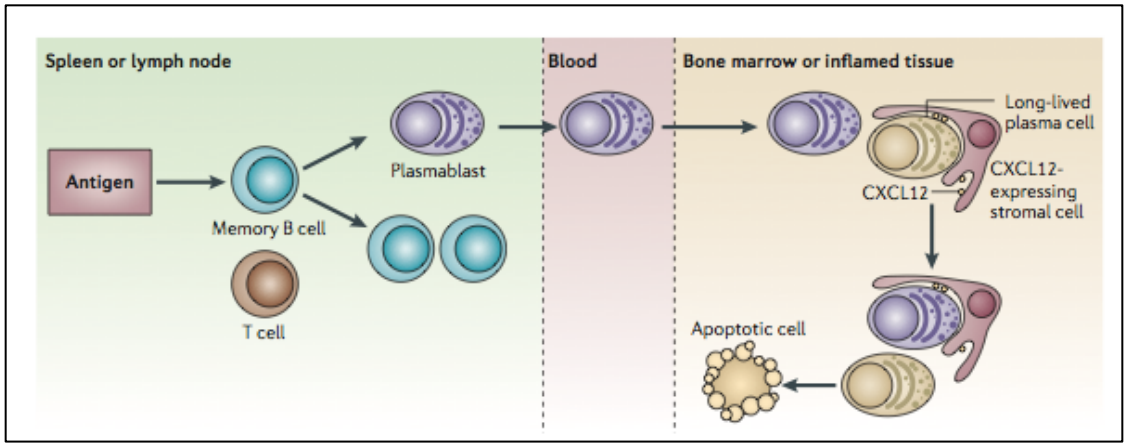

Figure 4.1: Antigen recognition and B-cell expansion initially occurs in the spleen or lymph node. Following recognition and expansion of antigen specific B cells, plasma blasts are generated which leave the lymph nodes and spleen and eventually travel to the survival niche present in the bone marrow (135).

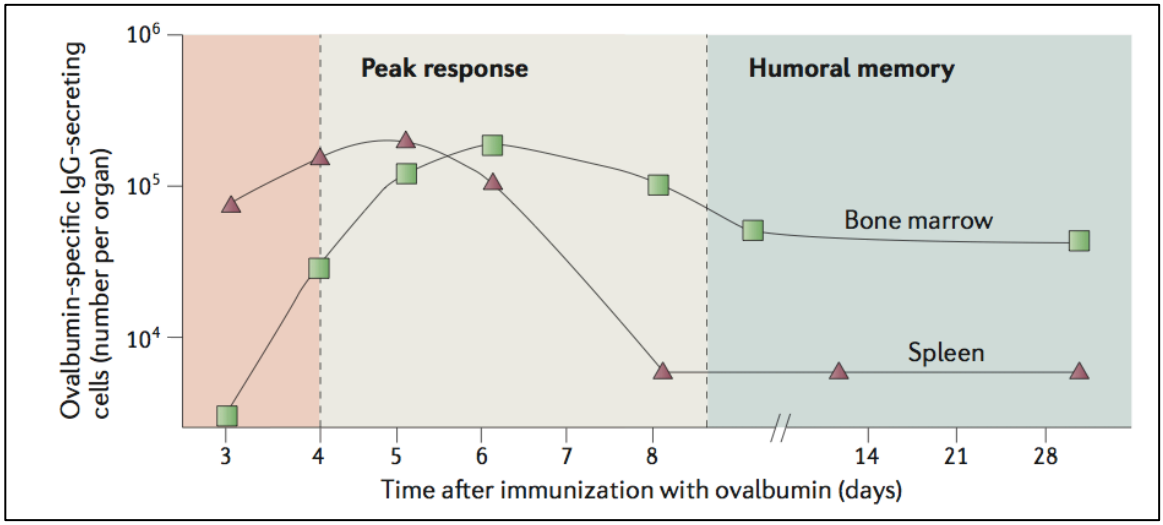

Figure 4.2: The bone marrow contains the appropriate environment for long-term persistence of IgG secreting plasmablasts and plasma cells thus promoting the persistence of these cells. However, the spleen or other secondary immune response sites do not contain the environment necessary for long term persistence of antibody producing cells (135).

Plasmablasts generated by the lymph node germinal center reaction no longer express the chemokine receptors CXCR5 and CCR7 that are expressed in the germinal center B cells from which they are derived; the loss of expression of these receptors is thought to allow them to leave germinal centers and become migratory (139). Nascent plasmablasts express instead CXCR4 and CXCR3 (the later of which occurs when the formation of plasmablasts is stimulated by the presence of interferon-γ), thereby attracting the cells from the lymph nodes to the bone marrow and inflamed tissue (139). A lymph node where lymphatic vessels carrying the antigen drain into is expected to contain germinal centers formed by antigen-stimulated B cells. Hence, that lymph node is unlikely to contain many antibody-secreting cells to unrelated antigens from prior exposure(s). Therefore, the repertoire of the local environment of a targeted lymph node should be filled with a much greater fraction of antigen specific antibody producing cells than the bone marrow. Experimental analysis confirms that extremely high levels of background antibody producing cells are present the bone marrow; quantification of the antibody producing cells from various anatomical locations of unimmunized mice shows that >70% of antibody producing are found in the bone marrow, while less than 3% of these cells are found in the lymph nodes (140).

In order to avoid the many irrelevant antibody-producing cells present in the bone marrow, we sought to generate highly polarized antibody repertoires composed largely of antigen specific antibodies by generating an antigen specific immune response in a specific lymph node. In order to target a specific lymph node with antigen, we immunized mice by injecting antigen and adjuvant into one of the rear footpads. Upon immunization, antigen was delivered via the lymphatic system to the popliteal lymph node located at the knee of the animal.

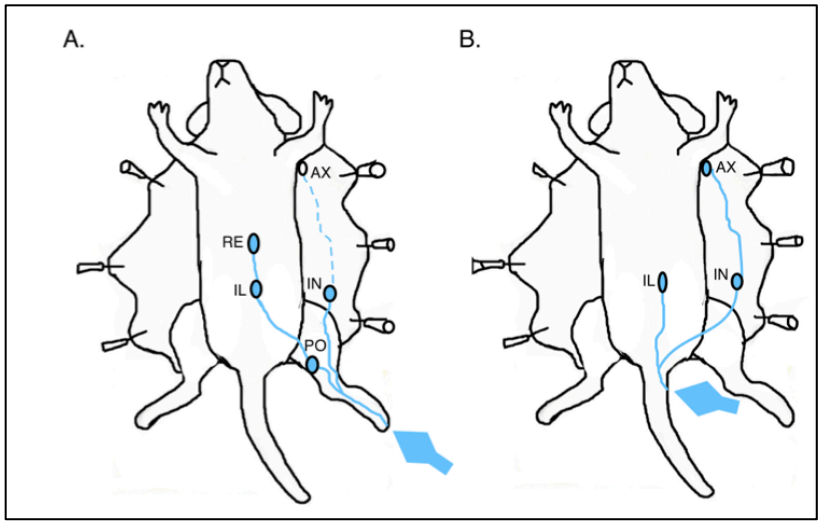

Figure 4.3: Targeting specific lymph nodes varies by injection route(141). Targeting the footpad in panel A results in antigen delivery to the popliteal lymph node (PO) and subsequently to other lymph nodes downstream from the PO.

Specific lymph nodes have previously been targeted with antigen in order to localize antigen-specific B cells for development of hybridoma fusions. Hybridomas produced from a splenic B-cell fusion effectively produce specific antibodies at wildly different frequencies; it is common to see reports that 1% -99% of successful fusions produced by a splenic B-cell fusion are antigen specific (142). However, most publications report that less than 10% of successful fusions generated from the spleen of an immunized mice are antigen specific (143). In order to improve the frequency of antigen specific hybridomas generated, researchers have targeted the popliteal lymph node by immunizing mice into the footpad. Targeting is effective because dendritic cell trafficking is regional and consequently antigen uptake by these cells at a distinct anatomic location leads to maturation and antigen presentation at the closest draining lymph node. Localization of antigen presentation at the lymph node nearest the site of

immunization leads to high levels of antigen-specific B cells. One study found that hybridomas developed from targeted popliteal and inguinal lymph nodes after immunizing into the proximal footpad produced only antigen specific clones (384/384) compared with only 8% antigen specify (29/352) from hybridomas developed from the spleen following a IP immunization (143).

Fusion efficiency (% positive wells): lymph node > spleen cell fusions.

Fusion cells and route of immunisation	Number of wells with colonies	Number of positive wells	% Colony formation	Proportion of positive wells
Lymph nodes: footpad	384	384	100	100%
Lymph nodes: hindleg intra-dermal	87	46	23	53%
Spleen: dorsal subcutaneous	352	29	92	8%

Table 4.1: Fusion efficiency of hybridomas developed from different anatomical origins. (143)

Targeting the popliteal lymph node for antibody discovery has been validated in subsequent studies (144, 145). Sado *et al*. also used lymph node targeting in order to generate antigen-specific hybridomas, however they targeted a different lymph node via tail vein injection. In their study, Sado *et al*. reported that 100% of the hybridomas from the targeted lymph node were antigen specific, while conventional spleen isolations yielded only 10% of antigen specific hybridomas (146). Antigen specific hybridomas have also been discovered in rats via popliteal lymph node targeting through footpad injection (147).

Based on these published results, anticipated that lymph node targeting would be an effective method to generate highly polarized libraries of antigen specific-antibodies. In initial studies to test this hypothesis, we immunized animals in the rear footpad with

the hapten phosphorylcholine (PC) conjugated to protein carrier BSA. Phosphorylcholine antigen is a highly immunogenic hapten commonly found covalently attached to LPS on the surface of many bacteria including *Streptococcus pneumoniae*, *Pseudomonas aeruginosa*, and *Neisseria* species (148). PC-BSA is an ideal proof-of-principle antigen because it produces a highly skewed immune response in certain mouse cell strains. When BALB/c mice are immunized with PC, >90% of antigen-specific antibodies produced from the primary immune response in this strain comprise a specific heavy chain V-D-J combination (V S107.1, D FL16.1, J JH1) (149, 150). A major advantage of using PC hapten is that the antigen-specific sequence is already known; therefore, relevant antibodies are visualized easily by DNA sequencing *in silico* thus it is not necessary to experimentally determine which antibody DNA sequences would yield antigen specific antibody proteins.

Following primary footpad immunization of two BALB/c mice with PC-BSA, we used PCR and Sanger sequencing of the antibody variable genes to investigate the repertoire of antibodies found in the targeted popliteal lymph node. PCR analysis of cDNA demonstrated that the targeted lymph node (ipsolateral to the site of injection) contained cells expressing IgG, while the control lymph node (contralateral to the site of injection) did not produce detectable levels of IgG. Furthermore, sequencing of the heavy chain V-gene repertoire revealed that mRNA transcripts isolated from the antigen-targeted lymph nodes were >20% of the heavy chain component of phosphorylcholine-specific T15 idiotype antibody. Therefore, the antibody repertoire from a lymph node targeted with hapten antigen is highly polarized with antigen-specific antibodies, allowing for simple *in silico* selection of antigen specific antibodies. We expect that this work will be the foundation of an overall improved protocol for monoclonal antibody

discovery that accelerates the speed and enhances the simplicity of therapeutic antibody discovery.

Because most therapeutically relevant antibodies bind complex protein targets, we applied the lymph node targeting technique to a complex antigen by repeatedly immunizing two additional BALB/c mice with Ebola virus-like-particles (VLPs) expressing the recombinant Ebola capsid glycoprotein-1 (GP1). Through PCR analysis of lymph node cDNA, we demonstrated that the targeted lymph nodes contained cells expressing IgG, while the control lymph node did not contain detectable levels of IgG. Furthermore, Sanger sequencing analysis of the antigen targeted lymph nodes revealed a highly polarized repertoire in one mouse (>20% of the antibodies corresponded to one heavy chain sequence) and a moderately polarized repertoire in another mouse (>5%). These results suggest that multiple immunizations with a complex antigen targeted at a specific lymph node will elicit a highly polarized antibody repertoire. However, additional work (discussed at the end of this chapter) is required in order to validate the antigen specificity of the highly represented antibody heavy chains from the Ebola VLP immunized mice.

RESULTS

PCR analysis of mRNA from PC-BSA Antigen Targeted Lymph Nodes

Two mice BALB/c mice were immunized in the footpad with 25ul of 20ug of PC-BSA (16 PC molecules per BSA) in PBS, pH 7.5 with 8ul of Titer Max Gold adjuvant. Both the antigen targeted and control popliteal lymph nodes were collected and processed 10 days after primary immunization. After harvest and CD138+ cell subtype selection via MACS, cDNA was generated from each cell fraction isolated from either the lymph node

or the spleen. PCR was performed on cDNA generated from the targeted popliteal lymph nodes and their control counterparts on the opposite foot in order to establish which relevant mRNA transcripts are present in the lymph node after targeting with an antigen. IgG, IgM, PC specific idiotype T15 and GapDH (a housekeeping gene) were analyzed via PCR with specific primers, resolved on a 3% agarose gel, then inspected under UV light. Both the targeted and control lymph nodes had sufficient levels of IgM and GapDH (a housekeeping gene) that they produced visually detectable bands of PCR product when resolved gels were run under UV light. Additionally, each of the targeted lymph nodes generated visually detectable PCR product bands when cDNA was amplified by a PCR reaction with IgG and PC-specific T15 primers, while the control lymph nodes did not. These PCR results demonstrate that targeted lymph nodes fill with antigen specific cells that have class switched to IgG, while the control lymph nodes do not. While these results do not confirm that all the IgG produced in the targeted lymph node are antigen specific, the prominence of the IgG and T15 bands suggest that there are many antigen specific clones in the targeted lymph node. However, a sequence-based approach is required in order to determine the relative frequency of antigen specific clones produced by the targeted lymph node.

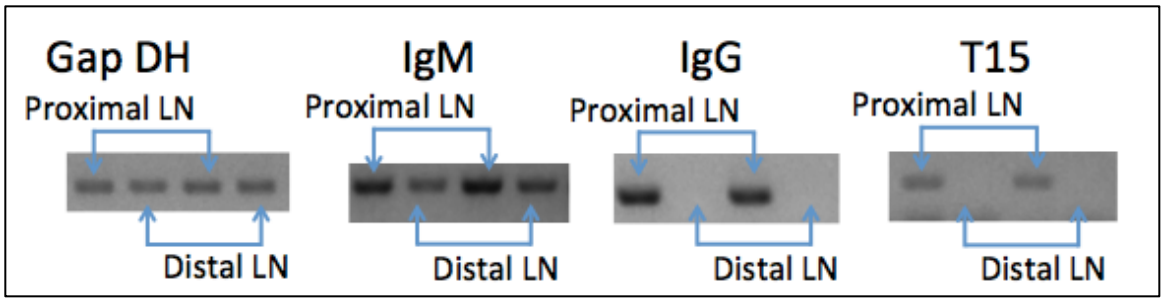

Figure 4.4: Comparing products on a gel from PCR reactions with specific primers (top line) using the cDNA from the targeted (proximal, or lateral, to the site of injection) and control (distal, or contralateral, to the site of injection) popliteal lymph node from mice immunized with PC-BSA.

In order to compare cell types and antibody specificities from the targeted lymph node and spleen, cDNA was created from the CD138+ cells (plasma cells) isolated from each organ from mice immunized with PC-BSA. These semi-quantitative PCR band results indicate higher mRNA transcript levels of antigen-specific T15 antibody in the targeted lymph node compared to the spleen. Additionally, the PCR results also indicate that the quantity of IgG mRNA transcripts is much higher in the lymph node than the spleen. These results suggest that the targeted lymph node has a much higher frequency of cells producing antigen specific IgG compared to the spleen, thus making the lymph node an ideal anatomical site for the discovery of antibodies.

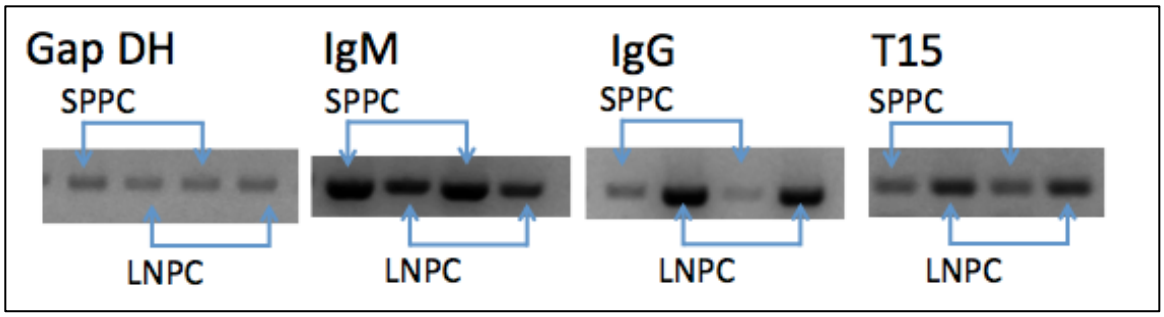

Figure 4.5: Comparing products on a gel from PCR reactions with specific primers (top line) using the cDNA from the targeted lymph node plasma cells and the plasma cells from the spleen of mice immunized with PC-BSA.

Sequencing Analysis of Lymph Nodes Targeted with PC-BSA

Heavy chain sequences collected from the CD138+ cells of the targeted lymph node and the spleen were analyzed in order to determine the frequency of the heavy chain component of phosphorylcholine-specific T15 idiotype from the primary immune response to phosphorylcholine immunization via the footpad. In order to amplify these genes from cDNA, we used standard PCR conditions with a 5' primer mix composed of primers specific for the entire heavy chain V gene repertoire and a 3' primer mix composed of primers specific for the constant region of each IgG subclass. After digesting, ligating into the APEx vector, and transforming PCR products using standard cloning techniques, individual colonies were sequenced via Sanger sequencing and the frequency of the heavy chain component of phosphorylcholine-specific T15 idiotype was determined (77).

	SPPC Mouse 1	LNPC Mouse 1	SPPC Mouse 2	LNPC Mouse 2
T15 seq	0	3	0	8
Total # of seq	43	33	32	36
%T15	0%	9%	0%	22%

Table 4.2: A comparison of T15 idiotype frequencies from two mice immunized with PC-BSA. SPPC = Spleen plasma cells, LNPC = lymph node plasma cells

These results indicate that the targeted lymph node has a much higher relative frequency of antigen-specific plasma cells than the spleen. In addition to the CD138+ subset, the mRNA from the whole lymph node was also collected and tested for the presence T15 IgG in the same manner as the CD138+ subset. Analysis of heavy chain V gene sequences generated from whole lymph node revealed that the IgG mRNA transcripts had two-fold more T15 sequences than the CD138+ subset. This is likely due to the contribution of other phosphorylcholine specific-cell subtypes such as CD138-low plasmablasts, CD138-negative memory cells and CD138-negative germinal center cells. Therefore, future investigations of sequence frequency should use whole lymph node mRNA in order to maximize polarization of the antibody repertoire.

	Total LN Mouse 1	Total LN Mouse 2
T15	10	22
Total Sequences	46	42
T15 % of total	22%	52%

Table 4.3: T15 idiotype frequency identified from IgG cDNA transcripts from the entire lymph node of two mice sacrificed 10 days after primary immunization.

It is interesting to note that the many T15 variable heavy chain regions sequenced were associated with various IgG subclasses with IgG1 and IgG2b were being the most frequent.

Antibody Titer and PCR analysis of mRNA from Ebola-VLP Hyper Immunized Mice

25 ug of Ebola virus like particles (VLPs) in 20ul PBS, pH 7.5 with 10ul of Imject Alum adjuvant (Pierce 77161) were injected into the footpad of two BALB/c mice on days 0, 21, 35 and 49. Ebola VLP specific IgG antibody titers were determined 7 days after each injection by collecting serum by tail vein bleed and performing an ELISA.

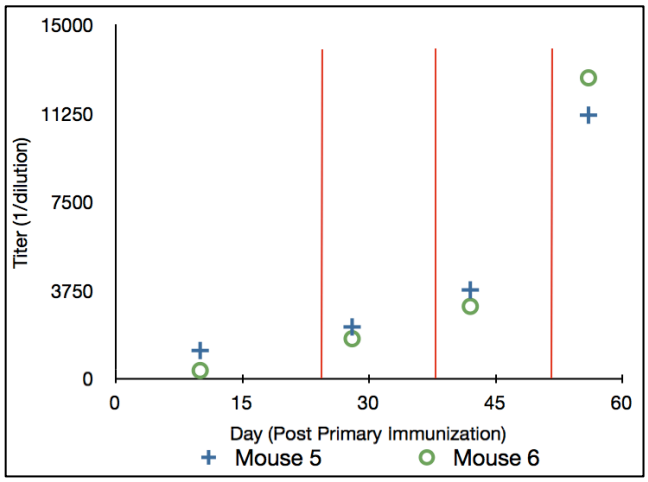

Figure 4.6: Ebola VLP Immunization Response to footpad injection: Serum IgG titers are reported for each day recorded. Red lines indicate boosts at days 21, 35 and 49.

At day 56, spleen and popliteal lymph node CD138+ cells and whole lymph node cells were isolated and cDNA was created as described for PC-BSA immunized mice in the previous section. PCR was performed on the cDNA generated from the targeted popliteal lymph nodes and their control counterparts on the opposite foot with primers specific for the constant regions of IgM, IgG and GapDH. PCR reactions were resolved on a 3% agarose gel then bands were inspected under UV light 3%. As with the PC-BSA immunized mice, visually detectable IgG bands were only present in the lymph node targeted with antigen. While these results do not confirm that all the IgG produced in the targeted lymph node are antigen specific, the prominence of IgG and the similarity of the response to the PC-BSA/T15 response suggest that there are many antigen specific antibody-producing cells in the Ebola VLP targeted lymph node. However, a sequence-based approach is required in order to determine the relative polarization of antibody mRNA transcripts within the targeted lymph node and high frequency antibodies should to be tested via ELISA in order to determine antigen specificity.

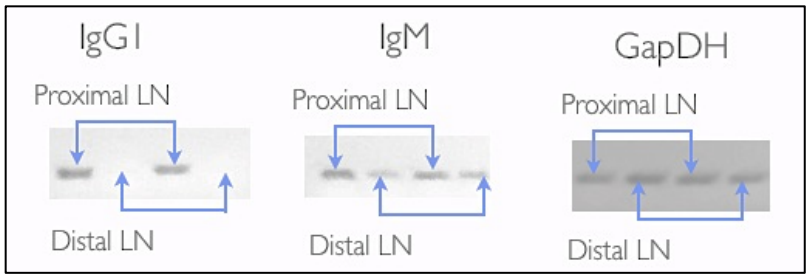

Figure 4.7: PCR bands from whole lymph node (LN) cDNA of two mice hyper immunized in the footpad with Ebola VLPs using specific primers for the constant regions of antibody heavy chains or GapDH.

Sequencing Analysis of Targeted Lymph Nodes Targeted with Ebola-VLPs

Individual sequences of IgG heavy chain variable regions were cloned and sequenced from the antigen-targeted whole lymph node mRNA of mice hyper immunized with Ebola-VLPs using the same methods described in the previous section for PC-BSA immunized mice.

Analysis of the sequences demonstrates that one of the targeted lymph nodes is highly polarized while the other is moderately polarized. Therefore, the antigen-targeted lymph nodes of mice hyper-immunized with complex antigen still generate highly polarized antibody repertoires. The CD138+ subset was not analyzed because data from the PC-BSA immunized mice suggested that the most polarized repertoires would be generated from whole lymph node mRNA.

	Mouse 5	Mouse 6
Total Number of Sequences	32	41
Frequency of Top Heavy Chain	8	3
Top Chain, % total	25%	7%
Frequency of Next Heavy Chain	1	2
Next Most Freq Chain % total	3%	5%

Table 4.4: Frequency of top heavy chains identified from the whole lymph node mRNA of two mice immunized repeatedly with Ebola VLPs. Identity was determined by identical V(D)J gene usage, identical CDRH3, and less than 3 nucleotide differences.

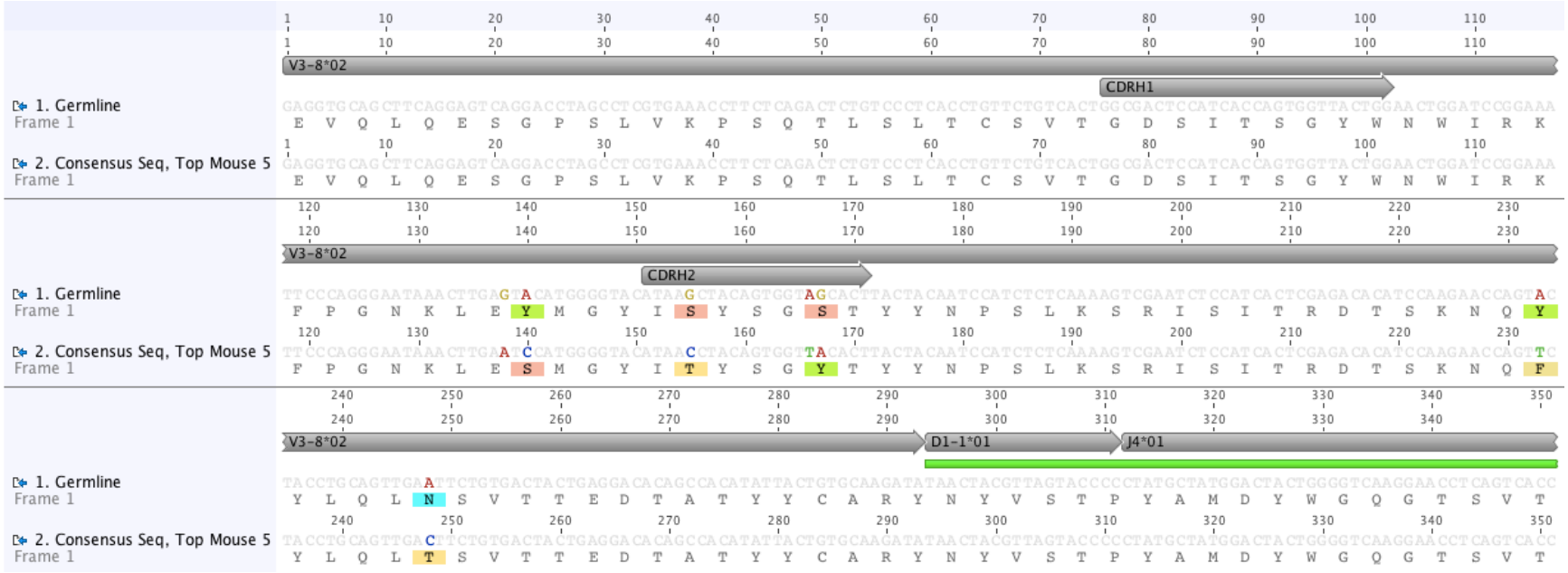

Figure 4.8: The heavy chain variable sequence from the high frequency antibody generated in Mouse 5 compared to the germline sequence.

DISCUSSION

In this work we set to produce the groundwork for a monoclonal antibody isolation protocol that improves the speed and simplicity of discovery. Our goal was to generate highly polarized antigen specific repertoires of antibodies. We demonstrate that a sequence frequency based approach combined with an immunization strategy that targets a specific lymph node with a hapten can generate an mRNA population within the lymph node in which over 50% of the transcript repertoire encodes for antigen specific antibodies. We further report highly polarized libraries following multiple lymph node targeted immunizations with the Ebola virus like particles (VLPs).

In order to target a specific lymph node, we chose to target the popliteal lymph node by immunizing in the rear footpad. The popliteal lymph node is an ideal lymph node to target because laboratory mice do not commonly experience antigen exposure in the footpad. An analysis of PCR products from the cDNA of antigen targeted and non-targeted popliteal lymph nodes reveals that IgG producing cells are locally restricted to the targeted popliteal lymph node (ipsilateral) and these cells are absent in the non-targeted popliteal lymph node (contralateral). In the more than 20 mice immunized using this method, we have never detected IgG via PCR from the non-targeted contralateral lymph node. This suggests that the IgG present in the targeted lymph nodes was specifically attracted by or generated in response to the node by the immunization. The frequency of PC-BSA specific T15 idiotype antibody in repertoires generated in mice immunized with PC-BSA suggests that the most frequent IgG variable regions generated in this manner are antigen specific.

The natural frequency of the T15 idiotype is very low in antibody repertoires generated from mice not immunized with phosphorylcholine. Analysis of previously

collected 454 data shows that among the lymph node plasma cells, only 3 of 16708 sequences utilize the same V and J combination as T15 (the V gene VHS107.1 is rarely used). Because T15 is normally found as such extremely low frequencies, our analysis of the immune response is simplified and we can fairly assume that any T15 presence is a response to the phosphorylcholine immunization. This estimation is further supported by the lack of T15 idiotype in the spleen plasma cells of mice immunized with phosphorylcholine.

The principle disadvantage of using a simple hapten with a simple monoclonal response such as phosphorylcholine is that any principles or strategies derived from such a response should be further validated by demonstration with a complicated antigen capable of a polyclonal response. We have performed immunizations with Ebola virus VLPs in order to demonstrate the strategy is effective for more therapeutically relevant immunizations. In order to attain satisfactory titers, mice were immunized four times with the antigen and adjuvant. After repeated immunizations and collection of relevant cells and mRNA, PCR was used to verify that IgG was localized to the targeting lymph node while no detectable IgG was found in the control popliteal lymph node. The localized IgG repertoire was also found to contain highly (>20%) or moderately (>5%) frequent heavy chain transcripts. This encouraging result implies that this method will likely prove useful for multiple immunizations and more complex antigens than phosphorylcholine. This encouraging antibody heavy chain is undergoing further analysis with random light chains to determine antigen specificity.

Interestingly, we found that phosphorylcholine specific T15 idiotype was more highly represented within the IgG heavy chain repertoire isolated from the total lymph node rather than just the CD138+ plasma cells. In both mice that were analyzed, the T15 idiotype was more than two-fold more frequent in the total lymph node cDNA than the

CD138+ subset from the same lymph node. However, an important part of the technology developed by Reddy *et al*. is the use of plasma cells for the identification of antigen specific antibodies. Plasma cells are of interest because they are responsible for a majority of circulating antibodies and the mechanisms involved in selecting for plasma cell differentiation and survival are complex and seem to be partially related to high affinity antibodies ((151), (152, 153). Therefore, mining the plasma cell repertoire is likely to yield the high affinity antibodies that are responsible for the serum titer. During plasma cell differentiation, immunoglobulin mRNA increases to superabundant levels, due to both increased transcription and stability of the mRNA (154). Therefore, despite the lack of enrichment for CD138+ cells, it is reasonable to suspect that whole lymph node isolations are mostly comprised of mRNA transcripts derived from antigen secreting cells that are either plasma cell or cells undergoing a transition to becoming plasma cells (i.e. plasmablasts). It then follows that mRNA frequency based antibody discovery techniques may be intrinsically biased towards selecting antibodies produced by plasma cells.

The most mature plasma cells are often considered those that have the highest level of CD138 and cells with the highest levels of CD138 are found in the bone marrow (28). However, B-cell development towards CD138 high plasma cells goes through many intermediate steps with low levels of CD138; certain development stages, such as plasmablasts, often have a heterogeneous level of CD138 (155). Therefore, developing plasma cells, especially the earliest stages of such development, have low or extremely low levels of CD138. Enrichment for CD138+ cells from the lymph node excludes many of the antigen specific cells being developed in the lymph nodes while enriching for irrelevant circulating CD138 high plasma cells found within the lymph node. Our evidence suggests that cells found within the targeted lymph node not isolated by

CD138+ selection contain an abundance of antigen specific mRNA transcripts, and therefore these cells should be included in further studies using lymph node targeting to discover antigen-specific antibodies.

Another possible explanation for the lower representation of T15 heavy chain in the CD138+ repertoire is that the other non-T15 idiotype antigen specific antibodies dominate the CD138+ population. While we cannot conclusively rule out this possibility, we find this unlikely as reports indicate that the primary response to PC should be >90% T15 (156). Additionally, neither serum showed significant titer against the carrier protein BSA, therefore most antibodies generated as a result of immunization with PC-BSA are suspected to be T15 idiotype.

One complication this work does not address is heavy chain and light chain pairing. By immediately lysing the cells upon isolation and relying on the mRNA frequency to discovery the relevant antibodies, the link between heavy chain and light is destroyed. Therefore, in order to discover antigen specific antibodies, heavy chain and light chain pairing must be addressed. While our technology does not directly address this issue, we anticipate that the highly polarized libraries generated by this technology will make the pairing between heavy chain and light chain of the top antibodies obvious. Even though we do not anticipate pairing to be a significant issue, we plan to combine our technology with an emerging technology developed within our lab that identifies heavy chain and light chain pairs by linking the pairs through single cell PCR. Once these methods are combined and refined, we anticipate no significant amount of time should be added to the process by solving the pairing problem through sequencing antibodies as heavy and light chain pairs.

MATERIALS AND METHODS

Footpad Immunizations

An emulsion of 1/3 adjuvant (CFA, imject alumn (Thermo, 77161), or Titer Max Gold (Sigma T2684-1ml)) with 25ug of antigen (PC-BSA Biosearch Technologies, PC1011H-10) in dPBS, pH 7.5 (Thermo, SH30028.02) was prepared at RT by mixing with a pipette then brief sonication until a stable emulsion is achieved (usually 30 seconds). Injection agent was drawn into the 29G syringe (BD, 309306). The maximum volume that can be injected into a footpad is 30ul (0.05 ml). Only one hind foot was used for injection (never inject both hind feet). Mice were immobilized by scruffing by one researcher. The rear hind foot to be injected was cleaned with water or alcohol to remove debris prior to injecting. The second person not scruffing the animal then held the foot with one hand and injected the foot subcutaneously using the loaded syringe into the center of the hind foot thereby forming a small bleb at the injection site.

All animals were then closely monitored for signs of pain, food consumption and ambulation. It was not observed in our studies, but there have been reports of self-mutilation occurring in which the foot is chewed off by the mouse. This is a sign of chronic pain. Any animal demonstrating self-mutilation should be called to the attention of the veterinary staff immediately. The animal must be euthanized when the lesion interferes with the animals' ability to ambulate or reach the food and water.

Titers

Serum IgG titers were determined by ELISA serial dilution. Briefly, high binding ELISA plates (Corning Costar 3590) were coated overnight at 4C with 50ul of 4ug/ml antigen in PBS, pH7.5. Plates were aspirated then blocked for 3 hours at 25°C with PBS,

pH7.5, 2% milk. Plates were again aspirated then incubated with 50ul of serum diluted 1/200 through 1/437000 in PBS, pH7.5, 2% milk and incubated at 25°C for 2 hours. Plates were washed 3X with PBS, pH 7.5 0.05% tween-20 (PBST) then incubated with 1/5000 anti-Mouse IgG HRP (Jackson Immuno, 115-065-209) at 25°C for half an hour. Plates were washed again 3X with PBST then incubated with 50ul of TMB substrate for 15 min at 25°C then quenched with 1M sulfuric acid. Plates were read at 450nm and analyzed with GraphPad Prism software. Titers were determined as the point where the non-linear fitted curve determined 3-fold signal above background.

Cell Subtype Isolation and cDNA amplification

The isolation procedure described in this section was adapted from Reddy *et al*. and Cato *et al*. (105, 157). Germinal center cells were not explicitly mentioned in the introduction or discussion, but the protocol for their isolation was developed for this project and is worth noting.

Half an hour before sacrifice of immunized mice, 25ul of 2% Evans Blue (Sigma, E2129) in PBS, pH 7.5 was injected into both the footpad previously injected with antigen and the unimmunized control foot. Sacrifice was performed using carbon dioxide according to IAUCUC protocol AUC-2011-00016. Following sacrifice, the skin and fur around the leg was removed to reveal the blue stained popliteal lymph node behind back of the knee. The antigen-targeted popliteal lymph node, unimmunized control lymph node, and spleen were isolated and collected into buffer 1 (PBS, pH 7.5, 0.1% BSA, 2mM EDTA) on ice.

A single cell suspension was made from isolated organs by passing cells through a 70uM strainer into a 50mL conical tube (large gauge needles and the rubber stopper of

a 3mL syringe are extremely helpful to break up the organ and allow single cells to pass). An additional 5ml of Buffer 1 was used to rinse strainer. Cells were then centrifuged at 500 x *g* for 10 min in a swinging bucket rotor.

For Spleen Single Cell Suspension:

Loosened spleen cell pellet was resuspended in 2mL of red blood cell lysis buffer (155mM NH4Cl, 12mM NaHCO3, .1mM EDTA in E-pure water) then incubated at 25°C for 3.5 min. Following incubation, the lysis reaction was quenched by adding 20mL of Buffer 1 at 25°C. Cells were then washed by centrifugation at 500 x *g* for 10 min at 25°C, resuspended with 5mL Buffer 1, then centrifuged again. Washed cells were resuspend in 1ml Buffer 1, then 200ul of washed spleen suspension were diluted in 300ul of Buffer 1 in a 2ml eppendorf at 4°C for further cell subset isolation.

For Lymph Node Single Cell Suspension:

The entire pellet from the lymph node single cell suspension was resuspended in a 2ml eppendorf with 0.5mL of Buffer 1 at 4°C. In order to compare antigen-targeted proximal lymph node and control distal lymph node, 50ul of proximal lymph node and all of distal lymph node were centrifuged and spin down at 500 x *g* for 10 min at 25°C. Each pellet was then resuspended in 400ul of TRI reagent (Ambion AM9738) and stored at -80°C until mRNA isolation. The remained of the fraction from the antigen-targeted lymph node was used for subsequent cell isolation steps outlined in the next sections.

Plasma Cell Isolation For Each 500ul Fraction:

For each suspension, 1.25ug (2.5ul) of biotin anti-CD138 antibody (BD Pharma, 553713) was added followed by incubation at 4°C for 20 min while rotating. Cells were

then washed twice by centrifugation (500 x *g*, 10 min, 25°C) and resuspension in 1/2ml of ice-cold buffer 1. Following wash, 25ul of preblocked Streptavidin M280 (Invitrogen 2014-04) beads were added to the suspension then rotated at 4°C for 20min. Next, cell-bead suspensions were incubated on a DynaMag-2 magnet (Invitrogen, 123-21D) followed by incubation at 4°C for 2min. The unbound fraction was removed with pipette and used for GC cell isolation protocol described below. Beads and bound cells were washed 2X by removing magnet, adding 1mL of buffer 1 at 4°C, applying magnet again, and pipetting away buffer 1 and unbound cells. Following wash, 400ul of TRI reagent was added to the beads with bound cells then vortexed briefly and stored at -80°C until mRNA isolation.

Germinal Center Cell Isolation For Each Pc Depleted 500ul Fraction:

To each plasma-cell-depleted cell suspension, 6.5ul of biotinylated antibody mix was added (antibody mix: 1.25ug biotin anti-CD43 (BD Pharma 553269), 1ug biotin anti-CD11c (eBioscience 13-0114-82) and 1ug biotin-anti-IgD (eBioscience 13-5593-85)). Cell suspension and antibodies were incubated at 4°C for 20 min then washed 2X by centrifugation (500 x *g*, 10min, 25°C) and resuspension in 0.5ml buffer 1 at 4°C. Following wash, 20ul of anti-biotin beads (Miltenyi Biotec 120-000-900) were added then the mixture was rotated at 4°C for 20min. LS columns were pre-washed (Miltenyi Biotec 130-042-401) with 3mL of buffer, and then cell, antibody, and bead mixture was added to the LS columns while columns were attached to the provided magnet (Miltenyi Biotec 130-090-544). Once the mixture entered the column, the column was washed 3X with 3mL of buffer at 4°C and the flow through was collected. The collected flow through was pelleted by centrifuging 500 x *g* 10 then resuspended in 400ul TRI reagent and stored at -80°C until mRNA isolation.

Purifying mRNA:

100ul of chloroform was added to 400ul TRI reagent and vortexed immediately. After incubation for 5 min at 25°C, the mixture was centrifuged for 10 min at 12000 x *g* and 4°C. The clear aqueous phase (upper phase) was collected into a new 1.5ml eppendorf (~220ul) then 1 volume (200-300ul) of 70% ethanol was added to the mixture and vortexed immediately at 25°C. The mixture was added to an RNeasy column (Qiagen 74004) then centrifuged for 30 seconds at 12000 x *g* 25°C, followed by a wash with 500ul of RPE solution (included with RNEasy kit) then 500ul 80% ethanol according to manufacturers instructions. Following wash, columns were transfered to a new 2ml collection tube (included with RNEasy kit) then centrifuged for 5 min at 12000 x *g* and 25°C. Columns were then transferred to a new 1.5ml collection tube included with the kit, 20ul RNase free water was added, and then centrifuged for 1 min at 12000 x *g* and 25°C. Collected mRNA was then quantified with a Nanodrop instrument according to manufacturers instructions.

PCR of cDNA for gel analysis

cDNA was created from 100ng of mRNA in 20ul reactions with using MMLV-RT and oligo(dT) according to manufacturers directions from RETROscript kit (Ambion, AM1710). Primers for PCR for amplification of the heavy and light chains were designed according to the mouse variable gene primer set outlined by Krebber, *et al*. with Sfi1 sites introduced for incorporation into the APEX1 and Mopac16 vectors (158). Individual primers were synthesized by IDT, dissolved in E-pure water to 100uM, and mixed according to Krebber *et al*. 1ul of the forward and reverse primer mixtures and 2ul of

cDNA were added to standard Phusion polymerase amplification conditions in a 50ul PCR reaction. The following PCR conditions were used to amplify cDNA:

Temperature	**Time (min, seconds)**
98 degC	3,0
a	**4 cycles**
98 degC	0,20
50 degC	1,0
72 degC	1,0
b	**4 cycles**
98 degC	0,20
55 degC	1,0
72 degC	1,0
c	**4 cycles**
98 degC	0,20
63 degC	1,0
72 degC	1,0
d	**16 cycles**
72 degC	7,0
4 degC	forever

Table 4.5: PCR conditions for the amplification of cDNA with Phusion polymerase and variable gene primer sets "VHf" and "IgG constant reverse"

After completion, PCR reactions were then resolved with a 1% agarose gel according to standard DNA electrophoresis conditions. Products at ~350bp were excised and used for subsequent analysis.

For specific amplification of IgG, IgM, T15, or GapDH, primers were designed in order to minimize possible overlaps and contaminations from homologous cDNA. Amplifications were done according to standard conditions for Phusion polymerase

(NEB, M0535L) with 1.5ul cDNA template included in a 50ul reaction. 20 cycles were performed with an annealing temperature set to 55°C for 30 seconds followed by a 30 second extension time at 72°C. After completion, PCR reactions were resolved with a 3% agarose gel according to standard DNA electrophoresis conditions.

IgG const for	TGACCTGGAACTCTGGATCCCTGTC
IgG const rev	CTGGGACTGTACATATGCAAGGCTTACAAC
Gapd for	GGTGAAGGTCGGTGTGAACG
Gapdh rev	CTCGCTCCTGGAAGATGGTG
T15 S107f	TTATTACTCGCGGCCCAGCCGGCCATGGCGCTGGAGTGGATTGCTGCAAGTAGAAACAAAGC
T15 J01r	GGCCGCGAATTCGGCCCCCGAGGCCGACTGAGGAAACGGTGACCGTGGTCCCTG
IgM for	CATCCACCTGCTGTGTACCTGCTG
IgM rev	CAACGCAGGTATAGGTCTCTCCGGAG

Table 4.6: Primers for cDNA analysis from targeted lymph nodes.

Sequencing Analysis

The frequency of T15 idiotype antibodies from various anatomical compartments and cell types was analyzed by amplifying a library of IgG transcripts from a mouse immunized via footpad injection with PC-BSA and Titermax Gold. The cDNA from the spleen plasma cells, lymph node plasma cells, or whole lymph nodes were amplified using the 5' heavy chain primer set "VHfor" based on designed from Krebber *et al*. and 3' heavy chain "IgG constant reverse" primers that amplify IgG1, 2a, 2b and 3 (158). Each primer from the "VHfor" set was resuspended in purified water to 100uM and mixed according to the table below.

Name	Sequence	% in mix
FOR 1	ATGGCCCAGCCGGCCATGGCGGAKGTRMAGCTTCAGGAGTC	7.6%
FOR 2	ATGGCCCAGCCGGCCATGGCGGAGGTBCAGCTBCAGCAGTC	7.6%
FOR 3	ATGGCCCAGCCGGCCATGGCGCAGGTGCAGCTGAAGSASTC	5.7%
FOR 4	ATGGCCCAGCCGGCCATGGCGGAGGTCCARCTGCAACARTC	7.6%
FOR 5	ATGGCCCAGCCGGCCATGGCGCAGGTYCAGCTBCAGCARTC	13.2%
FOR 6	ATGGCCCAGCCGGCCATGGCGCAGGTYCARCTGCAGCAGTC	3.8%
FOR 7	ATGGCCCAGCCGGCCATGGCGCAGGTCCACGTGAAGCAGTC	1.9%
FOR 8	ATGGCCCAGCCGGCCATGGCGGAGGTGAASSTGGTGGAATC	3.8%
FOR 9	ATGGCCCAGCCGGCCATGGCGGAVGTGAWGYTGGTGGAGTC	9.5%
FOR 10	ATGGCCCAGCCGGCCATGGCGGAGGTGCAGSKGGTGGAGTC	3.8%
FOR 11	ATGGCCCAGCCGGCCATGGCGGAKGTGCAMCTGGTGGAGTC	3.8%
FOR 12	ATGGCCCAGCCGGCCATGGCGGAGGTGAAGCTGATGGARTC	3.8%
FOR 13	ATGGCCCAGCCGGCCATGGCGGAGGTGCARCTTGTTGAGTC	1.9%
FOR 14	ATGGCCCAGCCGGCCATGGCGGARGTRAAGCTTCTCGAGTC	3.8%
FOR 15	ATGGCCCAGCCGGCCATGGCGGAAGTGAARSTTGAGGAGTC	3.8%
FOR 16	ATGGCCCAGCCGGCCATGGCGCAGGTTACTCTRAAAGWGTSTG	9.5%
FOR 17	ATGGCCCAGCCGGCCATGGCGCAGGTCCAACTVCAGCARCC	6.6%
FOR 18	ATGGCCCAGCCGGCCATGGCGGATGTGAACTTGGAAGTGTC	1.3%
FOR 19	ATGGCCCAGCCGGCCATGGCGGAGGTGAAGGTCATCGAGTC	1.3%

Table 4.7: The primer mix derived from Krebber *et al*. with 5' sfi site added

Each of the primers from IgG rev set described in the table below were diluted to 100uM each and a mix of the four primers at a 1:1:1:1 ratio created "IgG constant reverse" primer mix.

SC-IgG1-constrev	TTCGGCCCCCGAGGCCGAGCCAGAGTTCCAGGTCACTGTCACTG
SC-IgG2a-constrev	TTCGGCCCCCGAGGCCGAGCCAGAGTTCCAGGTCAAGGTCACTG
SC-IgG2b-constrev	TTCGGCCCCCGAGGCCGAGCCAGAGTTCCAAGTCACAGTCACTG
SC-IgG3-constrev	TTCGGCCCCCGAGGCCGAGCCATAGTTCCATTTTACAGTTACCG

Table 4.8: Reverse primers designed to amplify IgG1,2a,2b and 3.

cDNA was amplified with 1.5ul cDNA, 1ul of each forward and reverse primer mix, and the standard Phusion polymerase amplification conditions for a 50ul reaction (table 3.4). The reaction was performed via the PCR cycle described in the previous

section. Following amplification, the PCR reaction was resolved using standard electrophoresis conditions with a 1% agarose gel, then the ~450bp DNA band was excised and purified. Purified insert was digested using standard sfi1 conditions, followed by PCR cleanup then ligation into the pak200 vector. Ligations were transformed into Jude1 cells. Following overnight growth at 37°C on selective plates, individual colonies were selected and sequenced using standard Sanger sequencing.

The sequence for the T15 idiotype was compiled from the following publications (149, 150).

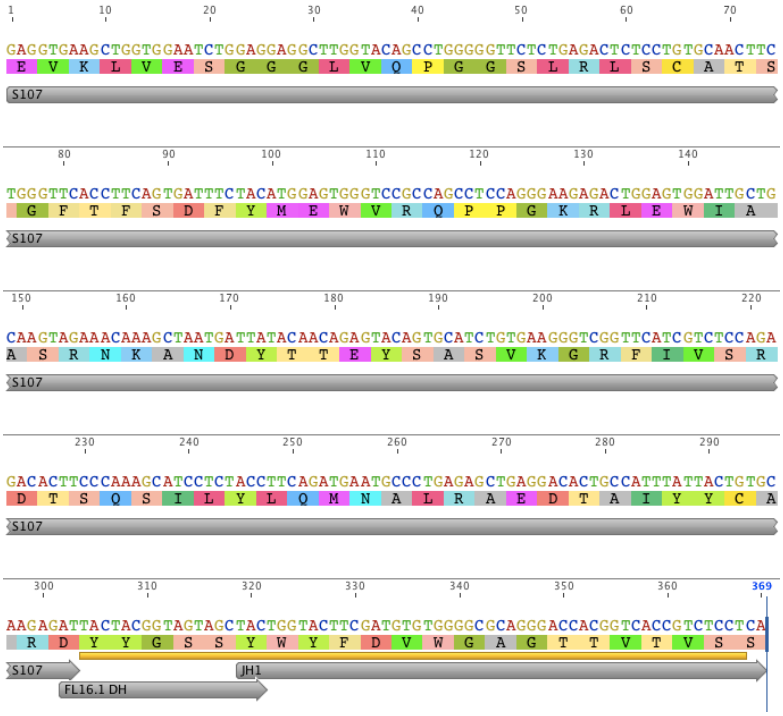

Figure 4.9: T15 DNA sequence, protein translation and V-D-J usage compiled from previous publications (149, 150).

DNA analysis software (Geneious Pro 5.4.6) was then employed to determine sequence homology to the established T15 sequence (Figure 3.9). Matches were determined by identical usage of V-D-J genes and identical CDRH3 sequences.

Chapter 5

Conclusions

The work detailed in this manuscript has resulted in the isolation of a high affinity antibody D, the first antibody shown to inhibit classical complement activity by inhibiting the C1s protease on the C1 complex. The disregulation of classical complement activation is associated with numerous human diseases including rheumatoid arthritis, transplant rejection, ischemic reperfusion injury and neurological disorders; therefore the regulation of this pathway is highly desirable. In order to discover antibody D, novel protocols and strategies were used for discovery and characterization. Extensive assay development was done with a focus on creating cell and plate based assays to demonstrate antibody D can regulate classical complement when the pathway is selectively activated by surface bound immunoglobulin. Through novel classical complement inhibition assays, we demonstrated the first example of an antibody that specifically regulates the classical complement pathway by targeting the C1s protease on the pathway initiating C1-complex.

It is further shown that affinity maturation of antibody D results in higher levels of complement inhibition at various antibody concentrations. The affinity-matured variant was only a 2-fold improvement over the parental antibody, but inhibition of classical complement activity was improved in all three assays we developed. We therefore assume that further affinity maturation should be pursued in the future in order to further increase the effectiveness of the antibody. However, we experienced great difficulty affinity maturing antibody D, while other studies performed using similar methods achieved much greater affinity improvement (>200 fold in some cases). The difficult in achieving a significant enhancement in the affinity of antibody D may be due

to its unusually long CDR3, which may be important for binding to the active site, cleft of C1s. In this case, further affinity improvements may need introducing mutations within the CDRH3 loop in order further optimize the contact interface.

The most significant limitation of antibody D and its affinity matured mutant D.35 is the high concentrations required to achieve ~50% inhibition of complement activity (>5uM in our studies). Even with a further affinity matured antibody D variant, it may be difficult to inhibit classical complement activity completely at more therapeutically relevant antibody concentrations (<1uM). In order to address the exceedingly high concentration of F_{AB} D.35 inhibitor required for complement inhibition, a combination of antibody inhibitors might be a desirable approach to limit complement activation at lower antibody concentrations. It is therefore particularly relevant that we have shown novel methodologies for discovering and affinity maturing such antibodies that can be easily tailored to different classical complement proteins or an entirely different pathway. Alternative antibody-based classical complement inhibition strategies that prevent C1 complex signaling could be developed by slightly modifying our discovery scheme for development of antibodies that bind the proenzyme form of C1s or C1r.

Another important aspect of the work detailed in this manuscript was the characterization of the lymphocytes and immune responses in humanized NSG ((NOD.Cg-Prkdc^{scid} Il2rg$^{tm1Wjl/SzJ}$) mice at 6- and 12-weeks post-engraftment. Humanized mice are generated through the engraftment of human CD34+ hematopoietic stem cells into immune-deficient mice. Once engrafted, the human stem cells home in to the bone marrow where they divide and differentiate into human cells of the myeloid and lymphoid lineages. Humanized mice are particularly relevant because they provide an important preclinical model that enables the investigation of human-specific infectious

diseases, most notably human-specific diseases such as HIV, Dengue virus and Epstein-Barr virus (EBV).

In order to better understand the model, we sought to characterize the human immune cells produced by humanized NSG mice, most notably the B and T lymphocytes, post-engraftment with human CD34+ HSC cells. We detected development of naïve human B and T cells and their various subtypes, as well as other human immune cells from engrafted mice. However, attempts to generate a robust antibody response to antigens were unsuccessful. Therefore, we conclude that NSG humanized mice developed in this study are suitable for studying the naïve B cells, however they are not suitable for the analysis of activated B-cells.

One reason thought to be partially responsible for the weak antibody response is that human T cell selection occurs against murine MHC I / II thereby altering human T cell help to mature B lymphocytes (1). It is important to determine all potential deviations humanized mice lymphocytes may have from their normal human counterpart that might impact the relevance of humanized mouse as a model for the study of human immune cells *in vivo*. Previous accounts describing the mature naïve B cell subsets generated in NSG humanized mice have not thoroughly characterized the B cell antibody repertoires in depth. One aspect that may deviate from normal human characteristics is the repertoire of antibodies produced by the naïve mature B cells and the active B cell immune response. In subsequent studies the mature naïve B cell population was sequenced and analyzed and it was determined that it was chiefly indistinguishable from those in human blood cells (2).

Last, we introduced a novel strategy for the generation of polarized antibody repertoires for use in therapeutic monoclonal antibody discovery. Reddy *et al*. showed that the most abundant antibody V genes (.5-10% frequency) expressed by bone marrow

plasma cells (BM-PCs) 7 days post-boost immunization correspond to antigen-specific antibodies. However, not all highly frequency V genes in the BM-PC repertoire are antigen specific necessitating the testing of several combinations of the most frequent VH and VL genes to find antibodies with desired affinity and specificity. Therefore, we sought to develop a technique that would isolate more polarized repertoires with many antigen specific antibodies and less irrelevant ones. Our technique for repertoire isolation involved targeted antigen delivery to a specific lymph node and isolation of that particular lymph node repertoire. Lymph nodes do not hold long-lived plasma cells, and therefore we expected less plasma cells producing irrelevant antibody.

Following primary footpad immunization of two BALB/c mice with a small hapten (phosphorylcholine conjugated to BSA), we used PCR and Sanger sequencing of the antibody variable genes to investigate the repertoire of antibodies found in the targeted popliteal lymph node. Sequencing of the heavy chain V-gene repertoire revealed that mRNA transcripts isolated from the antigen-targeted lymph nodes were >20% of antibodies in known idiotype (T15) that specifically binds the hapten. When two additional mice were repeatedly immunized with a more complex antigen (Ebola virus like particles), Sanger sequencing analysis of the antigen targeted lymph nodes revealed a highly polarized repertoire in one mouse (>20% of the antibodies corresponded to one heavy chain sequence) and a moderately polarized repertoire in another mouse (>5%).

We expect that this work will be the foundation of an overall improved protocol for monoclonal antibody discovery that accelerates the speed and enhances the simplicity of discovery techniques. Both of these repertoires were highly polarized and therefore accomplished our goals, however, future work should focus on the validation of these highly polarized libraries by making the antibodies for the polarized repertoire in order to

determine their specificity. The combination of polarized repertoires with confirmed antigen specificity is currently undergoing further study.

Appendix 1

Modeling Inhibition of C1s and Classical Complement by Antibody D

INTRODUCTION

Antibody D and its affinity-maturated variant D.35 described in Chapter 2 inhibit classical complement activity by inhibiting the C1s protease of the biochemical cascade. However, the concentrations of antibody required to inhibit the classical complement are much too high in order to be considered a serious therapeutic candidate. In the results of Chapter 2, we establish that affinity maturation of antibody D increases complement inhibition at the same concentrations. Furthermore, we established that the ~10-fold relative affinity increase via changing antibody format from fAb to IgG also increases the relative inhibition of C1s proteolysis of its substrate C2. Therefore, it is conceivable that further affinity maturation would lead to increased complement inhibition. In this work, we set to modeling the interaction between antibody and C1s to predict the dissociation constant necessary for inhibition of complement at therapeutically relevant antibody concentrations.

RESULTS

Modeling C1s inhibition by an Antibody Predicts Affinity Goals for further D Improvement

The mathematical model described in the materials and method section can predict substrate cleavage levels for a given set of inputs (time, K_D, concentrations, etc). In order to validate the model, it was used to predict outcomes for scenarios tested

experimentally. Once validated, it was then used to predict dissociation constants required for therapeutic effectiveness at physiological conditions.

Validating Mathematical Model using Experimental Results

Experimental conditions that are easily measured by SDS-PAGE were used in order to test the predictive abilities of the model. These experimental results were overlaid with the predicted outcomes for the same conditions with an antibody of various dissociation constants in the figure below (A.1).

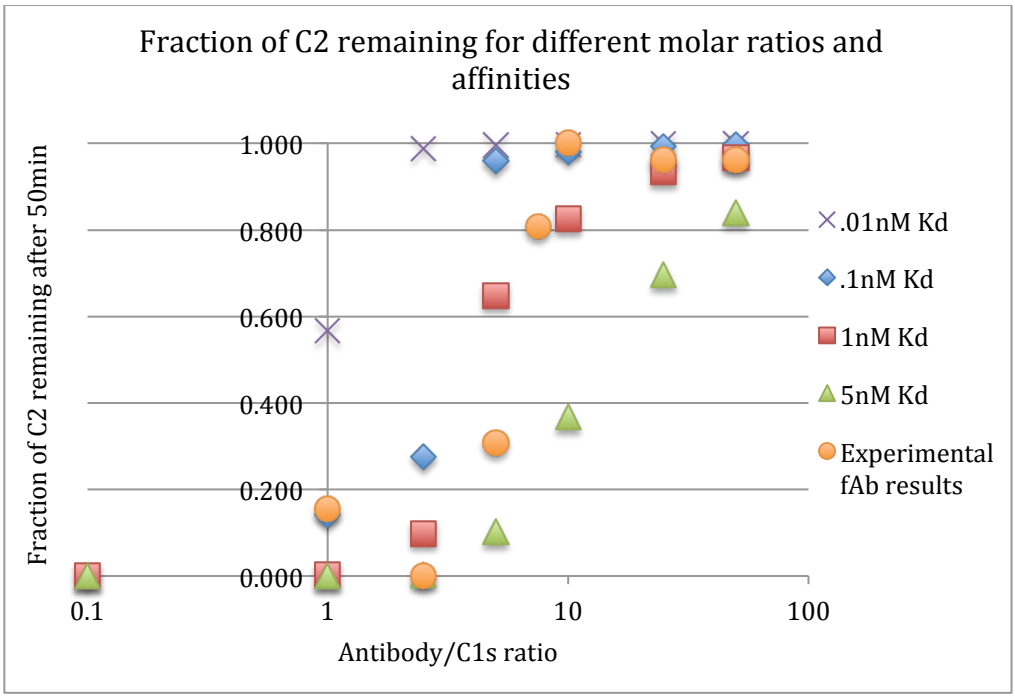

Figure A.1: Experimental Results Overlaid with Model Predictions

The inhibitor F_{AB} D has been shown to have a K_D = 1.7nM and the model accurately predicts the amount of substrate remaining for an antibody inhibitor with

roughly that concentration. These results confirm that the model can accurately predict the impact of a reversible inhibitor on C1s and substrate with user-defined inputs.

Employing Mathematical Model to Set K_D Goal for Therapeutic Relevance

Once the validity of the model was confirmed, the inputs were then changed to represent the actual concentrations *in vivo*. In order to determine the dissociation constant of an antibody necessary for inhibition of the classical complement at physiological substrate and enzyme concentrations, three important questions were proposed:

1. What is the expected serum concentration of a therapeutic antibody?
2. What is the acceptable free enzyme concentration required for inhibition of the entire pathway?
3. What Kd does antibody D need to have in order to achieve this level of inhibition at physiological conditions?

The first question was answered by reviewing the monoclonal antibody package inserts that come with such drugs as Herceptin. A review of published clinical information concerning therapeutic antibody serum concentrations found that the most common antibody trough concentration was ~660nM (159). Thus we can expect that a monoclonal IgG would need to be effective at this concentration. The model will ultimately be used to determine what dissociation constant will inhibit complement activity at 660nM of therapeutic antibody.

The model is able to determine the amount of C1s activity in the presence of an inhibitory antibody. However, it does not determine the level of C1s activity that is acceptable in order to effectively stop classical complement mediated cell lysis. In order

to determine the maximum acceptable active free C1s enzyme level that does not result in cell lysis, the free active enzyme predicted by the model is compared to the experimentally determined classical complement mediated lysis of RAMOS cell under the same conditions. The overlaid graph is shown below (figure A2)

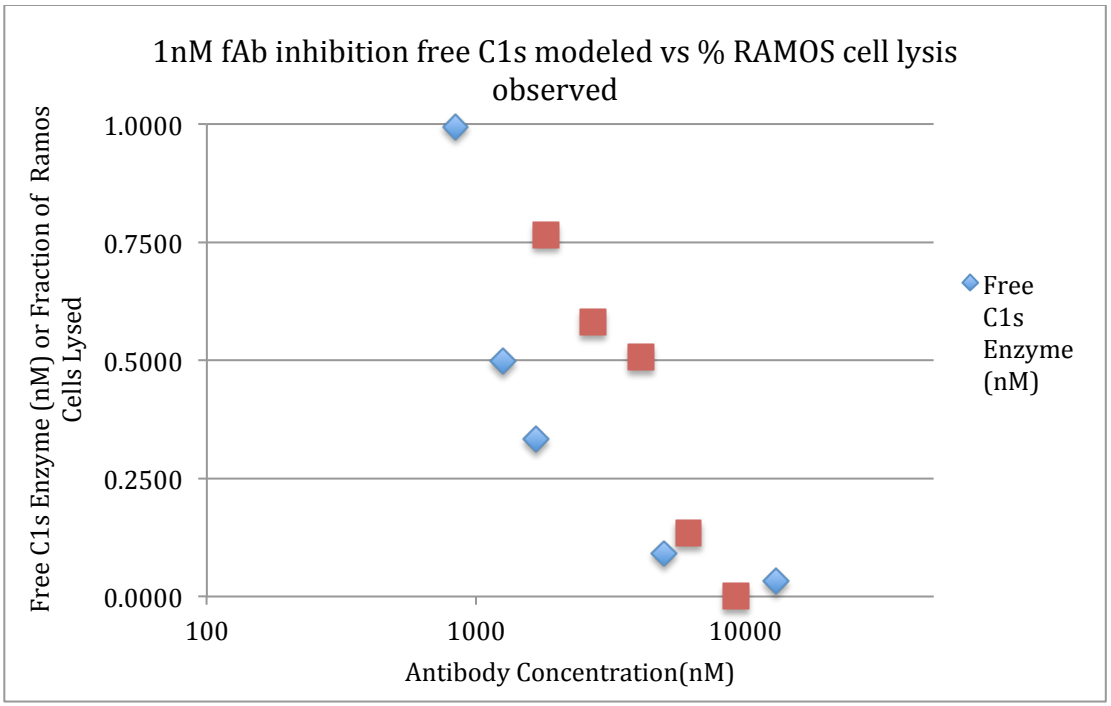

Figure A.2: Comparison of free enzyme (nM) predicted by model and experimentally determined fraction Ramos Cells lysed at simiar antibody concentrations.

In order to maintain cell integrity, the model predicts that ~25pM of C1s can be unbound by antibody and the cells will still maintain their integrity. Next different dissociation constants were modeled in order to predict the K_D necessary to achieve only .025nM free C1s enzyme with 660nM of antibody.

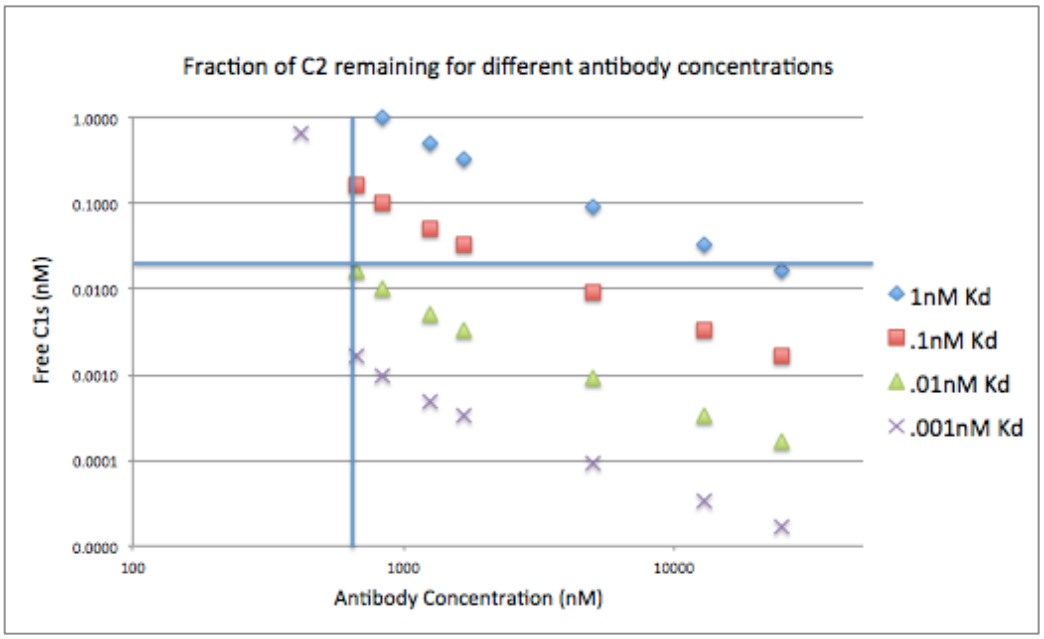

Figure A.3: Predicted free enzyme for antibodies with different dissociation constants and 660nM antibody (vertical blue line) and serum concentrations of other components. Horizontal blue line indicates .025nM free C1s goal.

An antibody with at least .01nM dissociation constant achieves .025pM of free C1s at 660nM. Therefore, according the model, an antibody that binds the same epitope as antibody D with a dissociation constant of .01nM will inhibit classical complement mediated lysis of RAMOS cells at therapeutically relevant concentrations.. This is the goal for future C1s inhibiting antibody dissociation constant.

DISCUSSION

The target dissociation constant for further affinity maturation was determined using the model herein described. While simplifying assumptions may flaw the model (listed in M&M), linking the experimental results to the model compensates for erroneous assumptions. Therefore, we confidently set the experimental goal of 10pM

dissociation constant in order to inhibit classical complement activity at therapeutic concentrations.

The goal determined from the model, 10pM K_D, may be attained in a number of ways: through the increase in apparent affinity associated with bivalency, through discovery of a new higher affinity antibody, or further affinity maturation. The difficulty in discovering another antibody that binds and inhibits the C1s enzyme is a daunting task because the antibody discovery techniques do not necessarily discover antibodies that both bind and inhibit C1s. Therefore the process could take an exceedingly long time to uncover the antibody with no guarantee that the antibody will have a higher affinity. Instead, antibody D.35 should be further improved by the strategies of affinity maturation and apparent affinity increase associated with bivalency.

MATERIALS AND METHODS

Mathematical Modeling of C1s Inhibition

The following is the derivation of the model for a system in which an antibody inhibits an enzyme by reversible binding. This section will derive the underlying equations for this model using constants that can be substituted for any enzyme-antibody-substrate system. The underlying assumption of this system is the antibody is a steric inhibitor; therefore enzyme bound by an antibody is not able to perform an enzymatic reaction. There are two important components to this model: enzyme kinetics that governs the rate of substrate proteolysis and reversible binding thermodynamics that governs the amount of free enzyme available for kinetic reactions. These two components are independently modeled, then combined.

Modeling Kinetic Parameters: Proteolysis

In order to model the impact of inhibitory antibodies on C1s, it is first necessary to model substrate C2 or C4 proteolysis in the absence of any inhibitor. This is commonly done in chemical engineering using Michaelis-Menten kinetic model of enzymes. This model is the best-known model of enzyme kinetics and relies on the assumption that enzymes form a reversible complex with their substrate before catalyzing an irreversible enzymatic reaction(160, 161). The Michaelis-Menten model is written as follows:

$$E + S \rightleftharpoons ES \longrightarrow E + P$$

Where E is the enzyme concentration, S is the substrate concentration and P is the product concentration. For the interaction modeled in this work, E is C1s, S is one of the C1s substrates C2 or C4, and P is the cleaved substrate concentration. This model can be expressed mathematically in terms of rate constants and product concentrations. The model is commonly used in textbooks to derive the Michaelis-Menten kinetic equation:

$$v_0 = \frac{v_{\max}[S]}{[S] + K_M} = \frac{k_{cat}[E][S]}{[S] + K_M} = \frac{\partial S}{\partial t}$$

K_M is the Michaelis-Menten constant, and k_{cat} is the turnover number; each of these numbers is a property of the enzyme and can be found in the BRENDA enzyme database. This model assumes the substrate is in instantaneous chemical equilibrium with the complex. This equation can be solved to express the free enzyme concentration (i.e. not in complex with substrate) as a function of substrate concentration and time:

$$[E] = \frac{[S_0] - [S] + K_M \ln(\frac{[S_0]}{[S]})}{k_{cat} t}$$

With this equation it is possible to model the fraction of substrate remaining after a set time (50mins in this case) as a function of free enzyme concentration.

Modeling Thermodynamic Parameters:

The other component of this model is the interaction between enzyme and antibody (C1s and D) that inhibits the ability of the enzyme to proteolyze substrate. In the case of an inhibitory reversible binder, such as antibody D, the free enzyme concentration is based on thermodynamic equilibrium. When the antibody binds the enzyme, it is not free to proteolyze substrate. Unbound enzyme is called "free enzyme" and is available to proteolyze substrate. The thermodynamic equilibrium can be expressed in terms of the dissociation constant and written in the following manner:

$$K_D = \frac{[\text{unbound C1s}][\text{unbound fAb}]}{[\text{fAb} - \text{C1s- complex}]} = \frac{[E_0 - X][F_0 - X]}{[X]}$$

E_0 is the total enzyme in solution, F_0 is the total antibody in solution, and X is the concentration of the antibody-enzyme complex. For simplicity, it is assumed the antibody is monovalent F_{AB}, which is true of the experiments performed in this study. This equation is rearranged to solve for the concentration of the antibody-enzyme complex, X:

$$[X] = \frac{K_D + [E_0] + [F_0] - \sqrt{(-K_D - [E_0] - [F_0])^2 - 4[[E_0][F_0])}}{2}$$

The antibody-enzyme complex can be expressed in terms of the "free enzyme concentration", [E]:

$$[E]+[X] = [E_0]$$

Combining these two equations expresses the thermodynamic term in terms of initial conditions and the free enzyme concentration.

Combined Parameters and Modeling in Excel

The combining the kinetic and thermodynaic equations from the previous two subsections allows for expression of the substrate concentration over time in terms of known input values such as k_{cat}, $K_{M,}$ substrate initial concentration, total antibody concentration, total enzyme concentration and the dissociation constant K_D. In order to use these values and model scenarios of interest, an excel file is built that first determines "free enzyme" concentration using the thermodynamic equations. The free enzyme concentration is then used as an input for the kinetic equation. This model can then be used to predict various outputs from defined input conditions. The most useful output parameter is the substrate concentration, [S]; however it is difficult to solve for this parameter using the final kinetic equation. Instead the excel file is set up such that [S] is an input and the output is time, a much simpler parameter to solve for. In order to determine the substrate concentration [S] at a given time, the Goal Seek function is employed to seek the substrate concentration present at a given time. For example, using the kinetic constants for C1s (enzyme) towards C2 (substrate) and known input concentrations of enzyme, substrate and inhibitor, the impact of the dissociation constant K_D can be determined on the amount of substrate cleaved in 50 minutes.

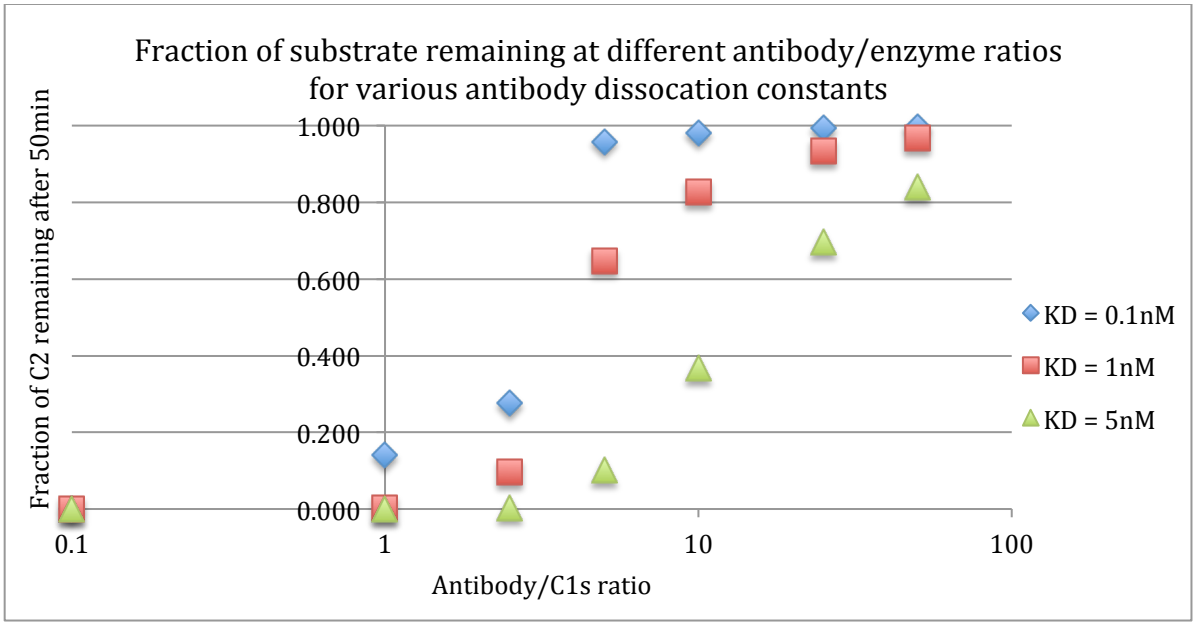

Figure A.4: Example output of model for various dissociation constants

In this example, it is clear that for the given inputs the dissociation constant impacts substrate cleavage dramatically at a 5-fold antibody to enzyme ratio. The dissociation constant does not have a significant impact when large excess of either component is present. For a given amount of substrate cleavage in 50 minutes, a lower dissociation constant (higher affinity) results in less inhibitor required. Sample inputs are shown in the table below, including the enzyme constants from BRENDA enzyme database that are used for all scenarios.

kcat (1/s)		5.1
Km (nM)		6100
C2 init conc (nM)	So	3000
C2 final conc (nM)	S	826.574296
Free Enzy conc (nM)	E	0.656
time (sec)	t	3000.000016
Frac Cleaved	S/So	0.275524765
50 mins = 3000 sec		

Table A.1: Example Inputs for Model

Assumptions Inherent in the Model

The model makes many simplifying assumptions.

1. C2 and C4 can be modeled as one substrate.
2. C1s is free floating in a solution, instead of immobilized to a surface bound antibody
3. The two C1s molecules present in the C1 complex can be assumed to be two C1s molecules free floating in solution
4. All available C1s is activated

The first assumption, that substrates C2 and C4 can be modeled as one substrate, is acceptable because the k_{cat} and K_M of C1s for these substrates is nearly identical. The other simplifying assumptions are necessary for simplicity. In the results section, the model will be linked to real-world data in order to compensate for any resulting flaws from these assumptions.

References

1. Murphy K, Travers P, Walport M. Janeway's Immunobiology. 7th ed. New York, NY 10016: Garland Science; 2008.
2. Rosenstiel P, Philipp EER, Schreiber S, Bosch TCG. Evolution and function of innate immune receptors--insights from marine invertebrates. Journal of innate immunity. 2009;1(4):291-300.
3. Medzhitov R. Recognition of microorganisms and activation of the immune response. Nature. 2007;449(7164):819-26.
4. Grommé M, Neefjes J. Antigen degradation or presentation by MHC class I molecules via classical and non-classical pathways. Molecular Immunology. 2002;39(3-4):181-202.
5. Lanzavecchia A, Sallusto F. Human B cell memory. Curr Opin Immunol. 2009;21(3):298-304.
6. Marasco WA, Sui J. The growth and potential of human antiviral monoclonal antibody therapeutics. Nat Biotechnol. 2007;25(12):1421-34.
7. Batista FD, Harwood NE. The who, how and where of antigen presentation to B cells. Nature Reviews Immunology. 2009;9(1):15-27.
8. Dall'Acqua WF, Kiener PA, Wu H. Properties of human IgG1s engineered for enhanced binding to the neonatal Fc receptor (FcRn). J Biol Chem. 2006;281(33):23514-24.
9. Kubota T, Niwa R, Satoh M, Akinaga S, Shitara K, Hanai N. Engineered therapeutic antibodies with improved effector functions. Cancer science. 2009;100(9):1566-72.
10. Tuma RS. Phase I antibody risks, trial safety examined. Journal of the National Cancer Institute. 2006 Jul 19;Sect. 956-8.
11. Aggarwal S. What's fueling the biotech engine--2010 to 2011. Nature Biotechnology. 2011;29(12):1083-9.
12. Carter PJ. Potent antibody therapeutics by design. Nat Rev Immunol. 2006;6(5):343-57.
13. Kindt TJ, Goldsby RA, Osborne BA. Kuby Immunology
. 6 ed. New York2006.
14. Schatz DG. V(D)J recombination. Immunological reviews. 2004;200:5-11.
15. Orange JS. Formation and function of the lytic NK-cell immunological synapse. Nat Rev Immunol. 2008;8(9):713-25.
16. Zalevsky J, Chamberlain AK, Horton HM, Karki S, Leung IWL, Sproule TJ, et al. Enhanced antibody half-life improves in vivo activity. Nature Biotechnology. 2010.
17. Roopenian DC, Akilesh S. FcRn: the neonatal Fc receptor comes of age. Nat Rev Immunol. 2007;7(9):715-25.
18. Morell A, Terry WD, Waldmann TA. Metabolic properties of IgG subclasses in man. The Journal of clinical investigation. 1970;49(4):673-80.

19. Tao MH, Morrison SL. Studies of aglycosylated chimeric mouse-human IgG. Role of carbohydrate in the structure and effector functions mediated by the human IgG constant region. J Immunol. 1989;143(8):2595-601.
20. Walport MJ. Complement. First of two parts. New England Journal of Medicine. 2001;344(14):1058-66.
21. Arlaud GJ, Gaboriaud C, Thielens NM, Rossi V. Structural biology of C1. Biochem Soc Trans. 2002;30(Pt 6):1001-6.
22. Anthony DeFranco RL, Miranda Robertson. Immunity: The Immune Response to Infectious and Inflammatory Disease: Oxford University Press, USA 2007.
23. Gál P, Barna L, Kocsis A, Závodszky P. Serine proteases of the classical and lectin pathways: similarities and differences. Immunobiology. 2007;212(4-5):267-77.
24. Carsetti R, Rosado MM, Wardmann H. Peripheral development of B cells in mouse and man. Immunol Rev. 2004;197:179-91.
25. Gatto D, Brink R. The germinal center reaction. The Journal of allergy and clinical immunology. 2010;126(5):898-907; quiz 8-9.
26. Pillai S, Cariappa A. The follicular versus marginal zone B lymphocyte cell fate decision. Nature Reviews Immunology. 2009;9(11):767-77.
27. Harwood NE, Batista FD. Early events in B cell activation. Annu Rev Immunol. 2010;28:185-210.
28. Oracki SA, Walker JA, Hibbs ML, Corcoran LM, Tarlinton DM. Plasma cell development and survival. Immunol Rev. 2010;237(1):140-59.
29. Todorovska A, Roovers RC, Dolezal O, Kortt AA, Hoogenboom HR, Hudson PJ. Design and application of diabodies, triabodies and tetrabodies for cancer targeting. Journal of Immunological Methods. 2001;248(1-2):47-66.
30. Kortt AA, Dolezal O, Power BE, Hudson PJ. Dimeric and trimeric antibodies: high avidity scFvs for cancer targeting. Biomolecular engineering. 2001;18(3):95-108.
31. Winau F, Winau R. Emil von Behring and serum therapy.2002.
32. Dunlop JM. The history of immunisation.1988.
33. Köhler G, Milstein C. Continuous cultures of fused cells secreting antibody of predefined specificity. Nature. 1975;256(5517):495-7.
34. Mechetner E. Development and characterization of mouse hybridomas. Methods in molecular biology (Clifton, NJ). 2007;378:1-13.
35. Maynard J, Georgiou G. Antibody engineering. Annual review of biomedical engineering. 2000;2:339-76.
36. Rathanaswami P, Roalstad S, Roskos L, Su QJ, Lackie S, Babcook J. Demonstration of an in vivo generated sub-picomolar affinity fully human monoclonal antibody to interleukin-8. Biochemical and Biophysical Research Communications. 2005;334(4):1004-13.
37. Bernett MJ, Karki S, Moore GL, Leung IWL, Chen H, Pong E, et al. Engineering fully human monoclonal antibodies from murine variable regions. Journal of Molecular Biology. 2010;396(5):1474-90.
38. Crowe JE. Recent advances in the study of human antibody responses to influenza virus using optimized human hybridoma approaches. Vaccine. 2009;27 Suppl 6:G47-51.

39. Yu X, McGraw PA, House FS, Crowe JE. An optimized electrofusion-based protocol for generating virus-specific human monoclonal antibodies. Journal of Immunological Methods. 2008;336(2):142-51.
40. Yamashita M, Katakura Y, Shirahata S. Recent advances in the generation of human monoclonal antibody. Cytotechnology. 2007;55(2-3):55-60.
41. Almagro JC, Fransson J. Humanization of antibodies. Frontiers in bioscience : a journal and virtual library. 2008;13:1619-33.
42. Zanella I, Verardi R, Negrini R, Poiesi C, Ghielmi S, Albertini A. New heteromyeloma cell lines for the production of human monoclonal antibodies. Journal of Immunological Methods. 1992;156(2):205-15.
43. Sheridan C. Fresh from the biologic pipeline-2009. Nat Biotechnol. 2010;28(4):307-10.
44. Brehm MA, Shultz LD, Greiner DL. Humanized mouse models to study human diseases. Curr Opin Endocrinol Diabetes Obes. 2010;17(2):120-5.
45. Shultz LD, Ishikawa F, Greiner DL. Humanized mice in translational biomedical research. Nat Rev Immunol. 2007;7(2):118-30.
46. Shultz LD, Schweitzer PA, Christianson SW, Gott B, Schweitzer IB, Tennent B, et al. Multiple defects in innate and adaptive immunologic function in NOD/LtSz-scid mice. J Immunol. 1995;154(1):180-91.
47. Kirchgessner CU, Patil CK, Evans JW, Cuomo CA, Fried LM, Carter T, et al. DNA-dependent kinase (p350) as a candidate gene for the murine SCID defect. Science. 1995;267(5201):1178-83.
48. Pearson T, Greiner DL, Shultz LD. Creation of "humanized" mice to study human immunity. Curr Protoc Immunol. 2008;Chapter 15:Unit 15.21.
49. Brehm MA, Cuthbert A, Yang C, Miller DM, DiIorio P, Laning J, et al. Parameters for establishing humanized mouse models to study human immunity: analysis of human hematopoietic stem cell engraftment in three immunodeficient strains of mice bearing the IL2rgamma(null) mutation. Clinical immunology (Orlando, Fla). 2010;135(1):84-98.
50. Ishikawa F, Yasukawa M, Lyons B, Yoshida S, Miyamoto T, Yoshimoto G, et al. Development of functional human blood and immune systems in NOD/SCID/IL2 receptor {gamma} chain(null) mice. Blood. 2005;106(5):1565-73.
51. Manz MG, Di Santo JP. Renaissance for mouse models of human hematopoiesis and immunobiology. Nature immunology2009. p. 1039-42.
52. Ito R, Takahashi T, Katano I, Ito M. Current advances in humanized mouse models. Cellular & Molecular Immunology. 2012;9(3):208-14.
53. Ippolito G, Hoi K, Reddy S, Carroll S, Ge X. Antibody Repertoires in Humanized NOD-scid-IL2Rγnull Mice and Human B Cells Reveals Human-Like Diversification and Tolerance Checkpoints in the …. PLoS ONE. 2012.
54. Hoogenboom HR. Selecting and screening recombinant antibody libraries. Nat Biotechnol. 2005;23(9):1105-16.
55. McCafferty J, Griffiths AD, Winter G, Chiswell DJ. Phage antibodies: filamentous phage displaying antibody variable domains. Nature. 1990;348(6301):552-4.

56. Clackson T, Hoogenboom HR, Griffiths AD, Winter G. Making antibody fragments using phage display libraries. Nature. 1991;352(6336):624-8.
57. Burton DR, Barbas CF, Persson MA, Koenig S, Chanock RM, Lerner RA. A large array of human monoclonal antibodies to type 1 human immunodeficiency virus from combinatorial libraries of asymptomatic seropositive individuals. Proc Natl Acad Sci USA. 1991;88(22):10134-7.
58. Marks JD, Hoogenboom HR, Bonnert TP, McCafferty J, Griffiths AD, Winter G. By-passing immunization. Human antibodies from V-gene libraries displayed on phage. Journal of Molecular Biology. 1991;222(3):581-97.
59. Fellouse, Sidhu. Sidhu protocol for Antibody Libraries-1. Making and Using Antibodies: A Practical Handbook by Howard and Kaser. 2006:1-24.
60. Sidhu SS. Engineering M13 for phage display. Biomolecular engineering. 2001;18(2):57-63.
61. Watkins NA, Ouwehand WH. Introduction to antibody engineering and phage display. Vox Sang. 2000;78(2):72-9.
62. Sidhu SS, Feld BK, Weiss GA. M13 bacteriophage coat proteins engineered for improved phage display. Methods in molecular biology (Clifton, NJ). 2007;352:205-19.
63. Sidhu SS, Fellouse FA. Synthetic therapeutic antibodies. Nat Chem Biol. 2006;2(12):682-8.
64. Daugherty PS, Iverson BL, Georgiou G. Flow cytometric screening of cell-based libraries. Journal of Immunological Methods. 2000;243(1,Äì2):211-27.
65. Ibrahim S, van den Engh G. Flow Cytometry and Cell Sorting
Cell Separation. In: Kumar A, Galaev I, Mattiasson B, editors.: Springer Berlin / Heidelberg; 2007. p. 19-39.
66. Sergeeva A, Kolonin MG, Molldrem JJ, Pasqualini R, Arap W. Display technologies: Application for the discovery of drug and gene delivery agents. Advanced Drug Delivery Reviews. 2006;58(15):1622-54.
67. Mazor Y, Van Blarcom T, Iverson BL, Georgiou G. E-clonal antibodies: selection of full-length IgG antibodies using bacterial periplasmic display. Nature Protocols. 2008;3(11):1766-77.
68. Varadarajan N, Cantor JR, Georgiou G, Iverson BL. Construction and flow cytometric screening of targeted enzyme libraries. Nature Protocols. 2009;4(6):893-901.
69. Varadarajan N, Pogson M, Georgiou G, Iverson BL. Proteases that can distinguish among different post-translational forms of tyrosine engineered using multicolor flow cytometry. Journal of the American Chemical Society. 2009;131(50):18186-90.
70. Varadarajan N, Georgiou G, Iverson BL. An engineered protease that cleaves specifically after sulfated tyrosine. Angewandte Chemie (International ed in English). 2008;47(41):7861-3.
71. Ibrahim SF, van den Engh G. Flow cytometry and cell sorting. Advances in biochemical engineering/biotechnology. 2007;106:19-39.
72. Mattanovich D, Borth N. Applications of cell sorting in biotechnology. Microbial cell factories. 2006;5:12.

73. Charbit A, Boulain JC, Ryter A, Hofnung M. Probing the topology of a bacterial membrane protein by genetic insertion of a foreign epitope; expression at the cell surface. The EMBO journal. 1986;5(11):3029-37.
74. Francisco JA, Campbell R, Iverson BL, Georgiou G. Production and fluorescence-activated cell sorting of Escherichia coli expressing a functional antibody fragment on the external surface. Proc Natl Acad Sci USA. 1993;90(22):10444-8.
75. Bereta M, Hayhurst A, Gajda M, Chorobik P, Targosz M, Marcinkiewicz J, et al. Improving tumor targeting and therapeutic potential of Salmonella VNP20009 by displaying cell surface CEA-specific antibodies. Vaccine. 2007;25(21):4183-92.
76. Chen G, Hayhurst A, Thomas JG, Harvey BR, Iverson BL, Georgiou G. Isolation of high-affinity ligand-binding proteins by periplasmic expression with cytometric screening (PECS). Nat Biotechnol. 2001;19(6):537-42.
77. Harvey BR, Georgiou G, Hayhurst A, Jeong KJ, Iverson BL, Rogers GK. Anchored periplasmic expression, a versatile technology for the isolation of high-affinity antibodies from Escherichia coli-expressed libraries. Proc Natl Acad Sci USA. 2004;101(25):9193-8.
78. Wörn A, Plückthun A. Stability engineering of antibody single-chain Fv fragments. Journal of Molecular Biology. 2001;305(5):989-1010.
79. Mazor Y, Blarcom TV, Mabry R, Iverson BL, Georgiou G. Isolation of engineered, full-length antibodies from libraries expressed in Escherichia coli. Nat Biotechnol. 2007;25(5):563-5.
80. Sidhu SS. Full-length antibodies on display. Nat Biotechnol. 2007;25(5):537-8.
81. Boder ET, Wittrup KD. Yeast surface display for screening combinatorial polypeptide libraries. Nature Biotechnology. 1997;15(6):553-7.
82. Higuchi K, Araki T, Matsuzaki O, Sato A, Kanno K, Kitaguchi N, et al. Cell display library for gene cloning of variable regions of human antibodies to hepatitis B surface antigen. Journal of Immunological Methods. 1997;202(2):193-204.
83. Zhou C, Jacobsen FW, Cai L, Chen Q, Shen WD. Development of a novel mammalian cell surface antibody display platform. mAbs. 2010;2(5):508-18.
84. Gai SA, Wittrup KD. Yeast surface display for protein engineering and characterization. Current Opinion in Structural Biology. 2007;17(4):467-73.
85. Gera N, Hussain M, Rao BM. Protein selection using yeast surface display. Methods (San Diego, Calif). 2012.
86. Weaver-Feldhaus JM, Lou J, Coleman JR, Siegel RW, Marks JD, Feldhaus MJ. Yeast mating for combinatorial Fab library generation and surface display. FEBS letters. 2004;564(1-2):24-34.
87. Walker LM, Bowley DR, Burton DR. Efficient Recovery of High-Affinity Antibodies from a Single-Chain Fab Yeast Display Library. Journal of Molecular Biology. 2009;389(2):365-75.
88. Hanes J, Plückthun A. In vitro selection and evolution of functional proteins by using ribosome display. Proceedings of the National Academy of Sciences of the United States of America. 1997;94(10):4937-42.

89. Amstutz P, Forrer P, Zahnd C, Plückthun A. In vitro display technologies: novel developments and applications. Current opinion in biotechnology. 2001;12(4):400-5.
90. Zahnd C, Amstutz P, Plückthun A. Ribosome display: selecting and evolving proteins in vitro that specifically bind to a target. Nature Methods. 2007;4(3):269-79.
91. Hanes J, Schaffitzel C, Knappik A, Plückthun A. Picomolar affinity antibodies from a fully synthetic naive library selected and evolved by ribosome display. Nature Biotechnology. 2000;18(12):1287-92.
92. Roberts RW, Szostak JW. RNA-peptide fusions for the in vitro selection of peptides and proteins. Proceedings of the National Academy of Sciences of the United States of America. 1997;94(23):12297-302.
93. Rother RP, Rollins SA, Mojcik CF, Brodsky RA, Bell L. Discovery and development of the complement inhibitor eculizumab for the treatment of paroxysmal nocturnal hemoglobinuria. Nature Biotechnology. 2007;25(11):1256-64.
94. Ji H, Ohmura K, Mahmood U, Lee DM, Hofhuis FMA, Boackle SA, et al. Arthritis critically dependent on innate immune system players. Immunity. 2002;16(2):157-68.
95. Jordan SC, Reinsmoen N, Peng A, Lai C-H, Cao K, Villicana R, et al. Advances in diagnosing and managing antibody-mediated rejection. Pediatr Nephrol. 2010;25(10):2035-45; quiz 45-8.
96. Bonifati DM, Kishore U. Role of complement in neurodegeneration and neuroinflammation. Molecular Immunology. 2007;44(5):999-1010.
97. Ricklin D, Lambris JD. Complement-targeted therapeutics. Nat Biotechnol. 2007;25(11):1265-75.
98. Schrezenmeier H, Höchsmann B. Drugs that inhibit complement. Transfusion and Apheresis Science. 2011:1-6.
99. Lunn M, Santos C, Craig T. Cinryze as the first approved C1 inhibitor in the USA for the treatment of hereditary angioedema: approval, efficacy and safety. Journal of blood medicine. 2010;1:163-70.
100. Davis AE, Mejia P, Lu F. Biological activities of C1 inhibitor. Mol Immunol. 2008;45(16):4057-63.
101. Nielsen EW, Waage C, Fure H, Brekke OL, Sfyroera G, Lambris JD, et al. Effect of supraphysiologic levels of C1-inhibitor on the classical, lectin and alternative pathways of complement. Mol Immunol. 2007;44(8):1819-26.
102. Herper M. The World's Most Expensive Drugs. Forbes; 2010 [updated 2010 June 25, 2012; cited]; Available from: http://www.forbes.com/2010/02/19/expensive-drugs-cost-business-healthcare-rare-diseases_print.html.
103. Chen CH, Lam CF, Boackle RJ. C1 inhibitor removes the entire C1qr2s2 complex from anti-C1Q monoclonal antibodies with low binding affinities. Immunology. 1998;95(4):648-54.
104. Hwang HY, Duvall MR, Tomlinson S, Boackle RJ. Highly specific inhibition of C1q globular-head binding to human IgG: a novel approach to control and regulate the classical complement pathway using an engineered single chain antibody variable fragment. Mol Immunol. 2008;45(9):2570-80.

105. Reddy ST, Ge X, Miklos AE, Hughes RA, Kang SH, Hoi KH, et al. Monoclonal antibodies isolated without screening by analyzing the variable-gene repertoire of plasma cells. Nature biotechnology. 2010.
106. Lee CV, Sidhu SS, Fuh G. Bivalent antibody phage display mimics natural immunoglobulin. Journal of Immunological Methods. 2004;284(1-2):119-32.
107. Bork P, Beckmann G. The CUB domain. A widespread module in developmentally regulated proteins. Journal of Molecular Biology. 1993;231(2):539-45.
108. Kerr FK, O'Brien G, Quinsey NS, Whisstock JC, Boyd S, de la Banda MG, et al. Elucidation of the substrate specificity of the C1s protease of the classical complement pathway. The Journal of biological chemistry. 2005;280(47):39510-4.
109. Wu TT. Length distribution of CDRH3 in antibodies. Proteins, structure, function, and bioinformatics. 1993;16(1):1-7.
110. Rani M, Bolles M, Donaldson EF, Van Blarcom T, Baric R, Iverson B, et al. Increased Antibody Affinity Confers Broad In Vitro Protection Against Escape Mutants of SARS-CoV. Journal of virology. 2012.
111. Van Blarcom TJ, Sofer-Podesta C, Ang J, Boyer JL, Crystal RG, Georgiou G. Affinity maturation of an anti-V antigen IgG expressed in situ through adenovirus gene delivery confers enhanced protection against Yersinia pestis challenge. Gene Therapy. 2010;17(7):913-21.
112. Ge X, Mazor Y, Hunicke-Smith SP, Ellington AD, Georgiou G. Rapid construction and characterization of synthetic antibody libraries without DNA amplification. Biotechnology and Bioengineering. 2010;106(3):347-57.
113. Zhou X, Hu W, Qin X. The role of complement in the mechanism of action of rituximab for B-cell lymphoma: implications for therapy. The oncologist. 2008;13(9):954-66.
114. Cardarelli PM, Quinn M, Buckman D, Fang Y, Colcher D, King DJ, et al. Binding to CD20 by anti-B1 antibody or F(ab')(2) is sufficient for induction of apoptosis in B-cell lines. Cancer immunology, immunotherapy : CII. 2002;51(1):15-24.
115. Farady CJ, Sun J, Darragh MR, Miller SM, Craik CS. The mechanism of inhibition of antibody-based inhibitors of membrane-type serine protease 1 (MT-SP1). Journal of Molecular Biology. 2007;369(4):1041-51.
116. Buerke M, Schwertz H, Seitz W, Meyer J, Darius H. Novel small molecule inhibitor of C1s exerts cardioprotective effects in ischemia-reperfusion injury in rabbits. Journal of Immunology. 2001;167(9):5375-80.
117. Nelson AL, Dhimolea E, Reichert JM. Development trends for human monoclonal antibody therapeutics. Nat Rev Drug Discov. 2010.
118. Wu Y, Eigenbrot C, Liang W-C, Stawicki S, Shia S, Fan B, et al. Structural insight into distinct mechanisms of protease inhibition by antibodies. Proc Natl Acad Sci USA. 2007;104(50):19784-9.
119. Fromant M, Blanquet S, Plateau P. Direct random mutagenesis of gene-sized DNA fragments using polymerase chain reaction. Anal Biochem. 1995;224(1):347-53.

120. Kubetzko S, Balic E, Waibel R, Zangemeister-Wittke U, Plückthun A. PEGylation and multimerization of the anti-p185HER-2 single chain Fv fragment 4D5: effects on tumor targeting. The Journal of biological chemistry. 2006;281(46):35186-201.
121. Morley BJ, Walport MJ. The Complement FactsBook. London: Academic Press; 2000.
122. Rossi V, Bally I, Thielens NM, Esser AF, Arlaud GJ. Baculovirus-mediated expression of truncated modular fragments from the catalytic region of human complement serine protease C1s. Evidence for the involvement of both complement control protein modules in the recognition of the C4 protein substrate. J Biol Chem. 1998;273(2):1232-9.
123. Hayhurst A, Happe S, Mabry R, Koch Z, Iverson BL, Georgiou G. Isolation and expression of recombinant antibody fragments to the biological warfare pathogen Brucella melitensis. Journal of Immunological Methods. 2003;276(1-2):185-96.
124. Ando K, Muguruma Y, Yahata T. Humanizing bone marrow in immune-deficient mice. Curr Top Microbiol Immunol. 2008;324:77-86.
125. Denton PW, Garcia JV. Humanized mouse models of HIV infection. AIDS reviews. 2011;13(3):135-48.
126. Jaiswal S, Pearson T, Friberg H, Shultz LD, Greiner DL, Rothman AL, et al. Dengue virus infection and virus-specific HLA-A2 restricted immune responses in humanized NOD-scid IL2rgammanull mice. PLoS ONE. 2009;4(10):e7251.
127. Strowig T, Gurer C, Ploss A, Liu Y-F, Arrey F, Sashihara J, et al. Priming of protective T cell responses against virus-induced tumors in mice with human immune system components. The Journal of experimental medicine. 2009;206(6):1423-34.
128. Ito M, Kobayashi K, Nakahata T. NOD/Shi-scid IL2rgamma(null) (NOG) mice more appropriate for humanized mouse models. Curr Top Microbiol Immunol. 2008;324:53-76.
129. Shultz LD, Saito Y, Najima Y, Tanaka S, Ochi T, Tomizawa M, et al. Generation of functional human T-cell subsets with HLA-restricted immune responses in HLA class I expressing NOD/SCID/IL2r gamma(null) humanized mice. Proceedings of the National Academy of Sciences. 2010;107(29):13022-7.
130. Marodon G, Desjardins D, Mercey L, Baillou C, Parent P, Manuel M, et al. High diversity of the immune repertoire in humanized NOD.SCID.gamma c-/- mice. Eur J Immunol. 2009;39(8):2136-45.
131. Watanabe Y, Takahashi T, Okajima A, Shiokawa M, Ishii N, Katano I, et al. The analysis of the functions of human B and T cells in humanized NOD/shi-scid/gammac(null) (NOG) mice (hu-HSC NOG mice). International Immunology. 2009;21(7):843-58.
132. Schmidt MR, Appel MC, Giassi LJ, Greiner DL, Shultz LD, Woodland RT. Human BLyS facilitates engraftment of human PBL derived B cells in immunodeficient mice. PLoS ONE. 2008;3(9):e3192.
133. Beerli RR, Rader C. Mining human antibody repertoires. mAbs. 2010;2(4).
134. Manz RA, Löhning M, Cassese G, Thiel A, Radbruch A. Survival of long-lived plasma cells is independent of antigen. International Immunology. 1998;10(11):1703-11.

135. Radbruch A, Muehlinghaus G, Luger EO, Inamine A, Smith KGC, Dörner T, et al. Competence and competition: the challenge of becoming a long-lived plasma cell. Nature Reviews Immunology. 2006;6(10):741-50.
136. Lu YF, Singh M, Cerny J. Canonical germinal center B cells may not dominate the memory response to antigenic challenge. International Immunology. 2001;13(5):643-55.
137. Mosser DM, Edwards JP. Exploring the full spectrum of macrophage activation. Nat Rev Immunol. 2008;8(12):958-69.
138. Shapiro-Shelef M, Calame K. Regulation of plasma-cell development. Nature Reviews Immunology. 2005;5(3):230-42.
139. Tarlinton D, Radbruch A, Hiepe F, Dörner T. Plasma cell differentiation and survival. Current opinion in immunology. 2008;20(2):162-9.
140. Benner R, Rijnbeek AM, Bernabé RR, Martinez-Alonso C, Coutinho A. Frequencies of background immunoglobulin-secreting cells in mice as a function of organ, age, and immune status. Immunobiology. 1981;158(3):225-38.
141. Harrell MI, Iritani BM, Ruddell A. Lymph node mapping in the mouse. Journal of Immunological Methods. 2008;332(1-2):170-4.
142. Fuller SA, Takahashi M, Hurrell JG. Fusion of myeloma cells with immune spleen cells. Current protocols in molecular biology / edited by Frederick M Ausubel [et al]. 2001;Chapter 11:Unit11.7.
143. Mirza IH, Wilkin TJ, Cantarini M, Moore K. A comparison of spleen and lymph node cells as fusion partners for the raising of monoclonal antibodies after different routes of immunisation. Journal of Immunological Methods. 1987;105(2):235-43.
144. Cliquet P, Cox E, Van Dorpe C, Schacht E, Goddeeris BM. Generation of class-selective monoclonal antibodies against the penicillin group. Journal of agricultural and food chemistry. 2001;49(7):3349-55.
145. Grivel JC, Ferrier P, Renard N, Jolly G, Jarry T, Leserman L. Rapid induction of anti-idiotypic responses to unmodified monoclonal antibodies from syngeneic mice following primary immunization. Journal of Immunological Methods. 1993;158(2):173-82.
146. Sado Y, Inoue S, Tomono Y, Omori H. Lymphocytes from enlarged iliac lymph nodes as fusion partners for the production of monoclonal antibodies after a single tail base immunization attempt. Acta histochemica et cytochemica. 2006;39(3):89-94.
147. Kishiro Y, Kagawa M, Naito I, Sado Y. A novel method of preparing rat-monoclonal antibody-producing hybridomas by using rat medial iliac lymph node cells. Cell structure and function. 1995;20(2):151-6.
148. Clark SE, Snow J, Li J, Zola TA, Weiser JN. Phosphorylcholine allows for evasion of bactericidal antibody by Haemophilus influenzae. PLoS pathogens. 2012;8(3):e1002521.
149. Crews S, Griffin J, Huang H, Calame K, Hood L. A single VH gene segment encodes the immune response to phosphorylcholine: somatic mutation is correlated with the class of the antibody. Cell. 1981;25(1):59-66.

150. Gearhart PJ, Sigal NH, Klinman NR. The monoclonal anti-phosphorylcholine antibody response in several murine strains: genetic implications of a diverse repertoire. The Journal of experimental medicine. 1977;145(4):876-91.
151. Manz RA, Hauser AE, Hiepe F, Radbruch A. Maintenance of serum antibody levels. Annu Rev Immunol. 2005;23:367-86.
152. Phan TG, Paus D, Chan TD, Turner ML, Nutt SL, Basten A, et al. High affinity germinal center B cells are actively selected into the plasma cell compartment. The Journal of experimental medicine. 2006;203(11):2419-24.
153. Radbruch A, Muehlinghaus G, Luger EO, Inamine A, Smith KGC, Dörner T, et al. Competence and competition: the challenge of becoming a long-lived plasma cell. Nat Rev Immunol. 2006;6(10):741-50.
154. Calame KL, Lin K-I, Tunyaplin C. Regulatory mechanisms that determine the development and function of plasma cells. Annual Review of Immunology. 2003;21:205-30.
155. Kallies A, Hasbold J, Tarlinton DM, Dietrich W, Corcoran LM, Hodgkin PD, et al. Plasma cell ontogeny defined by quantitative changes in blimp-1 expression. The Journal of experimental medicine. 2004;200(8):967-77.
156. Stall AM, Quintáns J, Loken MR. T15 idiotype expression in the murine response to phosphorylcholine is actively regulated by genes linked to the Igh-C locus. Journal of immunology (Baltimore, Md : 1950). 1986;136(7):2689-96.
157. Cato MH, Yau IW, Rickert RC. Magnetic-based purification of untouched mouse germinal center B cells for ex vivo manipulation and biochemical analysis. Nature Protocols. 2011;6(7):953-60.
158. Krebber A, Bornhauser S, Burmester J, Honegger A, Willuda J, Bosshard HR, et al. Reliable cloning of functional antibody variable domains from hybridomas and spleen cell repertoires employing a reengineered phage display system. Journal of Immunological Methods. 1997;201(1):35-55.
159. Genetech IU. Herceptin Package Insert.
160. Chen WW, Niepel M, Sorger PK. Classic and contemporary approaches to modeling biochemical reactions. Genes & Development. 2010;24(17):1861-75.
161. Fogler HS. Elements of Chemical Reaction Engineering. 3rd ed. Amundson N, editor. Upper Sadde River, New Jersey: A Simon & Shuster Company; 1999.

Vita

Sean Mathew Carroll was born in Ventura, California in 1984 and spent his youth in nearby Camarillo. He attended the University of California, Berkeley where he received his Bachelors of Science in Chemical Engineering in 2006. Afterward, he immediately enrolled at the University of Texas at Austin in order to pursue his doctoral degree in Chemical Engineering.

Permanent address: 2898 Avenida de Autlan, Camarillo, Ca 93010

This dissertation was typed by Sean M Carroll